

Technical University of Liberec

Faculty of Textile Engineering



DIPLOMA THESIS

2012

Mary Immaculate Sithembile Dlamini

Technical University of Liberec
Faculty of Textile Engineering
Chemical Technology of Textile
Department of Textile Chemistry

DIPLOMA THESIS

Photocatalytic properties of TiO₂ nanoparticles

Mary Immaculate Sithembile Dlamini

Supervisor: Assoc. prof. Jakub Wiener, MSc. PhD.

Consultant: Ing. Andrea Chladova

Number of text pages: 116

Number of pictures: 19

Number of tables: 10

Number of graphs: 18

Number of appendices: 3

STATEMENT

I have been informed that on my thesis is fully applicable the Act No. 121/2000 Coll. about copyright, especially §60 - school work.

I acknowledge that Technical University of Liberec (TUL) does not breach my copyright when using my thesis for internal need of TUL.

Shall I use my thesis or shall I award a licence for its utilisation I acknowledge that I am obliged to inform TUL about this fact, TUL has right to claim expenses incurred for this thesis up to amount of actual full expenses.

I have elaborated the thesis alone utilising listed and on basis of consultations with supervisor.

Date: 7 May 2012

Signature: Mary Immaculate Sithembile Dlamini

Mary Immaculate Sithembile Dlamini

ACKNOWLEDGEMENTS

I would like to thank my supervisor Assoc. Prof. Jakub Wiener who has greatly enriched my knowledge and for his guidance in my research work. A special thank you to Ing. Andrea Chladlova for her assistance and practical support of my laboratory work.

I would like to thank my family for their unconditional and invaluable support they have given me even though I was miles away from them. Their encouragement kept me going. I would like to thank my peers and friends for their continued support in my research work.

My sincere gratitude to the Department of Economic Development and CTFL SETA for funding my studies.

ABSTRACT

TiO₂ is extensively used as a photocatalyst due to the strong oxidizing power of its holes, high photostability and redox selectivity. The oxymetric method was investigated for testing of photocatalytic properties of TiO₂ on dye acid orange II and a saccharide to observe the influence of oxygen concentration which decreases under UV radiation. The oxymetric method was modified to test cotton and polyester samples coated with TiO₂ for photocatalysis and self-cleaning properties. The findings show that there is a linear correlation between the decrease of dissolved oxygen concentration as a function of time which shows photo catalytic behavior. The kinetic model is proposed for the degradation of acid orange II which resulted in slight decolourization of the dye acid orange II. Self-cleaning property tested on cotton samples stained with red wine and coffee and exposed to solar radiation for 1 day showed some decolourization of the stains.

Key words: Photocatalysis, TiO₂ nanoparticles, oxygen, UV light

Table of Contents

Table of Contents.....	6
List of tables	9
List of figures.....	10
1 Introduction	14
2 Literature Review	15
2.1 Photocatalysis.....	16
3 Physics and Chemistry of photocatalytic titanium dioxide	17
3.1 Energy bands in solids	17
3.1.1 Mode of action of TiO ₂	18
3.1.2 Mechanism of a photocatalytic process	19
3.2 Electronic processes	20
3.2.1 Moving to Visible Light Absorption Capability	22
3.2.2 N-doped TiO ₂	23
3.2.3 Increasing efficiency by incorporation of metal nanoparticles	24
3.2.4 Heterojunctions	25
3.2.5 Composite semiconductors	26
4 Advanced Oxidation Processes	26
4.1 Homogeneous photocatalysis	27
4.1.1 Heterogeneous photocatalysis	28
5 Kinetics	28
5.1 Catalyst.....	29
5.1.1 Toxicity studies of TiO ₂ particles	31
6 Acid Orange II.....	31
7 Applications of TiO ₂	32
7.1.1 Antibacterial property	32
7.1.2 Self -cleaning	33
7.1.3 UV protection.....	34
7.1.4 Self-cleaning property of cotton.....	34
7.1.5 Self cleaning properties of polyester.....	36
7.2 Practical applications of TiO ₂ photocatalysis	36

8	Analytical methods - TiO ₂ coating of cotton textiles using different pretreatments and techniques	37
8.1	Sol-gel method	37
8.1.1	RF plasma.....	37
8.1.2	MW-plasma.....	38
8.1.3	UV irradiation	38
8.1.4	Dip-pad-dry-cure.....	38
8.1.5	Dip-coating.....	38
8.1.6	Cross-linking	39
9	Experimental Methods and Procedures.....	40
9.1	Aim.....	40
9.2	Materials.....	40
9.2.1	Chemicals.....	40
9.2.2	Catalyst used	40
9.2.3	Equipment and Instruments.....	41
9.3	Method	46
9.3.1	Experiment 1	46
9.3.2	Experiment 2	47
9.3.2.1	<i>Measurement of photocatalytic activity of TiO₂</i>	47
9.3.2.2	<i>Testing of photocatalytic activity of TiO₂ photocatalyst with a saccharide (sugar) using the oxymetric method</i>	48
9.3.3	Experiment 3	48
9.4	Results and Discussion	50
9.4.1	Testing of oxymetric method to observe the influence of concentration of acid orange II in an open system -Experimental part 1	50
9.4.2	Temperature dependent system of photocatalytic activity of TiO ₂ photocatalyst with a saccharide (sugar) -Experimental part 2.....	57
9.4.3	Observation photocatalytic activity using white TiO ₂ coated cotton and polyester textile samples using the oxymetric method Experimental part 3.	61
9.4.4	Experimental part 3 - Observation photocatalytic activity using white TiO ₂ coated polyester textile samples using the oxymetric method	63
9.4.5	Self cleaning of cotton textile modified with TiO ₂ P25 Deegussa Experimental part 3 –	66
10	Conclusion.....	68
11	References	70

12	Appendices	74
12.1	Appendix A	74
12.2	Appendix B	88
12.3	Appendix C	98

List of tables

Table 3.1: Modes of microbe removal or killing action for various disinfection methods ...	19
Table 9.1 : Description (codes) of the samples.....	49
Table 9.2 Linear regression results of acid orange with TiO ₂ under UV light irradiation in a open system	55
Table 9.3: Linear regression results of acid orange with TiO ₂ under UV light irradiation in a closed system.....	57
Table 9.4: Linear regression of TiO ₂ and sugar irradiation under UV light.....	60
Table 9.5 : Linear regression of TiO ₂ in the absence of sugar irradiation under UV light.....	60
Table 9.6: Dissolved oxygen concentration change under UV radiation of cotton samples coated with TiO ₂	63
Table 9.7 : Dissolved oxygen concentration change under UV radiation of polyester samples coated with TiO ₂	65
Table 9.8: Coffee and wine stains on cotton samples exposed in the sun and kept in the dark.....	66
Table 9.9 : Coffee and wine stain on cotton samples after washing.....	66
Table 12.1: Oxygen concentration under UV irradiation 0.1 g/l TiO ₂	94

List of figures

Figure 3.1 : The energy band diagram for a semiconductor in contact with an electrolyte. ..	18
Figure 3.2: Top- Light of energy exceeding band gap results in charge separation, with electron reducing a donor (usually oxygen) and hole oxidising a donor (usually water); bottom: summary of processes occurring. Image based on Bahnmann (2004)[25]......	21
Figure 3.3 : N-doped TiO ₂ as explained by Nakoto and Irie. Doping with nitrogen results in a mid-band gap energy level which reduces the energy gap required for charge separation[25].	23
Figure 3.4: Incorporation of silver nanoparticles facilitate longer charge separation by trapping photogenerated electrons [25]......	25
Figure 3.5 : Photo-excitation in composite semiconductor-semiconductor photocatalyst [27].	26
Figure 5.1 :Band energies of typical semiconductors [26]......	30
Figure 6.1 :Chemical structure of acid orange II [18]	32
Figure 7.1: Electrostatic interaction of succinic acid with carboxylic group [14]......	35
Figure 7.2: Major areas of activity of titanium dioxide photocatalysis [26]	36
Figure 9.1: Dissolved Oxygen pocket meter - Oxi 315	41
Figure 9.2: Dissolved oxygen sensor –CellOx®325	41
Figure 9.3: UV box	42
Figure 9.4: UV/vis spectrophotometry	43
Figure 9.5: Vitrum centrifuga	43
Figure 9.6: Julabo thermostat	44
Figure 9.7: Bandelin ultrasonic homogeniser	45
Figure 9.8 :Experimental set up.....	45
Figure 9.9: Experimental set up.....	46
Figure 9.10: Decrease of oxygen concentration during degradation of acid orange II in the presence of TiO ₂	50
Figure 9.11: Linear regression showing decrease of dissolved oxygen during acid orange II degradation [0.01g/l] with TiO ₂ [0.1g/l]	50

Figure 9.12: Absorbance decrease at 485 nm showing some decolorization of acid orange II under UV light in the presence of TiO ₂	51
Figure 9.13: Derivation model of the change of oxygen concentration during degradation of dye acid orange II.....	53
Figure 9.14: Photocatalytic degradation of acid orange II under UV light in the presence of TiO ₂ in an open system	54
Figure 9.15: Linear regression showing decrease of dissolved oxygen during acid orange II degradation [0.01g/l] with TiO ₂ [0.1g/l] in a open system	54
Figure 9.16: Photocatalytic degradation of acid orange II under UV light in the presence of TiO ₂ in a closed system	56
Figure 9.17: Linear regression showing decrease of dissolved oxygen during acid orange II degradation [0.01g/l] with TiO ₂ [0.1g/l]	56
Figure 9.18: Change in temperature with irradiation in a closed system using a water cooling system.....	57
Figure 9.19: Maintenance of temperature 13.5°C using the Julabo thermostat in a closed system.....	58
Figure 9.20: Decrease of dissolved oxygen of TiO ₂ and sugar.....	59
Figure 9.21: Linear regression showing decrease of dissolved oxygen TiO ₂ with sugar	59
Figure 9.22 : Oxygen concentration behavior as a function of time under UV irradiation ...	61
Figure 9.23: Oxygen concentration decrease as a function of time under UV irradiation	62
Figure 9.24: Oxygen concentration behavior as a function of time under UV irradiation of cotton samples	62
Figure 9.25: Oxygen concentration behavior as a function of time under UV irradiation	64
Figure 9.26: Oxygen concentration behavior as a function of time under UV irradiation of polyester sample.....	64
Figure 9.27: Oxygen concentration behavior as a function of time under UV irradiation of polyester samples	65

List of symbols

TiO₂- titanium dioxide

CO₂- carbon dioxide

ZnO- zinc oxide

CdS- cadmium sulfide

Fe₂O₃- iron (III) oxide

H₂O₂-hydrogen peroxide

OH-hydroxyl

SiO₂- silicone dioxide

RuO₂- ruthenium oxide

Al₂O₂- aluminiu (II)oxide

List of Abbreviations

AOP- advanced oxidation process

ROS- reactive oxygen species

Ec-conduction band

Ev- valence band

E_{bg} - band gap energy

eV- electron volts

h^+ - positive hole

e^- -excited electron

HOMO- highest occupied molecular orbital

LUMO-lowest occupied molecular orbital

UV-ultraviolet light

UVA- ultra violet light long wavelength

UVB- ultra violet light middle wavelength

UVC-ultra violet light short wavelength

nm- nanometer

k- equilibrium constant

CO- cotton

PES- polyester

DSSC-dye sensitized solar cell

HEPA-high efficiency particulate air filters

1 Introduction

Photocatalytic chemistry of titanium dioxide has been extensively studied over the last 25 years for removal of organic and inorganic compounds from contaminated water and air and for the partial oxidation of organic compounds. The most active photocatalysts are formulations based on the anatase crystal phase, and most work has been done using the P25 form of TiO₂ produced by Degussa Chemical Company (Germany). This material is a mixture of phases with an approximate composition of 75% anatase and 25% rutile and has a BET surface area of about 50m²/g. The literature for the photocatalytic oxidation or reduction of organic and inorganic compounds has been the subject of expansive bibliographies and numerous reviews [19, 25].

In 1972, Fujishima and Honda discovered the photocatalytic splitting of water on TiO₂ electrodes. This event marked the beginning of a new era in heterogeneous photocatalysis. The main focus of previous studies has been to investigate the principal applicability of photocatalysis systems for efficient treatment of water polluted with toxic substances. But recently the application of nano-TiO₂ in textile finishing has become an important area of research because of self-cleaning effect imparted by nano-TiO₂ on textile substrates [7]. The vision for future technology about photocatalysis is that, the surface area of TiO₂ should be increased to absorb more photo energy and to enhance efficiency by allowing visible-light to activate the catalyst instead of ultraviolet. Second, we need to reduce the band-gap energy so that visible light can be used. Finally, effective methods need to be developed to prevent recombination of e⁻/h⁺ pairs [9]. With these changes, TiO₂ would be activated under visible light efficiently. In this paper the photocatalytic properties of TiO₂ on textiles will be reviewed. The photocatalysis will be tested using the oxymetric method on dye and a saccharide. The photocatalysis of cotton and polyester samples coated with TiO₂ will be tested using oxymetric method. The dissolved oxygen concentration will be measured as a function of time

2 Literature Review

In recent years, more attention has been paid to the application of semiconductors like ZnO, Fe₂O₃ and CdS as photocatalysts for the degradation of both inorganic and organic materials. As a popular photocatalyst, titanium dioxide has been widely used because of its various advantages such as, high photocatalytic activity, low cost, optical and electronic properties, chemical stability and nontoxicity [26]. Some characteristics of TiO₂ particles affecting the photocatalytic activity are particle size, crystal structure crystalline phase, hydroxylated level, intensity and wavelength of light irradiation, surface absorption of contaminants, pH of the solution and the preparation method. When TiO₂ particle size is reduced to the nano scale, photocatalytic activity increases as a result of the expansion of light band-gap for quantum size and due to the enhancement of the effective surface area. TiO₂, used for self-cleaning surfaces, has now become known in commercial products ranging from fabrics, kitchen and bathroom ceramic tiles, to indoor air filters and window glass sections. When TiO₂ catalysts are subjected to irradiation with photons of energy equal to or higher than their band gap, the generated electron-hole pairs can induce the formation of reactive oxygen species, such as hydroxyl radical and superoxide radical that are directly involved in the oxidation processes leading to the degradation of both contaminants and microorganisms [10].

Titanium dioxide is present in three crystalline phases: rutile, anatase and brookite. Among these three forms, rutile is more stable than the other two forms. Anatase and brookite, under the influence of heat, changes to rutile. Rutile and anatase structures are tetragonal while brookite structure is orthorhombic. Although some applications such as normal solution filtering do not require the crystalline phase, crystallinity is essential when biocompatible, photocatalytic or semiconducting properties are desired. For example, anatase phase titania is preferred in dye-sensitized solar cells and catalysis, whereas rutile is mostly used in the area of dielectrics and high temperature oxygen gas sensors. Previous studies have revealed that anatase TiO₂ is produced mainly from peroxide, while rutile TiO₂ produced superoxide radical is from oxygen. Among the crystalline phases of TiO₂, anatase has been reported to have the highest activity.

Synergy effect has also been reported for the high photocatalytic activity by mixing rutile TiO_2 into anatase TiO_2 . Both anatase and rutile have accessible band-gaps; their photoactive nature means that radical species are produced at their surfaces in the presence of sunlight and water [10].

High photocatalytic property of titanium dioxide nano-particles/coating have been widely used for water and air purification, sterilization/disinfection, photo-induced water splitting, organic compound degradation, dye-sensitized solar cell(DSSC), super hydrophilic effect and self-cleaning properties[7].

2.1 Photocatalysis

Photocatalysis is the acceleration of a photoreaction in the presence of a catalyst. Light is absorbed by an absorbent substrate in photolysis. Electron hole-pairs are created which generate free radicals ($\bullet\text{OH}$ hydroxyl radicals). The production of hydroxyl radicals can be used in various applications such as a commercial advanced oxidation process (AOP), in self-cleaning properties, used in disinfecting water, etc. Electron pairs known as excitons are generated when TiO_2 is subjected to radiation exceeding the materials band gap. These additional electrons enter the conduction band, while the holes remain in the valence band. Thus redox reactions are created by the formation of adsorbed radicals on TiO_2 surfaces because of the photogenerated electron hole pairs. Hence the photocatalysis activity of TiO_2 is dependent on the level of generation and recombination of the electron-hole pairs as well as the levels of adsorbed radical forming species on TiO_2 surfaces [5].

TiO_2 is used in the preparation of many composites where it is necessary to remove or kill microorganisms found in water, air, on surface, or in a biological host. Disinfection of water is required for human consumption, production of products that will be consumed by humans or animals. Disinfected air is required in medical facilities, in production processes where biological contamination must be prevented. Disinfection is a process that removes or deactivates pathogenic bacteria, virus, protozoa, or fungi. Disinfection of water has been a problem for many years particularly in rural areas and developing countries. The mostly used method in developed countries are chlorination,

ozonation, the use of germicidal lamps (low pressure mercury vapour lamps emitting at 254 nm) are being evaluated and used on a large scale. Disinfection of air is achieved by using germicidal lamps or size exclusion filter (high efficiency particle air, HEPA filters). Biocides are widely used for the control of biofilm growth in cooling towers and chilled water systems. Disinfection of surfaces can be achieved by ozone exposure, irradiation with UV light, washing with disinfectants or application of heat [19].

3 Physiscs and Chemistry of photocatalytic titanium dioxide

3.1 Energy bands in solids

Semiconductors of interest are network solids, not discrete molecules; the covalent bond network extends throughout the volume of the crystal. As required by molecular orbital theory, an energy level that exists for a discrete bond between a pair of atoms splits into a very large number of closely spaced energy levels in the microscopic solid. The accumulation of energy levels is called energy band gap (E_{bg}). An energy band is treated as a continuum of energy levels because the energy spacing between adjacent levels is so small. The energy level diagram of a net work solid consists of stacked series of energy bands some of which may overlap. The highest filled energy band and the lowest empty energy band are the most important in terms of charge transport and charge transfer. These bands are separated by a gap devoid of energy levels in a semiconductor or insulator, Figure (3.1).

The two bands overlap in metals, or a band is partially filled with electrons. The highest filled band is called the valence band (V.B.), and the lowest empty band the conduction band (C.B.) [3]. In most semiconductors the valence band is derived from a bonding molecular orbital and the conduction band from an anti-bonding molecular orbital. The band gap energy and the positions of E_v and E_c band edges on an electrochemical potential scale are the primary determinants of the properties and behavior of semiconductor electrodes. The preferred energy unit for E_{bg} is electron-volts (eV) [3].

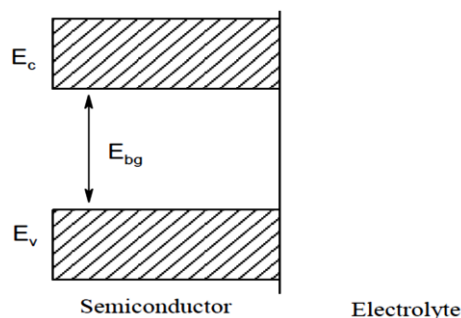


Figure 3.1 : The energy band diagram for a semiconductor in contact with an electrolyte.

E_c : conduction band; E_v : valence band; E_{bg} : band gap energy[1].

3.1.1 Mode of action of TiO_2

Titanium dioxide is a white powder, with titanium in oxidation state IV. Its d-electron configuration is therefore d^0 , and the white colour is explained by the lack of d-d or metal centered transitions. It exists in several polymorphs of titanium dioxide that are commonly used which are anatase and rutile. TiO_2 is a large band-gap semiconductor, its HOMO is termed a valence band and LUMO is termed a conduction band. The valence band of TiO_2 is composed primarily of oxygen 2p orbitals hybridized with Ti 3d states, while the conduction band is made up of pure 3d orbital of titanium [16, 25]. By conjuring the electronic energy band structure of TiO_2 , one can describe its photocatalytic activity. The outermost filled orbitals of elemental titanium (Ti) are 4s² and 3d² and that of oxygen (O) are 2s² and 2p⁴. In TiO_2 , the Ti ions are in a distorted octahedral environment and formally have a Ti^{4+} (3d⁰) electronic configuration. When TiO_2 is exposed to near-UV light, electrons in the valence band are excited to the conduction band leaving behind holes [25].

Rutile has a lower band gap 3.0 eV and for anatase it is 3.2eV which can be excited by irradiation at lower wavelengths, this region is in the UVA region resulting in a sharp absorption band at 390- 400nm [6,15] . Anatase has superior photocatalytic activity as a result of higher levels of adsorbed radicals and a higher surface area. The action spectrum for anatase shows a sharp decrease in activity above about 385 nm. Hence the combination of rutile and anatase increases the photocatalytic activity by improving the electron-hole separation. The photocatalytic process includes chemical steps that produce

reactive species that in principal can cause fatal damage to organic materials/microorganisms. The steps are summarized in Table 3.1 and include formation of the following species: hydroxyl radical, hydrogen peroxide, superoxide, conduction band electron, and valence band hole. The reactive oxygen species (ROS) may disrupt or damage various cell or viral functions or structures. The predominance of evidence on photocatalytic chemistry in aqueous solution suggests that the hydroxyl radical formed by whole transfer does not diffuse from the surface of the TiO₂ into bulk aqueous phase [15].

Table 3.1: Modes of microbe removal or killing action for various disinfection methods

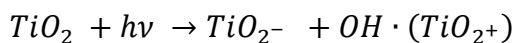
Method	OH	O ₂ ⁻ , H ₂ O ₂	Cl	hν	Adsorption	Trapping
UV (254 nm)				x		
Chlorine			x			
TiO ₂ (300-380nm)	x	x		(a)	x	(b)
TiO ₂ (254 nm)	x	x		x	x	(b)
HEPA filter						x

(a) Near ultraviolet light may have some killing effect on sensitive organisms.

(b) In some catalyst configurations the titanium dioxide layer may act as a particle filter [6].

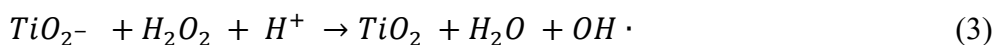
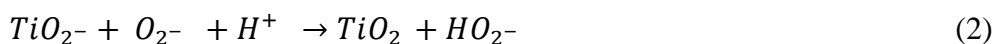
3.1.2 Mechanism of a photocatalytic process

Electron-Hole Pair Formation



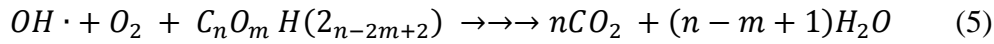
(conduction band electron and valence band hole) (1)

Electron removal from the conduction band

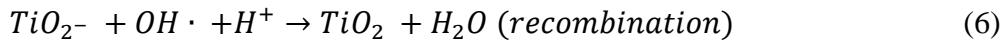




Oxidation of organic compounds



Nonproductive Radical Reactions.



Organic substances in contact with titanium dioxide surface may result in a direct electron transfer to the surface of the material. Light is essential for the photocatalytic system there can also be direct photochemistry as there would be from any UV source. There is a possibility of enhanced or unique photochemistry resulting from the irradiation of the organic substances while it is adsorbed on the oxidative surface [6].

3.2 Electronic processes

Looking more closely at the electronic processes leading in the promotion of an electron to the conduction band. Irradiation by UV light results in a 'hole' in the valence band where the electron density was localized on that orbital which leaves a positive sign to symbolize the loss of a negative electron [6]. The hole is powerfully oxidizing and the orbital very much wants to retrieve the electron density just lost after light irradiation. The lost electron density can be retrieved by the electron in the conduction band recombining with the valence band in process termed recombination, which is a sum of the radiative (i.e. emission may be observed) and non-radiative processes. Based on the energy gap law, rutile energy levels are closer which means that the non-radiative process is more efficient, and hence recombination is more efficient [9, 15].

The hole has the potential to oxidise water that may be on the surface of the material resulting in the formation of hydroxyl radicals. Hydroxyl radicals are very powerful

oxidisers hence they can oxidise any organic species that happens to be nearby, ultimately to carbon dioxide (CO₂) and water. At the same time as oxidation takes place, the hole in the conduction band has no hole to recombine with, since it has oxidized surface bound water. It quickly looks for an alternative to reduce, and rapidly reduces oxygen to superoxide anion. This is followed by a reaction with water to form, again the hydroxyl radical.

The processes are summarized below:

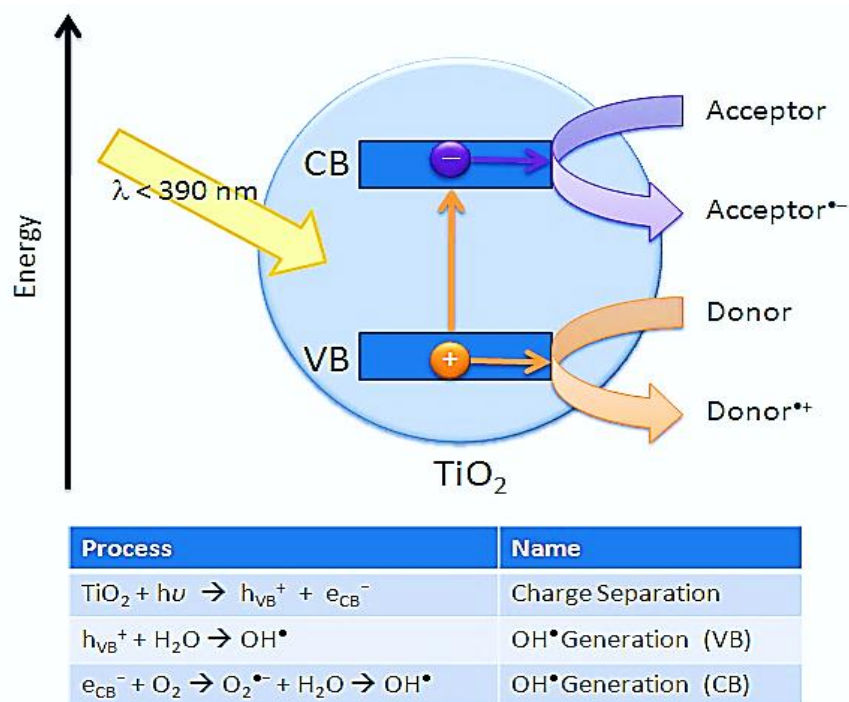


Figure 3.2: Top- Light of energy exceeding band gap results in charge separation, with electron reducing a donor (usually oxygen) and hole oxidising a donor (usually water); bottom: summary of processes occurring. Image based on Bahnemann (2004)[25].

The efficiency of photocatalysis can be deduced at the materials surface from the electronic reactions. The requirements are a surface bound water to allow efficient oxidation, and water should be aerated to provide oxygen to the solution. Additionally, the degradation of the pollutant by the catalyst requires for the pollutant to be adsorbed or very close to the surface of the material, and hence the greater the surface area of the material, the more pollutant can adsorb. Nanoparticulate materials are therefore preferred as they vastly increase the surface area [9].

Pilkington self-cleaning glass is an example of use of this technology in a commercial application. A thin film of nanoparticulate titanium dioxide is coated onto panes of glass (it is so thin that it is transparent). The glass accumulates dust in the normal daily events. The titanium dioxide on the glass, once exposed to sunlight, produces hydroxyl radicals which degrade any surface adsorbed dirt. Once washed down with rain, this decomposed dirt is removed and the glass is ready for another cycle. The same process is observed for any organic species they react with the hydroxyl radical to ultimately form carbon dioxide and water.

Given that the materials work readily, however there are some limitations. The primary limitation is that the materials absorb only UV light, so the activation by sunlight is completed by the 5% of sunlight that is in the UV region. A large amount of research has looked into ways to enhance the visible light activity of the materials. Another limitation is the fact that recombination is an efficient, competitive process, and given that this is a less efficient process with anatase, it is generally accepted that anatase is a preferred photocatalyst to rutile. The approaches are discussed below taken to both increase the visible light absorption capability and increase the efficiency of the reactivity that follows after the recombination process [25].

3.2.1 Moving to Visible Light Absorption Capability

Given the requirements for UV light activation of TiO_2 , researchers have become interested in tuning the materials so that they would become activated by visible light (e.g. room light) for applications for indoor use or by solar light for outdoor use. Various approaches were considered, and in 2001, a Japanese chemist named Asahi working out of Toyota labs, published a paper in the journal Science on nitrogen doped titanium dioxide materials. Nitrogen doping produced what is commonly called yellow TiO_2 which showed effective UV and visible light activity [2]. While there is some debate around how the activity is increased, the N-doped TiO_2 is shown to have a much greater absorbance in the visible region (extending from a sharp cut off at about 390 nm to a broad cut off at above 500 nm). This subsequently increased the amount of visible light activity the material could absorb, and hence meant that visible light-activated photocatalysis was achievable [25].

There has been some discussion in the literature on the mechanism on enhancement of nitrogen doping, and the mechanism described here is one put forward by Nakoto (2004) and Irie (2003), and counters Asahi's original explanation that the N-doping narrowed the gap between the valence band and conduction band of titania. These researchers proposed that the introduction of nitrogen introduced new occupied (i.e. electron rich) orbitals in between the valence band (which are comprised primarily of O-2p orbitals) and conduction band (which are comprised primarily of Ti-3d orbitals). These N-2p orbitals acted as a step up for the electrons in the O-2p orbital, which once populated had now a much smaller jump to make to be promoted into the conduction band. Once this process occurs, electrons from the original valence band can migrate into the mid-band gap energy level, leaving a hole in the valence band, which reacts as described before [25].

3.2.2 N-doped TiO₂

N-doping as explained by Nakoto and Irie. Doping with nitrogen results in a mid-band gap energy level which reduces the energy gap required for charge separation .

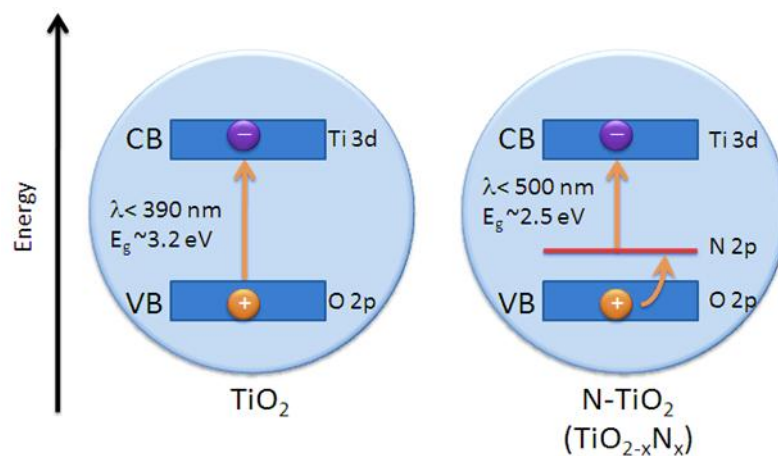


Figure 3.3 : N-doped TiO₂ as explained by Nakoto and Irie. Doping with nitrogen results in a mid-band gap energy level which reduces the energy gap required for charge separation[25].

3.2.3 Increasing efficiency by incorporation of metal nanoparticles

Photocatalytic mechanism can be further improved by designing higher and efficient photocatalytic materials, by increasing the e^-h^+ charge separation which decreases recombination. The charge separation requires a great deal of effort, as well as increasing visible light activity is to facilitate charge separation. One wise way of doing this is to incorporate noble metal nanoparticles such as silver, platinum or gold and metal oxides such as (RuO_2) into the titanium dioxide material. As an example, incorporation of a small amount of silver (1–5%) results in increased efficiency in photocatalysis. This process increases the e^-h^+ charge separation and hence reduces recombination causing increase in efficiency in oxidation and reduction reactions on the particle surfaces.

Silver has an electron accepting region at an energy just below the conduction band. Therefore, after light absorption and charge separation, the electron in the conduction band can be effectively trapped by the silver, while the hole oxidises water and forms hydroxyl radicals, without the threat of recombination. The trapping of electrons by silver is referred to as a “Goldilock’s zone” of silver. The requirement is to add just enough silver so that there are silver sites dispersed through the material to rapidly trap electrons, however too much silver may cover the titanium dioxide and prevent light absorption.

In addition, too much silver may mean that the silver acts as a recombination site itself essentially it will form a bridge between an electron and a hole[15]. The emission of titanium dioxide (and of similar studies with zinc oxide) can be interpreted as a measure of the recombination efficiency. Studies examining the emission of these metal oxides have demonstrated that the emission intensity reduces on increasing amounts of silver indicating that the silver is trapping electrons and reducing electron-hole recombination, as indicated in the diagram below. Incorporation of silver nanoparticles facilitate longer charge separation by trapping photogenerated electrons [25].

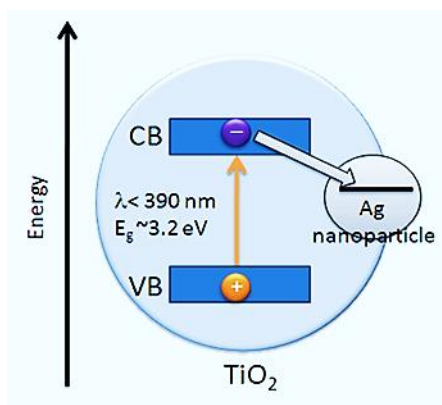


Figure 3.4: Incorporation of silver nanoparticles facilitate longer charge separation by trapping photogenerated electrons [25].

3.2.4 Heterojunctions

The idea of incorporating different semiconductors which have different conduction band energy levels, is a similar strategy to that described above, and a rapidly developing area. The strategy is as before, the electrons are trapped in order for the holes to have more time to react. A simple example is the anatase-rutile heterojunction. Rutile has a smaller band gap (by about 0.2 eV) to anatase, although their valence band levels are at similar energies. Therefore, in a similar fashion to the situation with silver, charge separation in anatase is followed by electron injection into the rutile conduction band which means that there is a hole in the valence band of anatase that can freely oxidise water. Heterogeneous photocatalysis is a promising method among advanced oxidation processes (AOPs), which can be used for degradation of various organic pollutants in water and wastewater. In photocatalysis systems a combination of semiconductors (such as TiO₂, ZnO, F₂O₃, CdS and ZnS) and UV or visible lights can be used. Various attempts have been made to reduce e⁻-h⁺ recombination in photocatalytic processes. These studies include doping metal ions into the TiO₂ lattice and coupling semiconductors have showed that the photonic efficiency of Pt deposited on TiO₂ is almost comparable with Au/TiO₂ but higher than Pd/TiO₂. TiO₂ doped with silver is more efficient than undoped TiO₂ at photocatalytic degradation, furthermore silver doped TiO₂ can be separated from treated effluent very easily than undoped TiO₂ [25]. It is no coincidence that the industry standard photocatalyst, Degussa P25, has a 75:25 ratio of anatase:rutile it also has a very small particle size.

3.2.5 Composite semiconductors

Coupled semiconductor photocatalysts provide an interesting way to increase the photocatalytic process by increasing the charge separation and extending the energy range of photo-excitation for the system. The energy of the excitation light is too small to directly excite the TiO_2 portion of the photocatalyst as shown in Fig 3.5. The hole produced in the CdS valence band by the excitation process remains in the CdS particle while the electron transfers to the conduction band of the TiO_2 particle. The electron transfer from CdS to TiO_2 increases the charge separation and efficiency of the photocatalytic process. The separated electron and hole are then free to undergo electron transfer with adsorbates on the surface. The quantum yield for the reduction of methylviolet drastically increased and approached an optimum value of 1 when the concentration of TiO_2 was increased in a CdS- TiO_2 system (Gopidas et al., 1990). Transient absorption spectra of the composite CdS- TiO_2 photocatalyst indicates trapping of the electron at Ti^{4+} sites on the TiO_2 surface. The CdS- TiO_2 system exhibits a broad absorption band in the 550-750 nm region after receiving a 355 nm (3.5 eV) picosecond laser pulse. This band is characteristic of chemical changes associated with the trapping of electrons on the TiO_2 surface. [27].

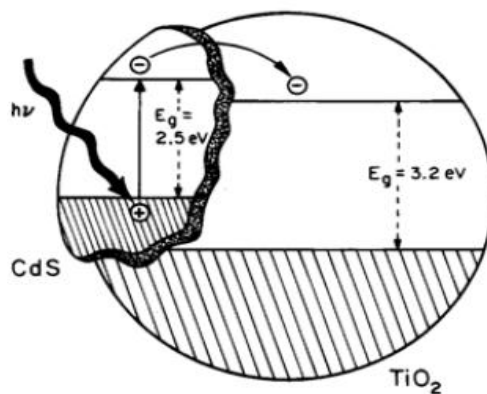


Figure 3.5 : Photo-excitation in composite semiconductor-semiconductor photocatalyst [27].

4 Advanced Oxidation Processes

Advanced oxidation process is one of the chemical treatment technique in water that has been developed to remove color from dye and contaminated waste waters. Advanced oxidation processes (AOP's), in combination with ozone and high output ultraviolet technologies, in conjunction with hydrogen peroxide and catalyst are successfully used to

decompose many toxic and bio-resistant organic pollutants in aqueous solution to acceptable levels, without producing additional hazardous by-products or sludge which require further handling. Advanced oxidation processes involve the generation of hydroxyl ($\bullet\text{OH}$) radicals which oxidize the pollutants [3]. After fluorine, the hydroxyl radical is the second strongest known oxidant having an oxidation potential of 2.8 eV. It is able to oxidize and mineralize almost every organic molecule, yielding CO_2 and inorganic ions as shown in Eq.11 and 12.



Different combinations of homogenous and heterogeneous methods which involve the generation of free radicals are, (i) photochemical irradiation with ultraviolet light (coupled with powerful oxidizing agents like ozone, hydrogen peroxide and /or a semiconductor), (ii) Fenton and Photo-Fenton catalytic processes (iii) Electron Beam Irradiation technique and (iv) Sonolysis.

All these processes use UV range for degradation. The UV spectrum is arbitrarily divided into three bands: UV-A (315 to 400 nm), UV-B (280 to 315nm) and UV-C (100 to 280 nm). Of these bands UV-A and UV-C are generally used in environmental applications. UV-A radiations are referred to as long wavelength radiations or black light and UV-C are referred to as short wave radiations [1].

Advanced oxidation processes can be broadly classified into the following groups:

1. Homogeneous photocatalysis
2. Heterogeneous photocatalysis

4.1 Homogeneous photocatalysis

The applications of homogeneous photodegradation (single-phase system) use in treatment of contaminated water, involves the use of an oxidant to generate radicals, which attack the organic pollutants to initiate oxidation. The major oxidants used are:

- Hydrogen peroxide (UV / H_2O_2)

- Ozone (UV /O₃)
- Hydrogen peroxide and Ozone (UV /O₃/H₂O₂)
- Photo-Fenton system (Fe⁺³ /H₂O₂)

4.1.1 Heterogeneous photocatalysis

Heterogeneous photocatalytic process consists of utilizing the near UV radiation to photo-excite a semiconductor catalyst in the presence of oxygen. Under these circumstances oxidizing species, either bound hydroxyl radicals or free holes, are generated. Using photocatalysis, organic pollutants can be completely mineralized reacting with the oxidizers to form CO₂, water and dilute concentration of simple mineral acids. The process is heterogeneous because there are two active phases, solid and liquid. This process can also be carried out utilizing the near part of solar spectrum ($\lambda < 380\text{nm}$) which transforms it into a good option to be used [1].

5 Kinetics

An understanding of reaction rates and how the reaction rate is influenced by different parameters is important for the design and optimization of an industrial system. The rate of photocatalytic degradation depends on several factors including illumination intensity, catalyst type, oxygen concentration, pH, presence of inorganic ions and the concentration of organic reactant. The destruction rates of organics in photocatalytic oxidation have been modeled by different kinetic models. Langmuir-Hinshelwood (L-H) kinetics seems to describe many of the reactions fairly well [27]. The rate of destruction is given by Eq 13:

$$\frac{dC}{dt} = k_1 \cdot k_2 \frac{C}{(1+k_2 C)} \quad (13)$$

In the ideal case, for which the L-H model is derived, C is the bulk solute concentration, k₁ the reaction rate constant, k₂ the equilibrium adsorption constant and t represents time. The L-H reaction rate constants are useful for comparing the reaction rate under different experimental conditions. Once the reaction constants k₁ and k₂ have been evaluated, the disappearance of the reactant can be estimated if all other factors are held constant. For

low solute concentration C , the L-H expression reduces to a pseudo first order expression:

$$-\frac{dC}{dt} = k_1 k_2 C = kC \quad (14)$$

This equation has been shown to apply to many photocatalysed reactions. The industrial pollutants levels are typically of the order of ppm, which are low enough for the reaction rate to follow pseudo first order kinetics.

5.1 Catalyst

Catalyst research over the last three decades has not only confirmed the capability of sunlight for detoxification and disinfection but also accelerated the natural process by the use of catalysts. For oxidation reactions to occur the valence band (VB) must have a higher oxidation potential than the material under consideration. The redox potential of the valence band and the conductance band for different semiconductors varies between +4.0 and -1.5 volts versus normal hydrogen electrode (NHE). Therefore, by careful selection of the semiconductor photocatalyst, a wide range of species can be treated via these photocatalytic processes. Metal oxides and sulphides represent a large class of semiconductor materials suitable for photocatalytic purposes. Figure 5.1 lists some of the selected semiconductor materials, which have been used for photocatalytic reactions, together with the VB and CB potentials, the band gap energy and wavelength required to activate the catalyst that produce this gap, the radiation must be of an equal or lower wavelength than that calculated by that Planck's equation (Eq15).

$$\lambda = hc/ E_{bg} \quad (15)$$

where E_{bg} is the semiconductor band-gap energy, h is the Planck's constant and c is the speed of light.

Among the listed semiconductors, TiO_2 has proven to be the most suitable for widespread environmental applications. ZnO also seems to be a suitable photocatalyst but it dissolves in acidic solutions and therefore, cannot be used for technical applications. Other semiconductor particles (e.g., CdS) absorb larger fractions of the solar spectrum than TiO_2 and can form chemically activated surface-bond intermediates, but

unfortunately, such catalysts are degraded during the repeated catalytic cycles usually involved in heterogeneous photocatalysis[27].

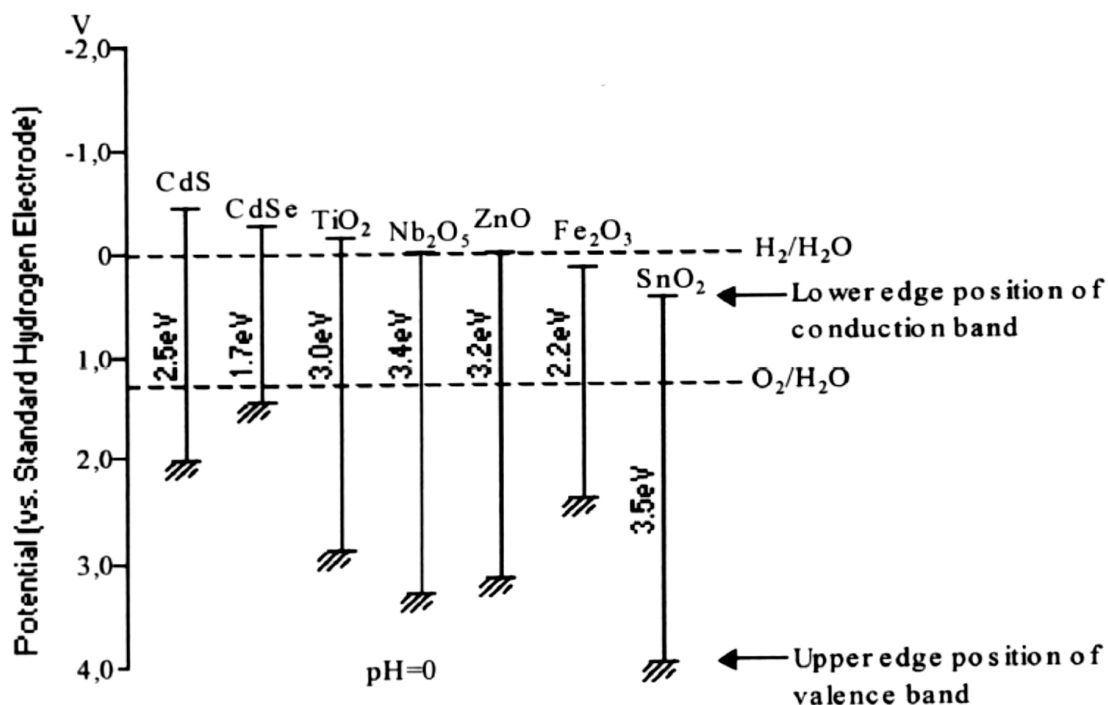


Figure 5.1 :Band energies of typical semiconductors [26].

Titanium dioxide is widely used as white paint pigment, sun blocking material, cosmetic, or as builder in vitamin tablets, among many other uses. It is biologically and chemically inert; it is stable to photo and chemical corrosion, and is inexpensive. Anatase and rutile are the most common forms and the former is the most effective in wastewater treatment. Anatase is thermodynamically less stable than rutile, but its formation is kinetically favored at lower temperature (<600°C), which could explain its higher surface area and its higher surface density of active sites for adsorption and catalysis. Furthermore, TiO₂ is of special interest since it can use natural (solar) UV radiation. This is because TiO₂ has an appropriate energetic separation between its valence and conduction bands, which can be exceeded by the energy of a solar photon.

The disadvantage that has been mentioned before of the particulate excitation of the semiconductors is the high degree of recombination between the photo-generated charge

carriers. As a result of this electron-hole recombination, the efficiency of the semiconductors decreases thereby, decreasing the quantum yield of the redox processes.

The other limitation of TiO_2 is that it utilizes only about 5% of the solar energy reaching the earth's surface which is in the UV region. This limitation is overcome by its modification. It can be modified by doping of metal ions and photosensitization by various colored organic and inorganic compounds, in order to extend the photo-response of large bandgap semiconductors into the visible region to use them for the degradation of colored organic contaminants and other organic pollutants. The metal ions added into polycrystalline TiO_2 or photo-deposited metals increase the absorption[27]

5.1.1 Toxicity studies of TiO_2 particles

Titanium dioxide has generally been regarded as a nuisance dust in man. The first epidemiologic survey of respiratory disease among 209 titanium metal production workers showed that 17% of the subjects had signs of pleural disease which suggests that reductions in ventilation capacity may be associated with the exposure to titanium tetrachloride and titanium dioxide. However, the epidemiologic study of 1576 workers exposed to TiO_2 particles shows no statistically significant association between TiO_2 exposure and risk of lung cancer and chronic respiratory diseases. No cases of pulmonary fibrosis has been found among TiO_2 exposed workers. The same conclusion was reached in another epidemiologic study of 2477 employees from TiO_2 plants that showed no statistically significant association between titanium tetrachloride exposure and risk of lung cancer and chronic respiratory diseases. However, some pathologic changes such as pulmonary fibrosis and skin necrosis may be associated with direct exposure to large quantities of TiO_2 particles. It is not clear whether the effect of ultraviolet or visible light is involved in these cases [15].

6 Acid Orange II

Orange II is one of the dyes that is commonly used in the textile industry. Textile dyes are intentionally designed to exhibit a high degree of chemical, photolytic, and microbial stability, as to fulfill the fastness requirements of consumers [24]. Acid orange II falls in the chemical class of Azo compounds. The color index of acid orange II is acid orange 7

and is a soluble acid. Azo compounds are an important class of synthetic dyes commonly used as coloring agents in the textile, paint, ink, plastics and cosmetics industries. They are characterized by the presence of one or more azo group (-N=N-) bound to aromatic rings as shown in Fig. The release of azo dyes into the environment is of great concern due to the coloration of natural waters, the toxicity, the mutagenicity, and carcinogenicity (Oh et al., 1997; Li and Bishop, 2002, 2004). TiO₂ has received considerable attention for its capability to completely mineralize organic contaminants, which can not be effectively removed by conventional methods [18].

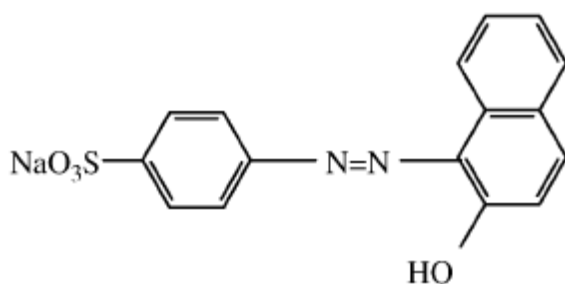


Figure 6.1 :Chemical structure of acid orange II [18]

7 Applications of TiO₂

Nano-technology in textiles and apparels is gaining increasing importance. Nano-technology uses structures that have at least one dimension that is nano-sized. Consequently, nano-technology improves the properties of materials due to such a small sizes. Nano particles have high surface area to volume ratio and have high affinity for fabric which leads to improve durability. Some of the finishing based on nano particles is found to maintain the breathability and soft hand. The most successful applications are UV protection, antibacterial and antistatic finishes as well as self cleaning property [14,27].

7.1.1 Antibacterial property

Nano-sized silver, titanium dioxide and zinc oxide are used to impart antibacterial properties on textiles. Metallic ions and metallic compounds display a certain degree of sterilising effect. Oxygen in the air or water is considered to become active oxygen relying on catalysis with the metallic ion, and dissolving organic substances to create a

sterilising effect. The number of nano-sized particles per unit area is increased, and thus antibacterial effects can be maximised.

Nano-silver particles are very reactive with proteins and have an extremely large relative surface area. When silver comes into contact with a bacteria, it will inhibit cell growth and multiplication. Titanium dioxide is a photocatalyst, when illuminated by light the e^-h^+ pairs will appear on the surface of the photocatalysts. The negative electrons and oxygen will combine into O_2 , the positive electric holes and water will bring hydroxyl radicals. These unstable chemical substances will combine with the organic compound and turn into carbon dioxide (CO_2) and water (H_2O). This cascade reaction is called oxidation reduction. A fabric treated with nano- TiO_2 could have effective protection against bacteria and the discolouration of stains, because of the photocatalytic activity of nano- TiO_2 . Zinc oxide is also a photocatalyst and has similar photocatalysis mechanism to that of titanium dioxide[14].

7.1.2 Self-cleaning

Nanocrystalline TiO_2 coating have received much attention because of its photocatalytic properties. It can chemically breakdown adsorbed organic contaminants in sunlight. Applications range from window glass, cement, textiles, more over self-cleaning paint is currently available in Europe. Self-cleaning window glass has made an impact with several multinational glazing companies marketing products. Recently other TiO_2 based self-cleaning products such as ceramics and plastics have become commercially available. Nanoscaled particles contained in these products can decompose organic contaminants and kill bacteria adhering to the surfaces under UV irradiation[13].

There are certain properties that should be considered when applying TiO_2 film to soft fibrous substrates such as textiles and garments. The first requirement, titania layer must be very thin and flexible so that the soft hand feel of the textile will not be adversely affected. Second, the titania film must adhere strongly to the textile substrate because textiles are often subjected to frequent washing. Third, the coated titania films must be optically transparent and colourless so as not to affect the original colour of the textile substrate [12]. Most importantly the mechanical properties such as tensile strength and tearing strength of the treated fabrics, as well as the breathability should be maintained.

TiO₂ could generate highly oxidative radical species (OH₂• –HO•) and oxidants (H₂O₂) form oxygen and water vapour under light irradiation. These reactive substances are able to discolour partially or totally organic stains like wine, coffee, curry stains and make-up. Cotton and polyester fabrics have also been treated with TiO₂ to obtain self-cleaning fabrics and textile. A single phase anatase-coated polyester studied by John H. Xin where fibers are pretreated with low-temperature oxygen plasma which shows significant improvement in self-cleaning performance under simulated day light irradiation. The adhesion between TiO₂ layers and polyester substrate is improved by plasma treatment. The UV absorption of titanium-coated polyester is significant enough to promote excellent UV protection to polyester [14].

7.1.3 UV protection

Nano-particle with a larger surface area per unit mass and volume leads to an increase of the effectiveness of blocking UV radiation. According to Rayleigh's scattering theory, the optimum particle size to scatter UV radiation between 200 and 400nm will be between 20 and 40nm. Inorganic UV blockers are better than organic UV blockers because they are non-toxic and chemically stable under exposure to high temperatures and UV. TiO₂, ZnO, SiO₂ and Al₂O₃ are usually used for inorganic UV blockers, TiO₂ and ZnO are commonly used. Nano-sized TiO₂ and ZnO are more efficient at absorbing and scattering UV radiation than the conventional size and are better able to block UV. The sol-gel method can be used on UV-blocking treatment for cotton fabrics. A thin layer of TiO₂ formed on the surface of cotton fabric which presents excellent UV-protection, the effect can be maintained after 50 home launderings [9].

7.1.4 Self-cleaning property of cotton

The incorporation of titania nanoparticles with cellulose or cotton surfaces has been reported to produce a self-cleaning phenomenon. The development of permanent self-cleaning cotton textiles with a life cycle of 25–50 washings or more is an objective sought by the textile industry in the framework of new products classified as intelligent textiles. Such a product could have applications in the European (EU) market of about 14 million meters of textiles per year. Cellulose is the most abundant and widespread biopolymer on the Earth [29]. Owing to its abundance, biodegradability and some physical properties (high moisture adsorption, softness, high strength, etc.), cellulose is a

very important renewable resource for the development of environmentally friendly, biocompatible and functional materials, as opposed to its traditional and massive use in papermaking and cotton textiles [10,7].

Cellulose fibers present a polar surface associated with the hydroxylated nature of cellulose constituting of the anhydroglucose units. Such a feature is responsible for the high hydrophilicity of cellulose, enabling the establishment of strong hydrogen bonding between fibers and the formation of three-dimensional fiber-based structures. On the other hand, the presence of these hydrophilic groups can promote the nucleation and growth of inorganic phases, such as TiO_2 and ZnO , at the cellulose fiber surfaces, thus allowing the production of nanocomposites with antimicrobial, UV blocking and unique infrared radiation properties. Several studies have reported that TiO_2 coating of cotton textiles could be performed using different pretreatments and techniques such as RF-plasma, MW-plasma, UV-irradiation, dip-pad-dry-cure and dip-coating. One way to graft nano TiO_2 on cotton fabrics is achieved by using the cross-link agent reported by Chen and Wang. The cross-link agent needs to have at least two free carboxylic groups to be able to bind both cotton and TiO_2 . The cross-link agent is introduced by the formation of a covalent ester bond. This implies esterification of one carboxylic group of the cross-link agent by a hydroxyl group of cellulose. The second cross-link agent carboxylic group is meant to attach TiO_2 by an electrostatic interaction. TiO_2 presents a strong electrostatic interaction with carboxylic group (Figure 7.1) [14].

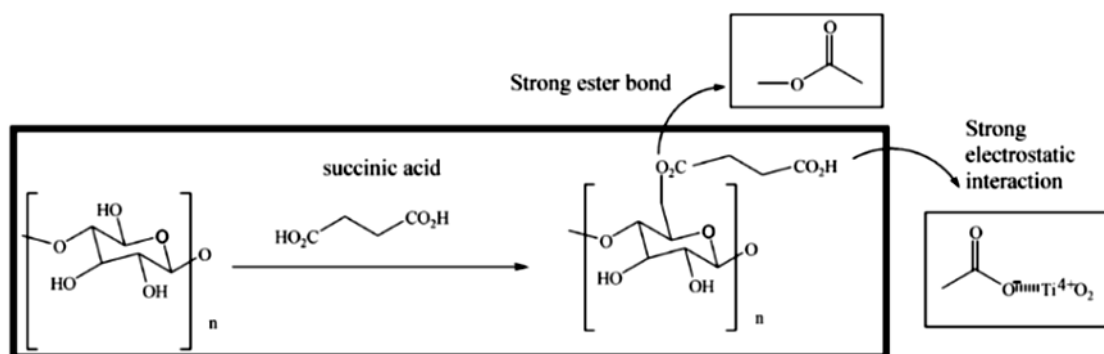


Figure 7.1: Electrostatic interaction of succinic acid with carboxylic group [14]

7.1.5 Self cleaning properties of polyester

Polyester is one of the most resistant low cost fabrics that have been coated for different uses by TiO_2 . This textile presents a large surface area making it suitable as a substrate for photocatalytic applications. The polyester fabrics are flexible and stable materials produced in large quantities. In recent years, the modification of textiles by TiO_2 aiming at pollutant degradation and self-cleaning processes has also been reported on polyester. This polyester presents a large surface area making it suitable as a substrate for photocatalytic applications [26].

7.2 Practical applications of TiO_2 photocatalysis

In Fig 7.2 the main areas of activity in titanium dioxide photocatalysis are shown. As already mentioned, in the last 10 years photocatalysis has become more and more attractive for the industry regarding the development of technologies for purification of water and air [26].

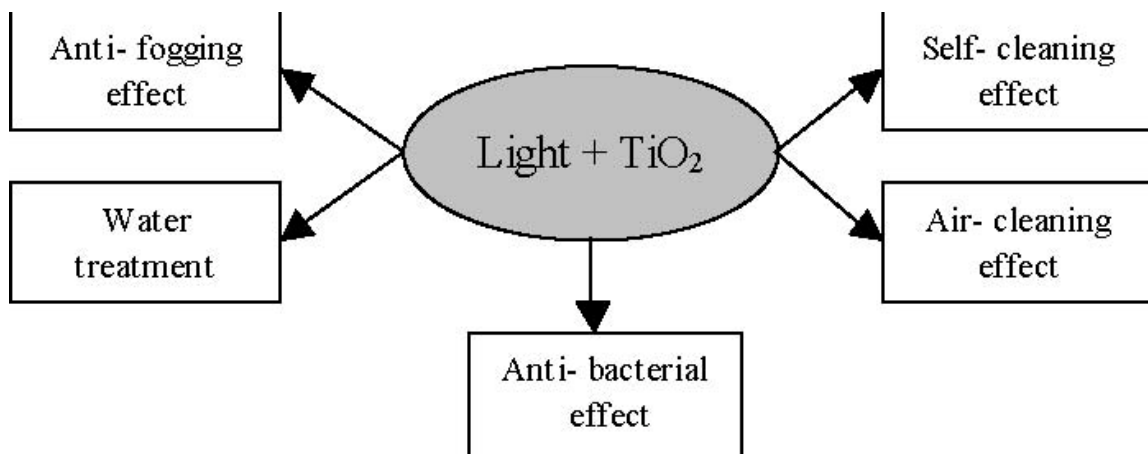


Figure 7.2: Major areas of activity of titanium dioxide photocatalysis [26]

8 Analytical methods -TiO₂ coating of cotton textiles using different pretreatments and techniques

8.1 Sol-gel method

A sol-gel process is an important method for preparing inorganic oxide-modified textiles. Hribernik et al grew a layer of silica on the surface of a regenerated cellulose fiber via a sol-gel process and studied the flame retardant activity of the coated regenerated cellulose fibers. Abidi et al modified lightweight cotton fabrics with titania and titania-silica nanosol for improved UV radiation protection. Wang et al reported a low-temperature growth approach for growing hexagonally oriented ZnO nanorod arrays onto cotton fabrics. The treated cotton fabrics provided an excellent UV protection[13]. In a typical sol- process, a colloidal suspension or a sol is formed due to the hydrolysis and polymerization reactions of the precursors, which on complete polymerization and loss of solvent leads to the transition from the liquid sol into a solid gel phase. This can be used to produce thin coating/films on textile substrated using dip coating. The wet gel fil, can be converted into anatase nano-crystals with further drying and hydrothermal treatment [16].

8.1.1 RF plasma

It is well known that low pressure plasma systems provide high stability and control of properties, but these devices also require expensive vacuum pumps and complex handling of textile materials. This can be avoided by applying the systems operating at atmospheric pressure (corona discharge and dielectric barrier discharge). Meji'a et al. demonstrated that fabrics pre-treated by air RF plasma at atmospheric pressure were able to bind TiO₂ due to the extreme localized heating of cotton (Meji'a et al. 2009). Corona discharge has an advantage of operating at atmospheric pressure where the reagent gas is ambient air. Corona discharge at atmospheric pressure and air RF plasma for deposition of colloidal TiO₂ nanoparticles at low pressure can be efficiently exploited for the activation of cotton fiber surface prior to deposition of colloidal TiO₂ nanoparticles [29].

8.1.2 MW-plasma

MW-plasma in air (air- MW-Plasma) is a process used to oxidize the cotton surface. The pretreatment time can be varied between 5 and 45 s and usually 120 °C is not exceeded. This is below the temperature of 180 °C the upper limit for cotton textiles. The ionized gas is composed atomic oxygen, ionic forms of oxygen (negative and positive), radicals formed due to the interaction of O-excited species and residual water vapor [21].

8.1.3 UV irradiation

The UV light excites electrons from the valence to the conduction band of the semiconductor catalyst, leaving holes behind. The electron–hole pairs can initiate redox reactions with surface species. UV light is light with a wavelength shorter than that of visible light. Electromagnetic radiations of wavelength between 150 and 400 nm are termed as Ultraviolet rays with energies from 3 eV to 124 eV. UV light is more energetic than visible light and has a shorter wavelength, letting it penetrate more readily through obstacles [1]. When TiO₂ is irradiated with UV light at ambient temperature it lead to the degradation of organic materials.

8.1.4 Dip-pad-dry-cure

TiO₂ finishing on white cotton fabrics has been reported which be done through a dip-pad–dry-cure process. The cleaned cotton fabrics were firstly dipped in TiO₂ sol for 1 min and padded with an automatic padder with a fixed nip pressure to standardize the amount of TiO₂ on each of the cotton substrates (wet pick-up is about 70%). The substrates were then dried at 80 °C for 5 min in a preheated oven (and finally cured at 120 °C for 3 min in a preheatedcuring machine [13].

8.1.5 Dip-coating

The incorporation of TiO₂ particles into the structure of nonwoven polyester fabric can be realised by dip-coating the fabric with a water dispersion containing 3% wt. of unmodified or modified TiO₂, poly(ethylene glycol) as a wetting agent in the amount of 10% wt. and hydroxyethylcellulose as a thickening agent [22].

8.1.6 Cross-linking

One way to graft nano TiO_2 on cotton fabrics is achieved by using the cross-link agent reported by Chen and Wang . The cross-link agent needs to have at least two free carboxylic groups to be able to bind both cotton and TiO_2 . The cross-link agent will be introduced by the formation of a covalent esterbond. This implies esterification of one carboxylic group of the cross-link agent by a hydroxyl group of cellulose. The second cross-link agent carboxylic group is meant to attach TiO_2 by an electrostatic interaction. TiO_2 presents a strong electrostatic interaction with carboxylic group [14].

9 Experimental Methods and Procedures

9.1 Aim

The aim of this research is to determine the photocatalytic properties of TiO₂ nanoparticles . The experiment was done to determine:

1. The effect of using the oxymetric method for testing photocatalytic properties of TiO₂ nanoparticles.
2. The effect of the oxymetric method on testing target chemicals such as a saccharide and textile dye .
3. The effect of using the oxymetric method for testing the oxygen concentration on cotton and polyester cotton textile samples.

9.2 Materials

9.2.1 Chemicals

1. Acid orange II , purchased from Synthesia –Pardubice
C.I. Acid Orange 7, chemical class -Azo
2. Normal white sugar
3. White woven TiO₂ coated cotton and polyester samples purchased from Inotex, spol. s r.o. .

Structure of cotton is a woven S twill 3/3, and the polyester woven structure is a plain weave 1/1

9.2.2 Catalyst used

1. TiO₂P25 Degussa, was purchased from Degussa Company, Germany. It has a BET surface area of $50 \pm 15 \text{ m}^2\text{g}^{-1}$ and is 70% in anatase crystal form with average particle size of 30 nm.

9.2.3 Equipment and Instruments

1. Dissolved oxygen pocket meter - Oxi 315i, robust, water-proof, battery-operated hand held dissolved oxygen meter with temperature compensation. The simplified keypad helps to prevent operating errors. AutoRead enables reproducible results. Automatic calibration.



Figure 9.1: Dissolved Oxygen pocket meter - Oxi 315

2. Dissolved oxygen sensor –CellOx®325, Galvanic Dissolved Oxygen Sensor which measures dissolved oxygen concentration.



Figure 9.2: Dissolved oxygen sensor –CellOx®325

3. UV box- UV N36K Flächenstrahler, watt 4x 6, Volt 220 V, was used to irradiated the TiO₂ suspensions and textile samples. Aqueous solutions irradiated with

ultraviolet light (UV) at 13.5 °C. The process carried out using TL[®] 6W /05 Philips fluorescent lamps with UV irradiant intensity of 3120 $\mu\text{W}/\text{cm}^2$.The irradiation time of experiment was 120 and 60 minutes .

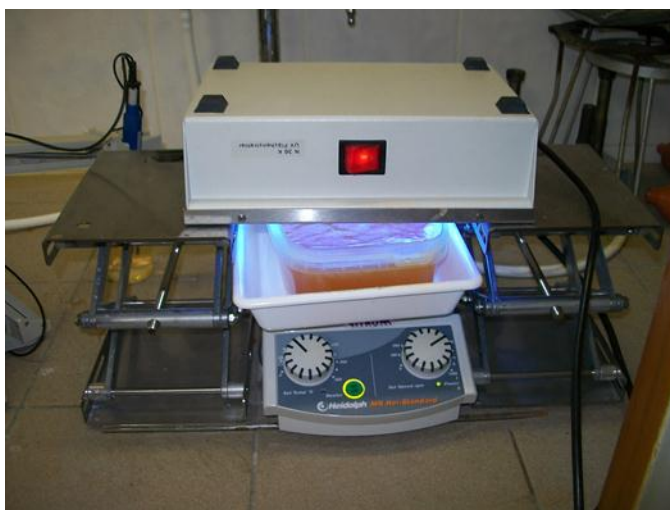


Figure 9.3:UV box

4. UV/Vis spectrophotometry, a Helios Epsilon ThermoFischer Scientific spectrophotometry for electronic absorbance measurements. The system was switched on and warmed up, the spectrophotometry was calibrated with water.



Figure 9.4: UV/vis spectrophotometry

5. Vitrum Centrifuga EBA20, centrifuges solution at high speed. The speed can be as high as 6000 rpm.



Figure 9.5 Vitrum centrifuga

6. JULABO thermostat- has a circulation thermostat for temperature control loop for internal or external circulation thermostats. JULABO bath with stainless steel set for internal and external temperature has an LED display for actual temperature and setpoint temperature display accuracy 0.1 ° C. The keypad is used to enter the set value protected by a film, with automatic return to the display of the actual value.



Figure 9.6 Julabo thermostat

7. Bandelin ultrasonic homogeniser , ultrasonic homogenizers are typically used for ultrasonic disruption. This helps in the reduction of hard particles and/or agglomerates of TiO_2 . The process was carried for 60 seconds at ultrasonic capacity of 50 KHz. The homogenization is based on cavitation. During this implosion very high pressures and high speed liquid jets are generated locally. The resulting currents and turbulences disrupt particle agglomerates and lead to violent collisions between individual particles.



Figure 9.7: Bandelin ultrasonic homogeniser

8. Experimental set up ,the Julabo thermostat is connected to the cooling pot. The dissolved oxygen sensor is immersed into the reaction mixture with the stirrer . The UV box was placed above of the pot using the supporting stands.



Figure 9.8 :Experimental set up



Figure 9.9 : Experimental set up

9.3 Method

9.3.1 Experiment 1

9.3.1.1 Testing of oxymetric method to observe the influence of concentration of acid orange II in an open system

Photocatalytic degradation of dye Acid orange II was studied with P25 TiO_2 catalyst by irradiating the aqueous solution with UV light over 120 minutes. The content of dissolved oxygen concentration was measured using an Oxi 315i meter (dissolved oxygen meter). TiO_2 photocatalyst was prepared at a concentration of 0.1g/l, acid orange II was prepared at 0.01mg/l. Acid orange II was selected as a model dyeing pollutant as Azo dyes are amongst the largest group of colourants used in the textile and paper industry. The TiO_2 powder was first dissolved in about 10 ml of water and ultrasonically agitated since the photocatalyst would not dissolve properly by simple stirring. The experiment was prepared in a metal pot in an open system. The metal pot worked as a cooling system where water runs in and out of the pot connected to the tap of running water in order to stabilise the temperature. The reaction mixture was stirred at 500 rpm between each measurement interval to prevent TiO_2 from settling in the pot. Each photocatalytic experiment was repeated four times and the results are plotted as an average of the four experiments.

Spectrophotometric absorbance measurements were measured at each time interval, by taking out 15 ml of the solution and placing them in the dark cupboard so that light will not cause further photocatalysis. The absorbance at 0 minute was measured in the absence of UV radiation and placed in a dark cupboard. The solution of acid orange with TiO₂ nanoparticles was centrifuged at 6000 rpm for 20 minutes before the absorbance measurements were taken at 486 nm. TiO₂ nanoparticles settle after some time as a result they result in scattering on the quartz cuvettes. The absorbance was plotted as an average of four repeated absorbance measurements.

9.3.1.2 Testing of oxymetric method to observe the influence of concentration of acid orange II in a open and closed system

Photocatalytic degradation of dye Acid orange II was studied with P25 TiO₂ catalyst by irradiating the aqueous solution with UV light over 60 minutes. The content of dissolved oxygen concentration was measured using an Oxi 315i meter. TiO₂ photocatalyst was prepared with the sugar at 0.2, 0.1, and 0 g/l of TiO₂, acid orange II was prepared at 0.01 mg/l. The temperature of the system was only stabilised by the water cooling system where water runs in and out of the pot connecting to a running tap of water.

The first experiment was not covered to make the experiment an open system and the second experiment was prepared in a metal pot covered by a polyethylene plastic film to make it a closed system so that the oxygen from the outside environment would not interfere with the level of oxygen of the reaction. The reaction mixture was stirred at 500rpm between each measurement interval to prevent TiO₂ nanoparticles from settling in the pot. Each photocatalytic experiment was repeated two times and the results are plotted as an average.

9.3.2 Experiment 2

9.3.2.1 Measurement of photocatalytic activity of TiO₂ photocatalyst with a saccharide (sugar) showing a temperature dependent system

The photocatalytic activity of TiO₂ suspension was tested by measuring the concentration of oxygen. White normal sugar of 0, 1 g/l was dissolved into 0.2, 0.1 and 0 g/l of TiO₂. The TiO₂ and sugar solution was irradiated with UV light over 60 minutes, and the

content of dissolved oxygen concentration was measured using an Oxi 315i. Two experiments were conducted; the first experiment was conducted with the water cooling pot to stabilize the temperature. The second experiment was conducted with the same concentrations under the temperature stabilization by using Julabo thermostat. The Julabo thermostat stabilized the temperature at 13.5°C which was taken as an average from the previous experiments which were conducted. Each photocatalytic experiment was repeated two times

9.3.2.2 Testing of photocatalytic activity of TiO₂ photocatalyst with a saccharide (sugar) using the oxymetric method

The photocatalytic activity of TiO₂ was tested by measuring the concentration of oxygen. White normal sugar of 0.1 g/l was dissolved into 0.2, 0.1 and 0 g/l of TiO₂ powder. The TiO₂ and sugar solution was irradiated with UV light over 60 minutes. The temperature of the reaction system was stabilized at 13,5 °C by the Julabo thermostat connected to the metal pot where water runs in and out of the pot. The reaction mixture was stirred at 345 rpm between each measurement interval. Each photocatalytic experiment was repeated two times.

9.3.3 Experiment 3

9.3.3.1 Observation photocatalytic activity using white TiO₂ coated cotton and polyester textile samples using the oxymetric method

White cotton and polyester samples coated with TiO₂ nanoparticles purchased from Nikato spol, s.r.o in Czech Republic were used. The samples were cut into a square and positioned on the metal pot by metal sieve. The cotton structure samples are an S twill 3/3 and the polyester samples is a plain weave 1/1. The concentration of the samples is not known the samples are given special codes so as to protect the company's recipe. The samples have a silicone polymer supporting the titanium nanoparticles which vary in the ratio of silicone to TiO₂ ratio. Irradiation of the samples was carried out in the cavity of the pot, with cooled water at 13.5 °C cooled by the Julabo thermostat. Sugar solution of concentration 0.1 g/l was prepared the solution and the textile sample was irradiated for

60 minutes under UV light. The dissolved oxygen concentration was measured using an Oxi 315i meter in a closed system, the solution was stirred at 245 rpm. Different codes of the cotton and polyester samples were tested as shown in the table below.

Table 9.1 : Description (codes) of the samples

Cotton	Polyester
4AE3CO	4AE3 PES
4AD3CO	4AD3 PES
4A2CO	4A2 PES
4AH3 CO	4AH3 PES
4AF3 CO	4AF3 PES
Cotton without TiO ₂	PES without TiO ₂

9.3.3.2 Self-cleaning of cotton textile modified with TiO₂ P25 Degussa

Self-cleaning is one of the properties of titanium dioxide nanoparticles. Four cotton samples were stained one drop of with coffee and red wine. The red wine is a product of Lambrusco rosso produced in Italy with a concentration of 7.5% alcoholic volume. Nescafe classic coffee 100g made of 100% Arabica beans, 200 mg per 100ml was used one teaspoon was dissolved in 100 ml of water. Two cotton samples 4A2 with TiO₂ nanoparticles and two samples of cotton without TiO₂ nanoparticles were stained. Four samples were exposed to the solar radiation for 1 day and four samples were kept in a dark place. After the exposure the sample were washed at 40°C with water.

9.4 Results and Discussion

9.4.1 Testing of oxymetric method to observe the influence of concentration of acid orange II in an open system -Experimental part 1

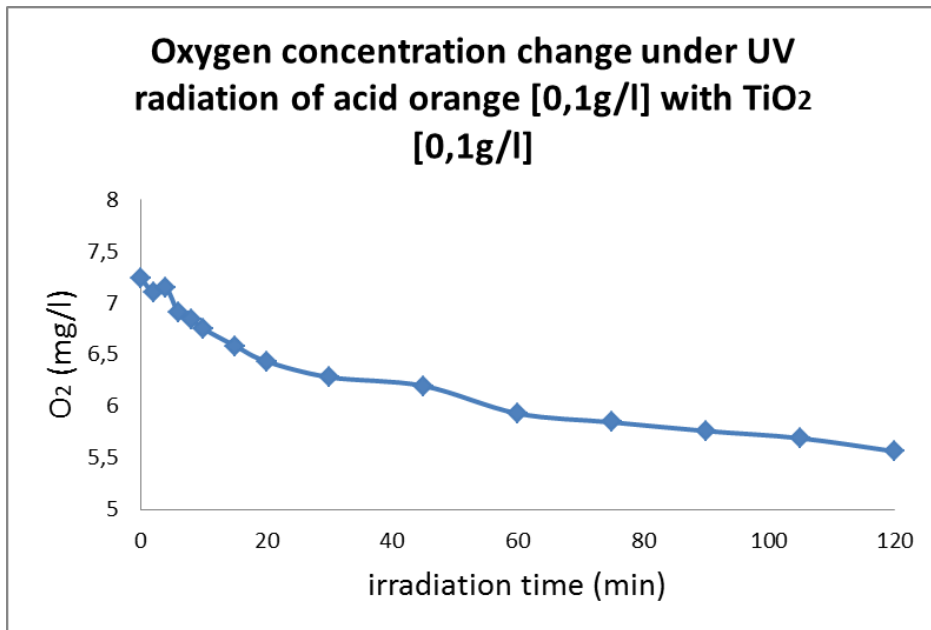


Figure 9.10 : Decrease of oxygen concentration during degradation of acid orange II in the presence of TiO₂

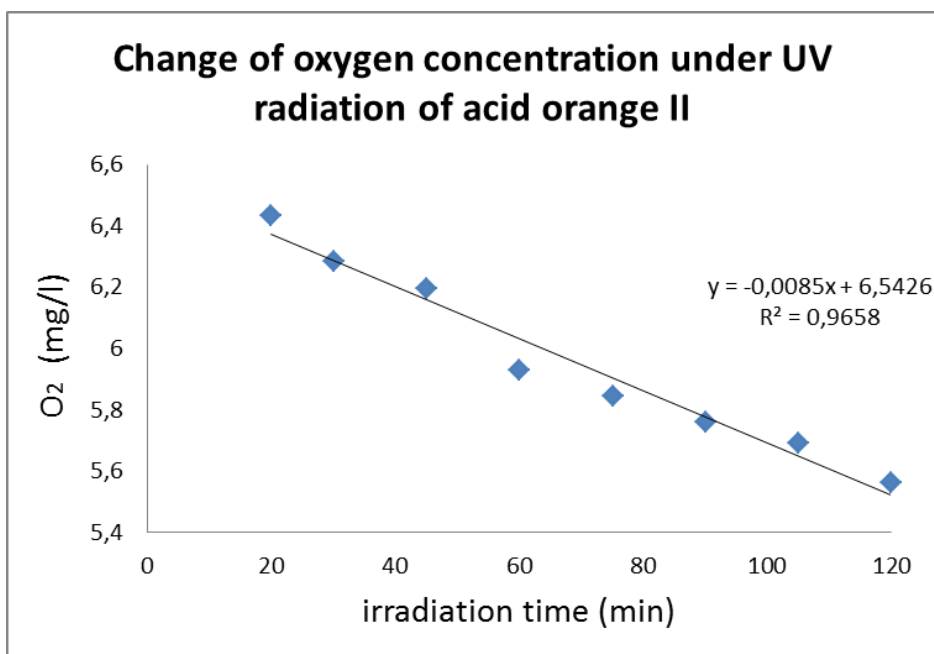


Figure 9.11: Linear regression showing decrease of dissolved oxygen during acid orange II degradation [0.01g/l] with TiO₂ [0.1g/l]

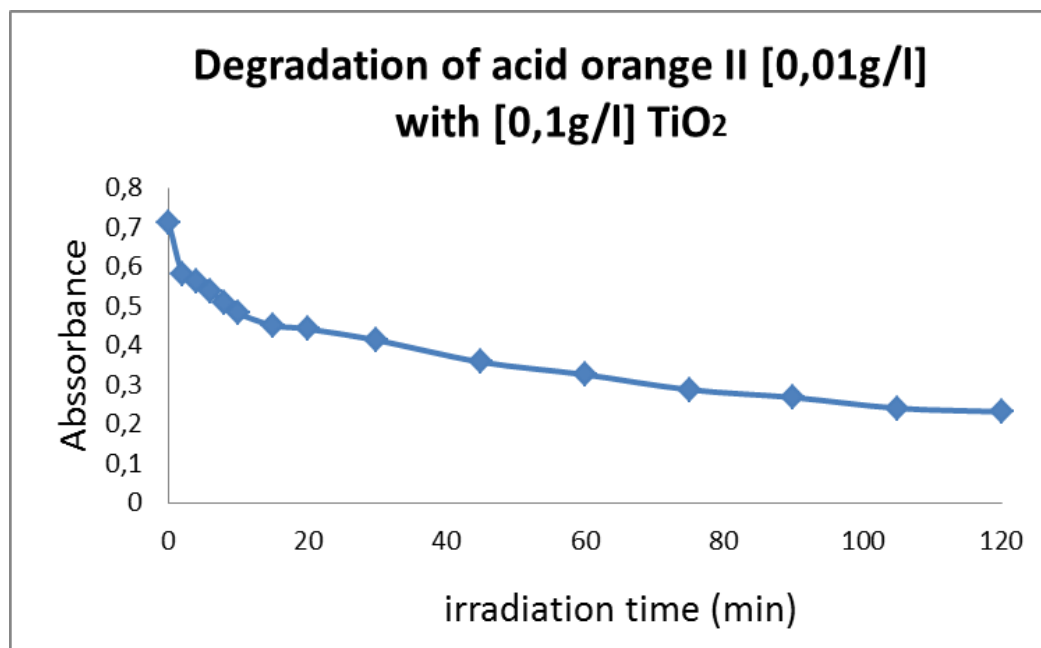


Figure 9.12: Absorbance decrease at 485 nm showing some decolourization of acid orange II under UV light in the presence of TiO₂

Fig 9.10 and Fig 9.11 show a kinetic model experiment which shows that the rate of photocatalytic degradation depends on several factors including illumination intensity, catalyst type, oxygen concentration, stirring of the solution, and the concentration of organic reactant acid orange. The solution was irradiated for 120 minutes it was found that the oxygen concentration decreases as well the absorbance curve in Fig 9.12. The absorbance results shows that there is some degradation of acid orange II to some extent resulting in a slight colour change. The absorbance was measured at 486 nm because that is where acid orange absorbs in the spectrum. With UV radiation of the photocatalyst highly oxidizing radicals are produced, these radicals react with the dye to produce colourless products. The colourless products can react further forming other intermediate colourless products.

The linear regression shows clearly the decrease of the dissolved oxygen concentration in the system. The results show that photocatalytic treatment of the acid orange–TiO₂ system with visible light irradiation may lead to oxidative fragmentation of the dye molecule mainly attacking the nitrogen double bond resulting to colorless compounds of progressively lower molecular weight and, eventually, to CO₂, water and inorganic ions.

A first order rate of reaction for the degradation of acid orangeII is proposed. If the amount of dye concentraion C_D is decreasing at a rate that is proportional to the intensity of radiation $I_{(UV)}$, the amount of concentration C_D remaining in the system, then the rate of the decrease of concentration C can be described as:

$$\frac{dC_D}{dt} = I_{(UV)} \cdot \frac{C_{(D)} \cdot K_D}{C_{(D)} \cdot K_D + C_{(CLP)} \cdot K_{CLP}} \quad (16)$$

where k is the rate constant, C_D is the concentration of the dyestuff

$I_{(uv)}$ is the intensity of the UV light, C_{CLP} is the concentration of the colourless products at the begining of the radiation to end of radiation.

$$C_{CLP} = C_{D(t=0)} - C_{D(t)} \quad (17)$$

Therefore, with irradiation the dye oxidizing radicals are produced which attack the dye forming colourless products .

$$\frac{dC_D}{dt} = I_{(UV)} \cdot \frac{C_{D(t)}}{C_{D(t)} + (C_{D(0)} - C_{D(t)}) \cdot \frac{K_{CLP}}{K_D}} \quad (18)$$

However, the concentration of the dye stuff was not measured directly during the degradation, the degradation of dye was measured according to decrease of oxygen content. C_{O_2} is the concentration of oxygen. The ratio of the degradation of dye is the same to the decrease of oxygen in the system.

$$\frac{dC_D}{dt} = \frac{dC_{O_2}}{dt} \quad (19)$$

The equation is inverted to get an estimation of the the decrease of oxygen concentration

$$\frac{dt}{dC_D} \cong \frac{C_{O_2(t)}}{C_{O_2(t)}} + \frac{C_{O_2(0)}}{C_{O_2(t)}} - K \quad (20)$$

$$\frac{dt}{dC_D} \cong 1 + K \frac{C_{O_2(0)}}{C_{O_2(t)}} - K \quad (21)$$

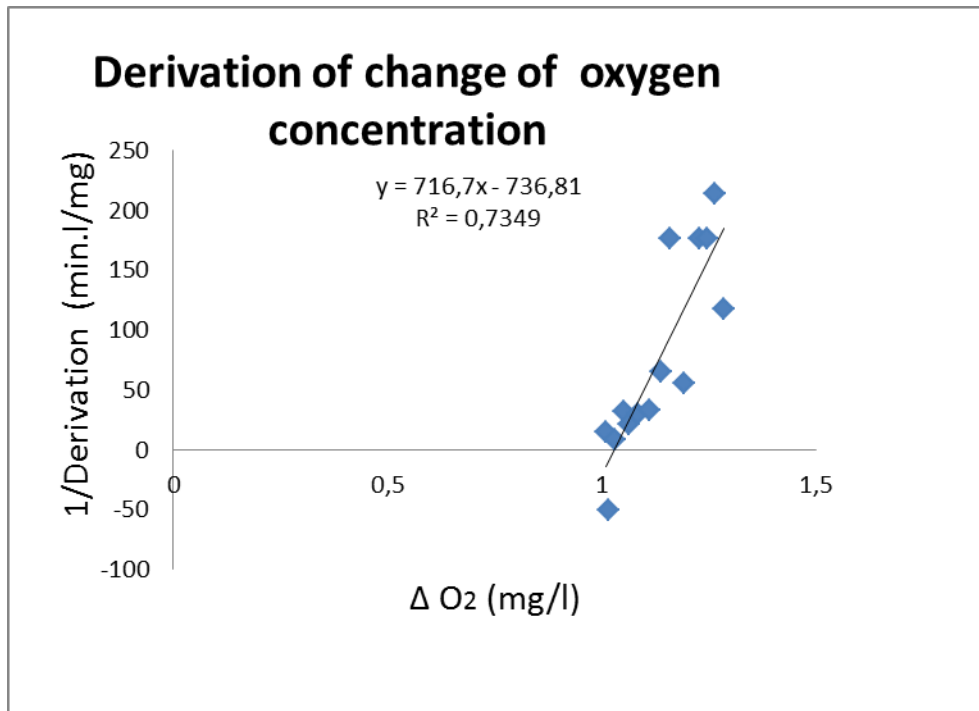


Figure 9.13: Derivation model of the change of oxygen concentration during degradation of dye acid orange II

Fig 9.13 show derivation model is a proposed model which shows the decrease of oxygen concentration with change in time resulting in the production of colourless products of the dye. It shows how quickly oxygen is removed from the system.

However the temperature of the reaction system was increasing with increasing degradation time due to the fact that the experiment was conducted in an open system. There is an influence of the outside environment which results in the diffusion of heat and oxygen from the outside environment to the reaction system. Hence as the temperature increases the concentration of oxygen in the system decreases because of this diffusion.

9.4.1.1 Testing of oxymetric method to observe the influence of concentration of acid orange II in a open system -Experimental part 1

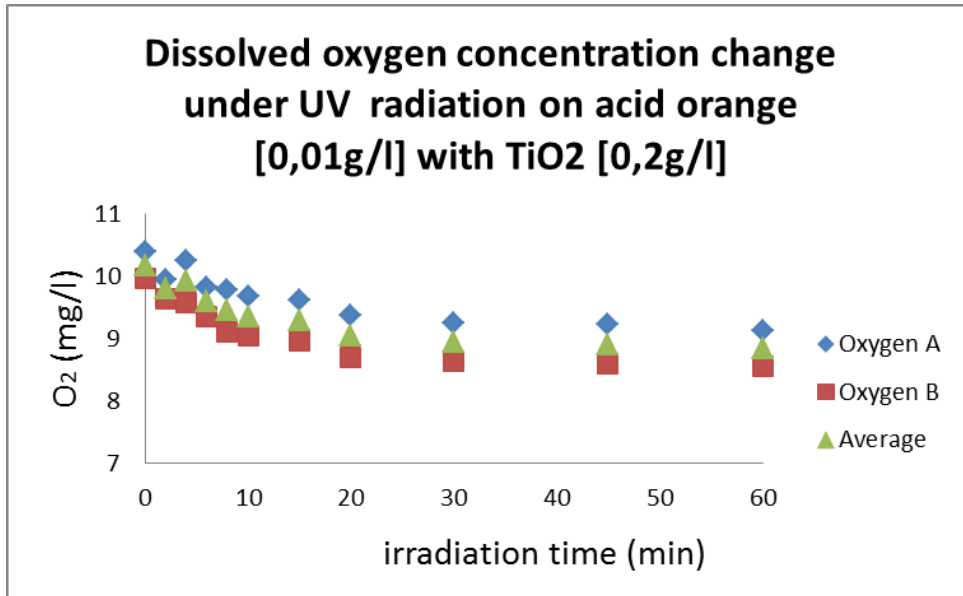


Figure 9.14 Photocatalytic degradation of acid orange II under UV light in the presence of TiO₂ in an open system

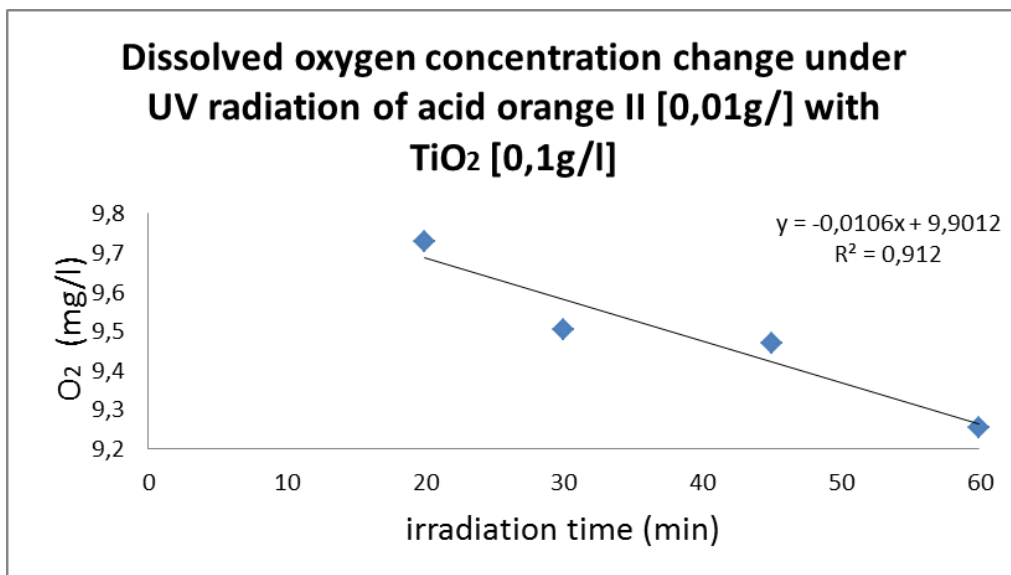


Figure 9.15 : Linear regression showing decrease of dissolved oxygen during acid orange II degradation [0.01g/l] with TiO₂ [0.1g/l] in a open system

Table 9.2 Linear regression results of acid orange with TiO₂ under UV light irradiation in a open system

TiO ₂ (mg/l)	Acid orange II (mg/l)	Decrease of oxygen (slope)	Correlation (R ²)
0.2	0.01	0.016	0.912
0.1	0.01	0.0043	0.9242
0	0.01	0.0146	0.9882

Figure 9.14 and Fig 9.15 show a high decrease of the oxygen concentration in an open system between 0.2 and 0.1 g/l of TiO₂ photocatalyst. The temperature of the reaction system was increasing with increasing degradation time due to the fact that the experiment was conducted in an open system. From the beginning of radiation the temperature of the reaction system temperature is low. As the radiation progressed the temperature increased because the reaction was conducted in an open system. There was an influence of the external temperature which results in the diffusion of heat and oxygen from the reaction. Hence as the temperature increases the concentration of oxygen in the system decreases because of this diffusion.

9.4.1.2 Testing of oxymetric method to observe the influence of concentration of acid orange II in a closed system- Experimental part 1

Fig 9.16 and Fig 9.17 show that the dissolved oxygen concentration in the system was decreasing fast from 0-20 minutes. From 20-60 minutes the amount of oxygen in the system was reaching stability. The experiment was conducted in a closed system where there was some oxygen available in the water with the progression of time the level of oxygen in the system decreased. This behaviour shows that photocatalytic oxidation reaction was taking place since photocatalysis of the semiconductor TiO₂ involves the photogeneration of strongly oxidising hydroxyl radicals when the catalyst TiO₂ is activated by UV light.

Table 9.2 show the change of dissolved oxygen concentration under UV radiation of TiO₂ with acid orange II at different concentrations. A higher dose of titanium dioxide show higher photocatalytic activity. In the absence of the photocatalyst the decrease in the dissolved oxygen concentration was minimal. Linear regression model was used to

show the relationship between oxygen and irradiation time. The linear regression was plotted from points of 20-60 minutes because this where the decrease in oxygen starts to stabilize.

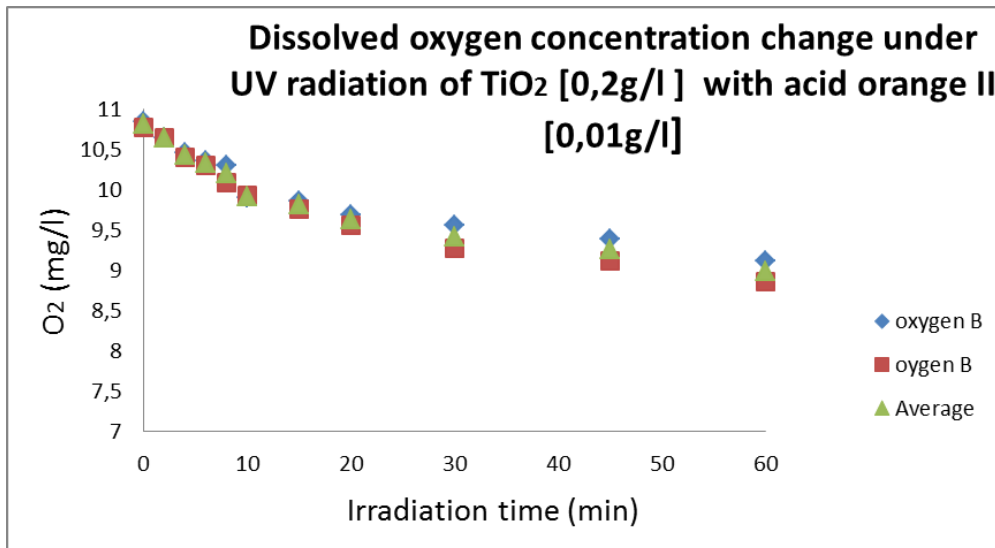


Figure 9.16: Photocatalytic degradation of acid orange II under UV light in the presence of TiO₂ in a closed system

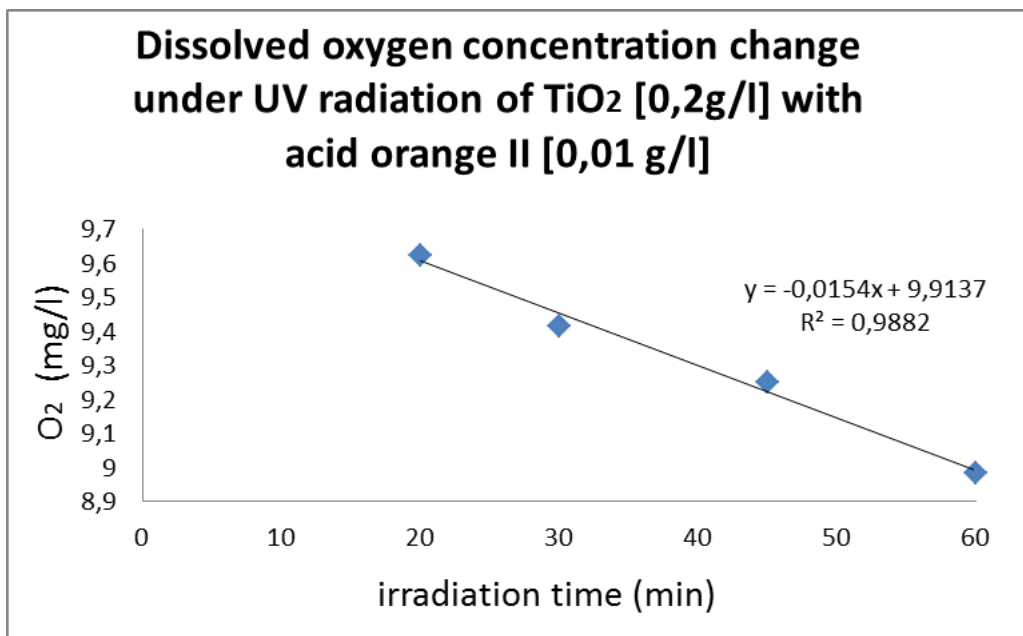


Figure 9.17: Linear regression showing decrease of dissolved oxygen during acid orange II degradation [0.01g/l] with TiO₂ [0.1g/l]

Table 9.3: Linear regression results of acid orange with TiO_2 under UV light irradiation in a closed system

TiO_2 (mg/l)	Acid orange II (mg/l)	Decrease of oxygen (slope)	Correlation (R^2)
0.2	0.01	0.0154	0.9882
0.1	0.01	0.0108	0.976
0	0.01	0.0019	0.99

It can be seen that the decrease in oxygen concentration in the closed system is minimal compared to the open system where there is an influence of diffusion with the external environment.

9.4.2 Temperature dependent system of photocatalytic activity of TiO_2 photocatalyst with a saccharide (sugar) -Experimental part 2

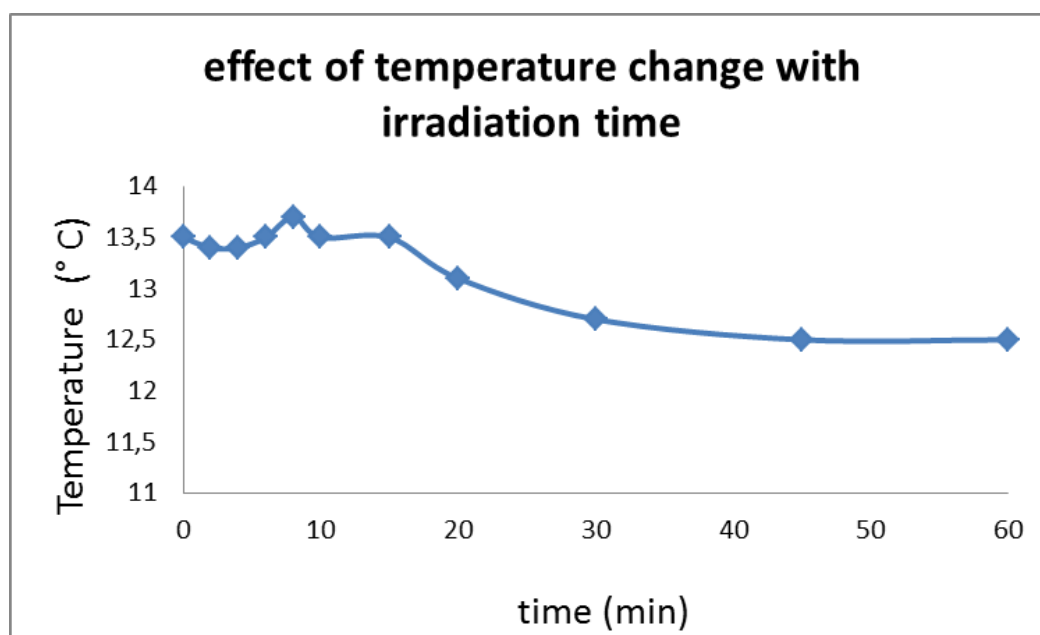


Figure 9.18: Change in temperature with irradiation in a closed system using a water cooling system

Fig 9.18 show an experiment performed with the cooling water pot system. These results show that the temperature was fluctuating with the irradiation time. This shows that the cooling pot with water was ineffective at stabilizing the temperature.

Fig 9.19 shows the same experiment which was conducted but the photo catalytic reaction was stabilized with the Julabo thermostat with a set point temperature display accuracy 0.1°C. The temperature was kept at 13.5°C which was taken as an average value based on the previous experiments that were conducted. Stabilization of the temperature during the photocatalytic experiment allows the system to cool down and the closed system prevents the influence of the external environment temperature and the removal of the oxygen from the system.

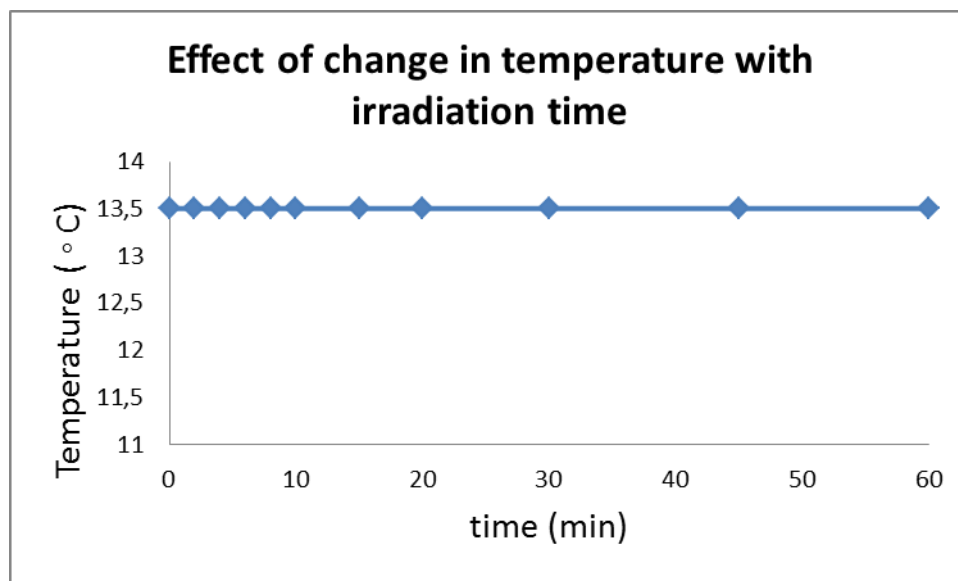


Figure 9.19 :Maintainance of tempearature 13.5°C using the Julabo thermostat in a closed system

9.4.2.1 Testing of photocatalytic activity of TiO₂ photocatalyst with a saccharide (sugar) using the oxymetric method -Experimental part 2

Fig 9.20 and Fig 9.21 show the decrease in the concentration of dissolved oxygen ater 60 mininutes of radiation. The sugar that was used as a target chemical into the TiO₂ suspension it did not have affect the amount of oxygen in the sytem. It has has a relatilvely low asbsorption in the spectrum, hence sugar is oxidised easily and dissolves easily in water.

The experiments were reapeated twice and the results plotted as an average. Linear regression model in table 9.4 was used to show the relationship between oxygen and irradiation time. The decrease in oxygen concentration is higher in the presence sugar

compared to the linear regression when sugar is absent in table 9.5. The linear regression was plotted from points of 20-60 minutes because this is where the decrease in oxygen starts to stabilize.

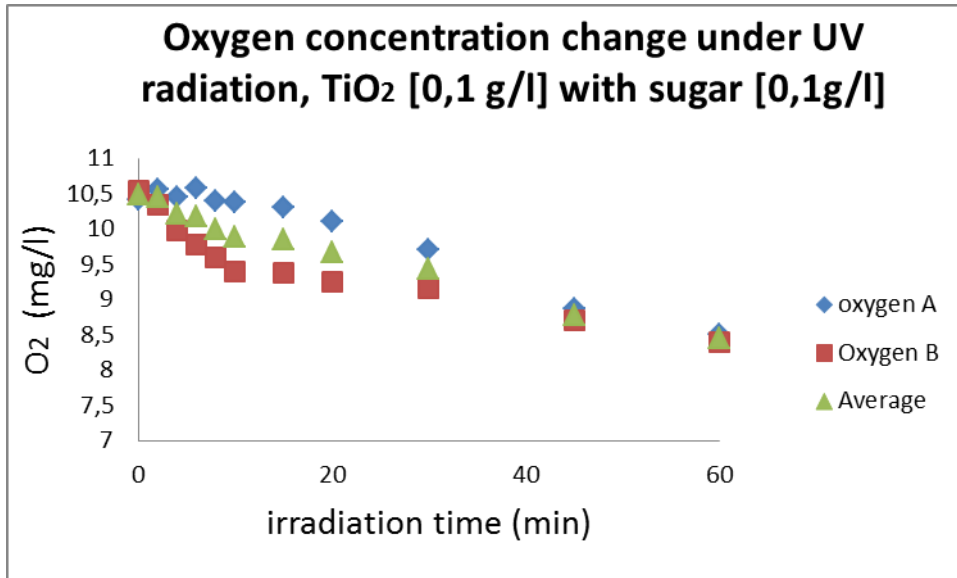


Figure 9.20: Decrease of dissolved oxygen of TiO₂ and sugar

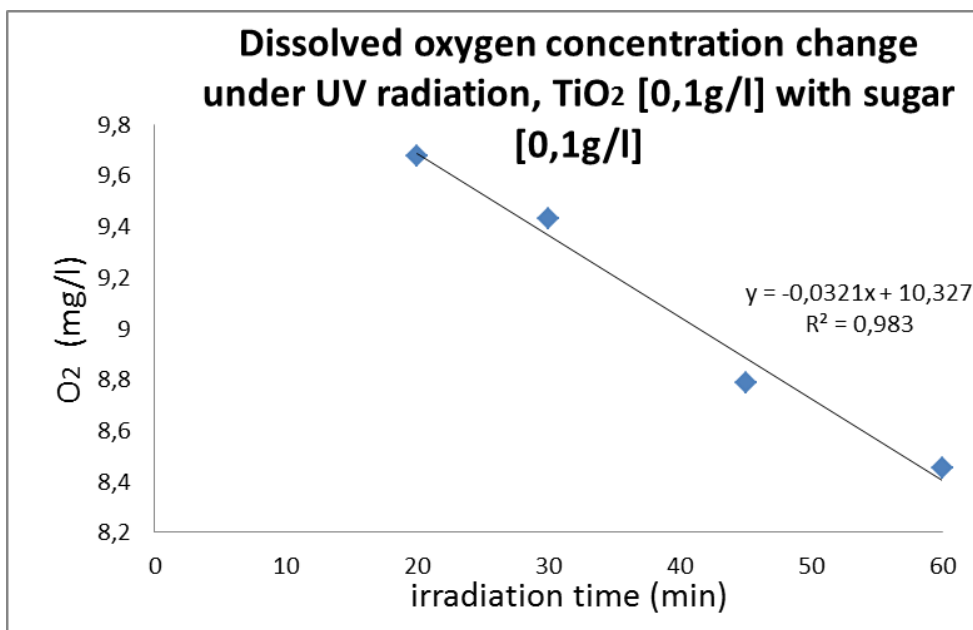


Figure 9.21: Linear regression showing decrease of dissolved oxygen TiO₂ with sugar

Table 9.4: Linear regression of TiO₂ and sugar irradiation under UV light

TiO ₂ (mg/l)	Sugar (mg/l)	Decrease of oxygen (slope)	Correlation (R ²)
0.2	0.1	0.0459	0.9635
0.1	0.1	0.0252	0.9776
0	0.1	0.0143	0.9653

Table 9.5 : Linear regression of TiO₂ in the absence of sugar irradiation under UV light

TiO ₂ (mg/l)	Decrease of oxygen (slope)	Correlation (R ²)
0.2	0.023	0.944
0.1	0.0299	0.9435
0	0.0147	0.9412

The linear regression results of photocatalysis in the presence of the target chemical sugar show a higher decrease of the oxygen concentration. The decrease can be contributed to the fact that sugar is easily oxidized in the presence of the titanium photocatalyst hence a oxidation chain reaction is initiated, more OH radicals are produced and more oxygen is scavenged during the reaction. In the absence of the target chemical the decrease of the oxygen concentration is rather lower.

The decrease of oxygen concentration in all the experiments which are in agreement with literature can be explained in terms of the heterogeneous photocatalysis. There exist several works in the literature, which mentioned that the primary oxidizing agent in the TiO₂ semiconductors were OH• radicals formed by reactions of with surface OH groups and electrons with adsorbed oxygen followed by and attack of water according to the reaction:



It is indicated that the presence of a large amount of OH groups on the surface of photocatalyst enhances O₂ adsorption and consequently, its increase photoreactivity. The oxygen provided within the reaction scavenges the generated electrons preventing the recombination of electrons and holes. However in this case the dissolved oxygen concentration was decreasing which could have been caused by the electron hole recombination. The electron hole competes with the photochemical oxidation process. In absence of a catalyst, the oxidation would proceed rather slowly. A photocatalyst decreases the activation energy of a given reaction.

9.4.3 Observation photocatalytic activity using white TiO₂ coated cotton and polyester textile samples using the oxymetric method Experimental part 3

Fig 9.22 shows the decrease of the dissolved oxygen concentration under irradiation of cotton sample 4AF3 coated with titanium nanoparticles. Fig 9.23 shows the linear regression model showing the relationship between time of irradiation and the decrease in oxygen in the system. The linear regression was plotted from points of 20-60 minutes because this where the decrease in oxygen starts to stabilize. This behavior also shows that photocatalytic oxidation reaction was taking place hence the decrease of dissolved oxygen.

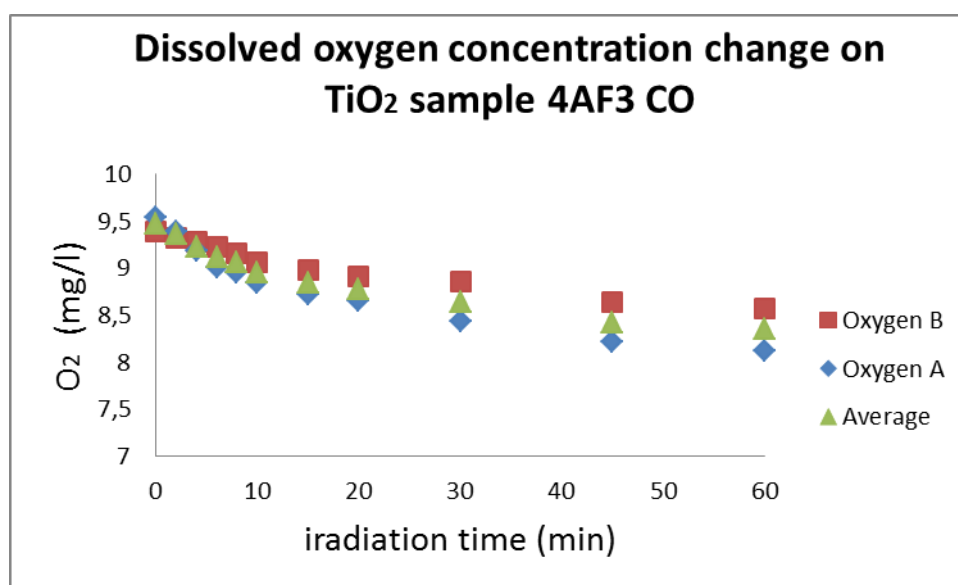


Figure 9.22 : Oxygen concentration behavior as a function of time under UV irradiation

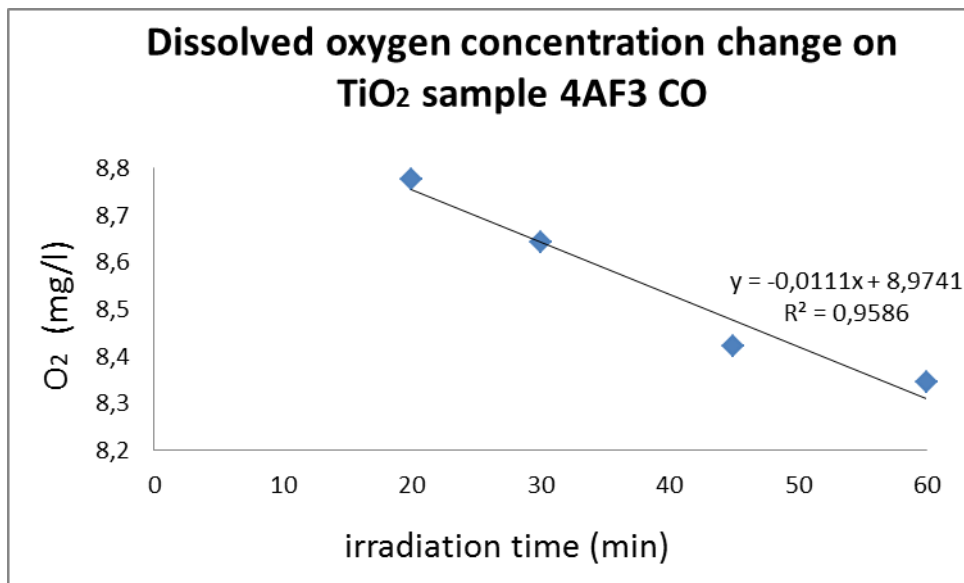


Figure 9.23: Oxygen concentration decrease as a function of time under UV irradiation

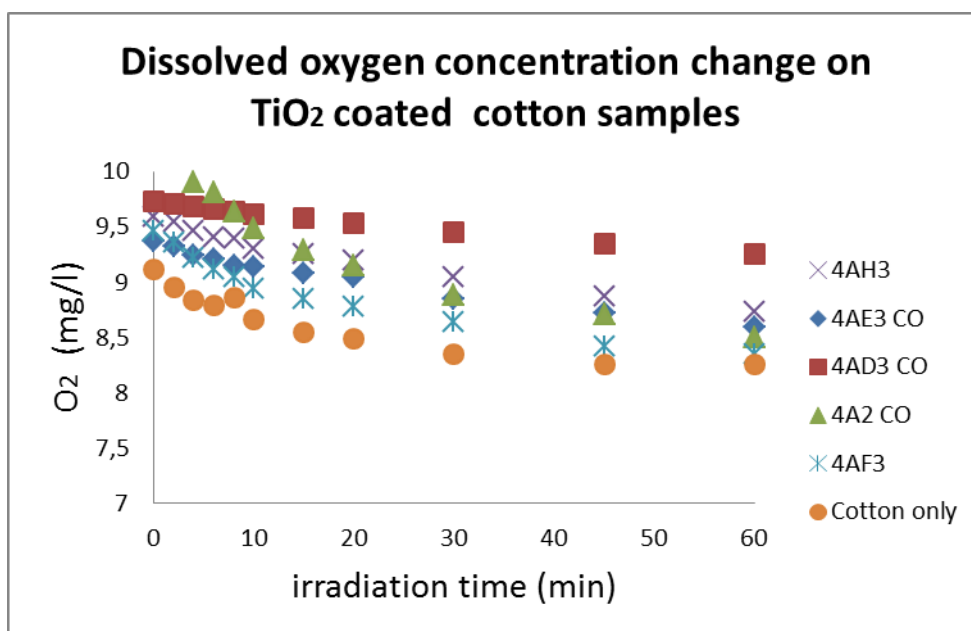


Figure 9.24: Oxygen concentration behavior as a function of time under UV irradiation of cotton samples

Fig 9.24 also shows the same relationship of the used cotton samples. Cotton sample 4AD3 has a higher photocatalytic activity compared to the other cotton samples. The cotton without TiO₂ nanoparticles has the lowest photocatalytic activity which is in agreement because it was not coated with nanoparticles.

Table 9.6: Dissolved oxygen concentration change under UV radiation of cotton samples coated with TiO₂

Cotton samples coated with TiO ₂	Sugar (mg/l)	Decrease of oxygen (slope)	Correlation (R ²)
4A2CO	0.1	0.0156	0.9851
4AH3 CO	0.1	0.0114	0.9906
4AF3 CO	0.1	0.0111	0.9586
4AE3 CO	0.1	0.0108	0.9581
4AD3 CO	0.1	0.0069	0.9965
Cotton without TiO ₂	0.1	0.0056	0.8108

9.4.4 Experimental part 3 - Observation photocatalytic activity using white TiO₂ coated polyester textile samples using the oxymetric method

Fig 9.25 shows the decrease of the dissolved oxygen concentration under UV irradiation of 4A2 polyester sample coated with titanium nanoparticles. Fig 9.26 shows the linear regression model showing the relationship between time of irradiation and the decrease in oxygen in the system. The linear regression also shows photocatalytic behavior hence the decrease of dissolved oxygen. Fig 9.27 also shows the decrease of the oxygen concentration with UV irradiation all the polyester samples. Polyester sample 4AE3 has a higher photocatalytic activity compared to the other samples, and polyester sample without titanium dioxide nanoparticles had the lowest photocatalytic activity compared to the rest of the samples.

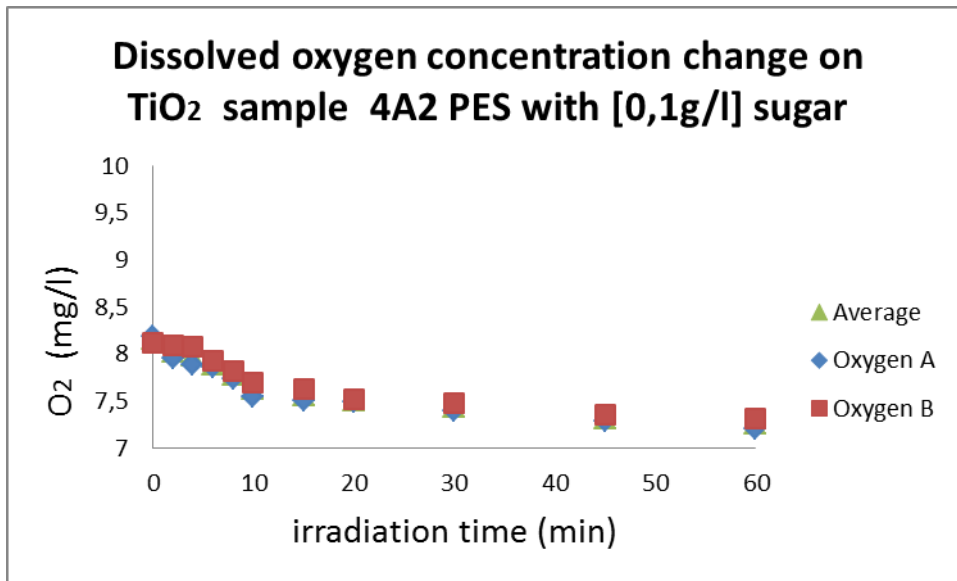


Figure 9.25 : Oxygen concentration behavior as a function of time under UV irradiation

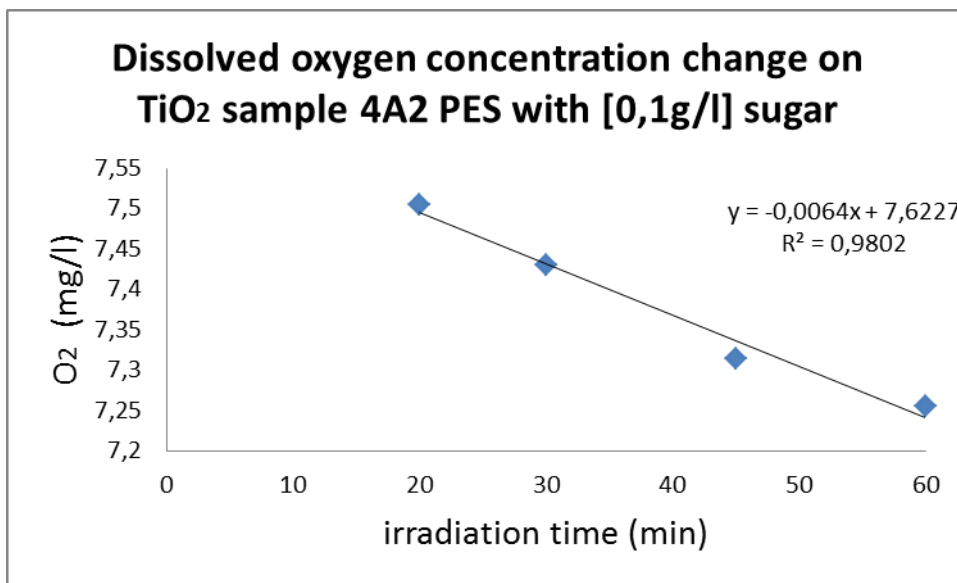


Figure 9.26 : Oxygen concentration behavior as a function of time under UV irradiation of polyester sample

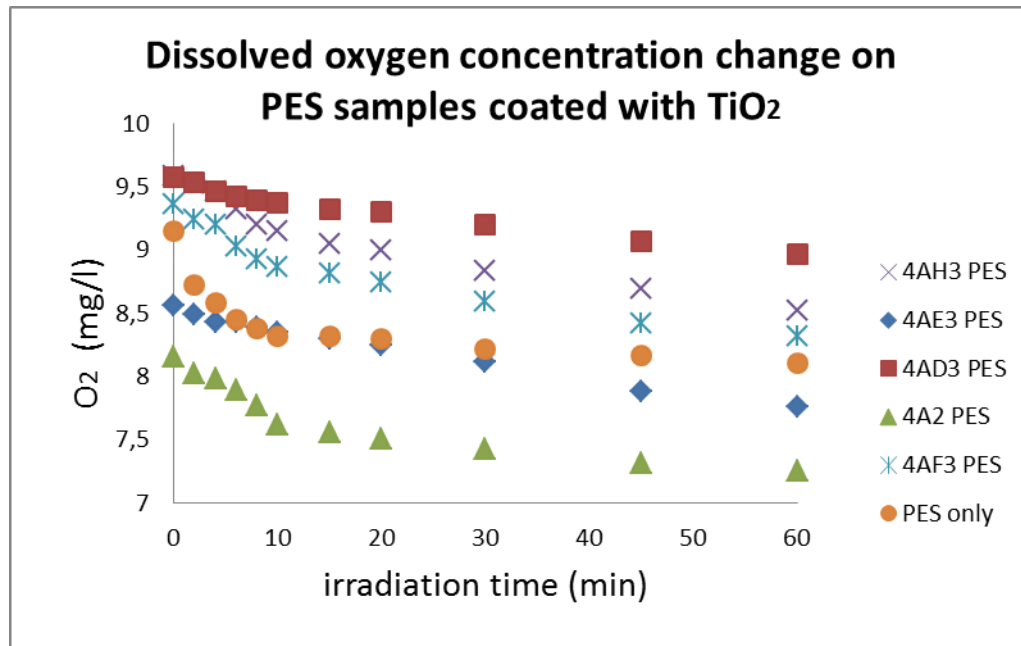


Figure 9.27: Oxygen concentration behavior as a function of time under UV irradiation of polyester samples

Table 9.7 : Dissolved oxygen concentration change under UV radiation of polyester samples coated with TiO₂

PES samples coated with TiO ₂	Sugar (mg/l)	Decrease of oxygen (slope)	Correlation (R ²)
4AE3	0.1	0.0125	0.9847
4AH3	0.1	0.0122	0.9922
4AF3	0.1	0.0111	0.9959
4AD3	0.1	0.0074	0.9747
4A2	0.1	0.0065	0.9842
PES without TiO ₂	0.1	0.0044	0.9723

Fig 9.27 shows that polyester sample 4AD3 has a higher photocatalytic activity compared to the other samples. The tested textiles of cotton and polyester samples both show photocatalytic behavior which is shown by the linear regression results. The polyester sample without TiO₂ shows a moderately higher photocatalytic activity compared to the other samples, the reason could be explained by some contamination of

the reactor pot with residues of TiO₂ nanoparticles. The photocatalytic behavior is different in all the samples which mean that the titanium nanoparticles concentration in the samples is different. However the concentrations of the samples could not be presented as the supplier is does not release the company's recipe.

**9.4.5 Self-cleaning of cotton textile modified with TiO₂ P25 Degussa
Experimental part 3 -**

Table 9.8: Coffee and wine stains on cotton samples exposed in the sun and kept in the dark

Type of stain	1 Day in the sun (Sample 4A2)	In the dark (Sample 4A2)	Untreated cotton 1 Day in the sun	Untreated cotton – in the dark
Coffee				
Wine				

Table 9.9 : Coffee and wine stain on cotton samples after washing

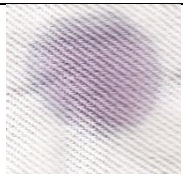
Type of stain	1 Day in the sun (Sample 4A2)	In the dark (Sample 4A2)	Untreated cotton 1 Day in the sun	Untreated cotton – in the dark
Coffee				
Wine				

Table 9.1 and table 9.2 show the slight decolourization of cotton samples that were stained with coffee and red wine. Four samples were exposed to solar radiation for 1 day, two samples were treated with TiO_2 and two samples were untreated. The treated samples appear much lighter which show that TiO_2 was efficient at partly decolorizing the stains. It can also be seen that samples treated with TiO_2 even if they were placed in a dark cupboard there was some decolourization but the effect is very small. The untreated cotton samples show no colour change after washing. When coffee stains the cotton it turns from white to brown and the wine stain appears dark red on the cotton sample. The decolourization of the stains exposed to solar radiation is result of the formation of strongly oxidizing radicals on the surface of TiO_2 nanoparticles deposited on the cotton when they were activated by the solar radiation. The efficiency of photocatalysis can be deduced at the materials surface from the electronic reactions. The requirements are a surface bound water to allow efficient oxidation. The stains of coffee and red wine were adsorbed very close to the surface of the material, and hence the TiO_2 nanoparticles having a greater surface area, the more pollutant was adsorbed to be photocatalytically oxidised.

10 Conclusion

UV radiation of acid orange II 0.01g/l with 0.1g/l TiO_2 results in the slight decolourization of acid orange to a certain extent as shown by the decrease in the absorbance measured at 486nm. The linear regression model used to quantify the decrease of oxygen concentration is very sensitive to differences in oxygen therefore they can be easily seen on the graphs. The decrease of oxygen concentration is from 7 to about 5.5 mg/l with irradiation time of 120 minutes. The proposed kinetic model shows how oxygen quickly oxygen is removed from the system it is quite similar to other kinetic models discussed in literature. The diffusion of oxygen and the influence of external temperature in an open system seem to be a problem as it leads to a very low concentration of oxygen in the system. Hence the experiments conducted in a closed system show higher concentrations of oxygen in the system. The decrease of oxygen concentrations of the conducted experiments show photocatalytic behavior since photocatalysis results in the generation of strongly oxidizing hydroxyl radicals and the interaction of the surface adsorbed oxygen, hence the reduction of oxygen in the system. The oxymetric method is robust and relatively easy with easy calibration.

The photocatalytic reactions of acid orange II 0.01g/l show a high photocatalytic activity at 0.2g/l TiO_2 . The saccharide used as a target chemical is oxidized easily, non-toxic and does not affect the photocatalysis. From the conducted experiments the trend of the decrease of concentration of dissolved oxygen is from 10 to about 7.5 mg/l which was observed during the irradiation time of 60 minutes. The oxymetric method on testing cotton and polyester samples coated with TiO_2 nanoparticles also show some photocatalytic behavior. The cotton and polyester sample 4AD3 shows higher photocatalytic activity compared to the rest of the samples. The exact concentration of the cotton and polyester samples could not be quantified as they are not released by the Nikato spol s.ro company. Self-cleaning properties tested on cotton samples that were exposed to solar radiation for one day show some decolourization but the stains were not totally removed as the limitation of the solar radiation is that it only absorbs 3- 5% in the UV region. The cotton samples that were placed in a dark cupboard showed no decolourization.

Future recommendations will be the usage of higher dosage of the photocatalyst titanium dioxide could achieve a complete decolourization and mineralization of the dye. Since the oxygen concentration was decreasing in the system, to achieve higher rates of photocatalysis the oxygen can be injected into the reaction system. The decrease in the oxygen concentration is caused electron hole which is a process that competes with the photochemical oxidation process because of the electron hole recombination. The cotton samples could be irradiated under UV light to eliminate the solar radiation limitation hence substantial self-cleaning could be achieved.

11 References

1. Al-Nour G.Y.M (2009). Photocatalytic degradation of Organic contaminant in the presence of Graphite-supported and unsupported ZnO modified with CdS particles. <http://scholar.najah.edu/publication/thesis/photocatalytic-degradation-organic-contaminants-presence-graphite-supported-and-u>
2. Asahi R *et al.* (2001). Visible light photocatalysis in nitrogen doped Titanium oxides. *Science* Volume 293 no.5528, pages 269-271.
3. Behnajady M.A *et al.* (2008). Enhancement of Photocatalytic Activity of TiO₂ Nanoparticles by Silver Doping: Photodeposition versus Liquid Impregnation Methods. *Global NEST Journal* Vol 10, No 1, pages 1-7.
4. Banerjee S *et al.* (2006). Physics and chemistry of photocatalytic titanium dioxide: Visualization of bactericidal activity using atomic force microscopy. *Current science*, Vol. 90, no. 10 pages 1378-1383.
5. Benedix R *et al.* (2000). Application of Titanium Dioxide Photocatalysis to Create Self-Cleaning Building Materials. *LACER* (5): pages 157-168.
6. Blake D. M (1999). Application of the Photocatalytic Chemistry of Titanium dioxide to Disinfection and the killing of Cancer cells. *Separation and Purification Methods* Volume 28(1), pages 1-50.
7. Bozzi A *et al.* (2005). Self-cleaning of modified cotton textiles by TiO₂ at low temperatures under daylight irradiation. *Journal of Photochemistry and Photobiology A: Chemistry* 174, pages 156–164.
8. Fernández J (2004). Orange II photocatalysis on immobilised TiO₂ Effect of the pH and H₂O₂. *Applied Catalysis B: Environmental* 48, pages 205–211

9. Fujishima A, Hashimoto K, Watanabe T (1999). *TiO₂ Photocatalysis, Fundamental and Applications*, Bkc Inc., Tokyo, Japan.
10. Gupta K. K, Jassal M and Agrawal A. K (2007). Functional Finishing of Cotton Using Titanium Dioxide and Zinc Oxide Nanoparticles. *Research Journal of Textile and Apparel*, 11(3), pages 1-10.
11. Gupta K, Manjeet J and Agrawal A (2008). Sol-gel derived titanium dioxide finishing of cotton fabric for self-cleaning. *Indian Journal of Fiber and Textile Research* Vol.33, pages 443-450.
12. Hanaor D.A, Sorrell C.C (2011). Review of the anatase to rutile phase transformation. *Journal of Materials Science* 46: pages 855-874.
13. Hu J (2001). Adaptive and functional polymers, textiles and their application. Chapter 5 pages 169-178 of *Adaptive polymeric composites and applications*. Imperial College Press.
14. Kaneko M, Okura I (Eds) (2002). *Photocatalysis Science and Technology, Biological and Medical physics series*. Chapter 2 of *Fundamental Aspects of photocatalysts*. Kodansha, Springer, page 24.
15. Karmi L et al. (2010). Effect of Nano TiO₂ on Self-cleaning Property of Cross-linking Cotton Fabric with Succinic Acid under UV Irradiation. *Photochemistry and Photobiology*, Volume 86, Issue 5, pages 1030–1037.
16. Katarzyna S.S *et al.* (2011). Evaluation of the Photocatalytic Properties of Textile Fabrics Modified with Titanium Dioxide of Anatase Structure. *Fibres & Textiles in Eastern Europe* Vol. 19, No. 2 (85) pages 76-8.
17. Kim T-w and Lee M-J (2010). Effect of pH and Temperature for Photocatalytic Degradation of Organic Compound on Carbon-coated TiO₂. *Journal of Advanced Engineering and Technology*, Vol. 3, No. 2 pages 193-198.

18. Laoufi N.A, Tassalit D, Bentahar F (2008). The degradation of phenol in water solution by TiO₂ photocatalysis in a helical reactor. *Global NEST Journal*, Vol 10, No 3, pages 404-418.
19. Liu Y et al (2005). Photocatalytic degradation of azo dyes by nitrogen doped TiO₂ nano crystals. *Chemosphere* 61, pages 11-18.
20. Meji'a M.I et al (2010). Preparation, testing and performance of a TiO₂/polyester photocatalyst for the degradation of gaseous methanol. *Applied Catalysis B: Environmental* 94, pages 166–172.
21. Mihailovic' D *et al.* (2011). Functionalization of cotton fabrics with corona/air RF plasma and colloidal TiO₂ nanoparticles. *Polymer Composites Volume 32, Issue 3*, pages 390–397.
22. Montazer M and Seifollahzadeh S (2011). Enhanced Self-cleaning, Antibacterial and UV Protection Properties of Nano TiO₂ Treated Textile through Enzymatic Pretreatment. *Photochemistry and Photobiology* 87: pages 877–883.
23. Ozdural P *et al.* Catalytic Wet Air Oxidation of Azo-Dye Orange II: In Search Of an Efficient Catalyst. <http://www.nacatsoc.org/20nam/abstracts/P-S4-03A.pdf>
24. Qi K, Wang X and Xi J.H. (2010). Photocatalytic self-cleaning textiles based on nanocrystalline titanium dioxide. *Textile Research Journal*, 0(00) pages 1–10.
25. Seery M.K (2009). Metal oxide Photocatalysis. *Photochemistry Portal*. Principles, Applications and Experimentation in Modern Photochemistry. <http://photochemistryportal.net/home/index.php/category/semi-conductor-photocatalysis/>

26. Stamate M, Lazar G (2007). Application of titanium dioxide Photocatalysis to create Self-cleaning materials. Mocom 13 – Volume 3 – Romanian Technical Sciences Academy 280.
27. Sumandeep K.V (2011). Light induced oxidative degradation studies of organic dyes and their intermediates. PhD thesis, Thapar University. <http://hdl.handle.net/123456789/450>
28. Xue C-H *et al.* (2008). Superhydrophobic cotton fabrics prepared by sol–gel coating of TiO₂ and surface hydrophobitization. IOP Publishing, Science and Technology of Advanced Materials 9, 035001 (5pp).
29. Yuranova T *et al.* (2006). Self-cleaning cotton textiles surfaces modified by photoactive SiO₂/TiO₂ coating. Journal of Molecular Catalysis A: Chemical 244, pages 160–167.

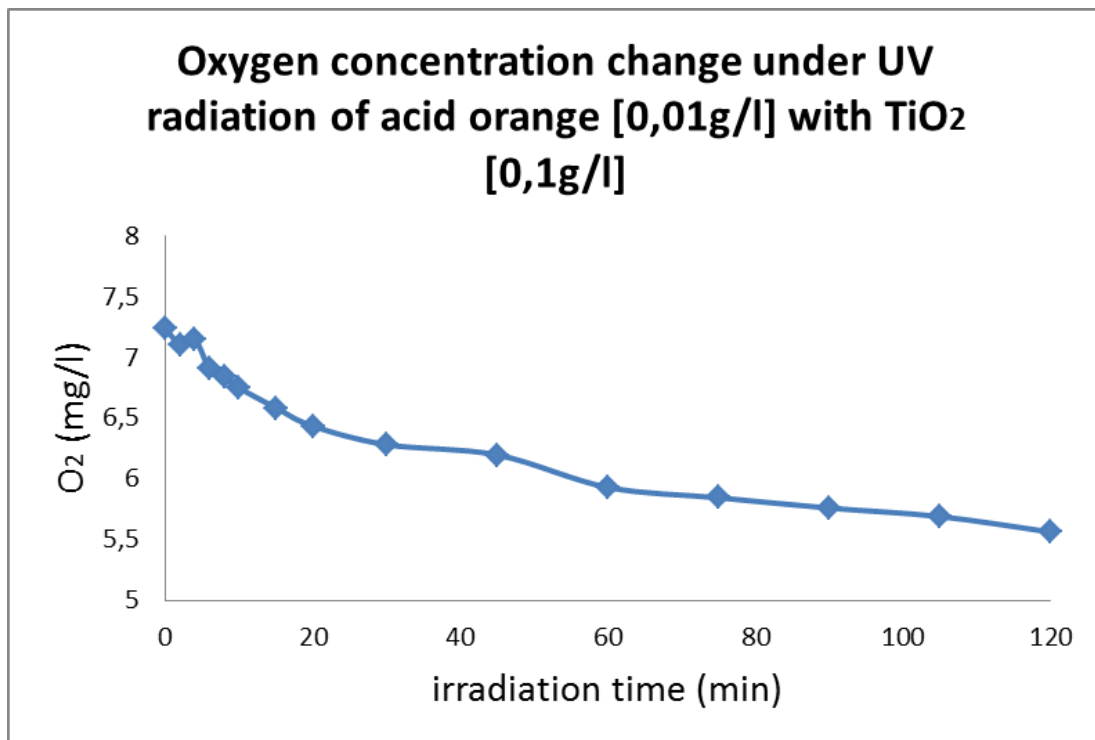
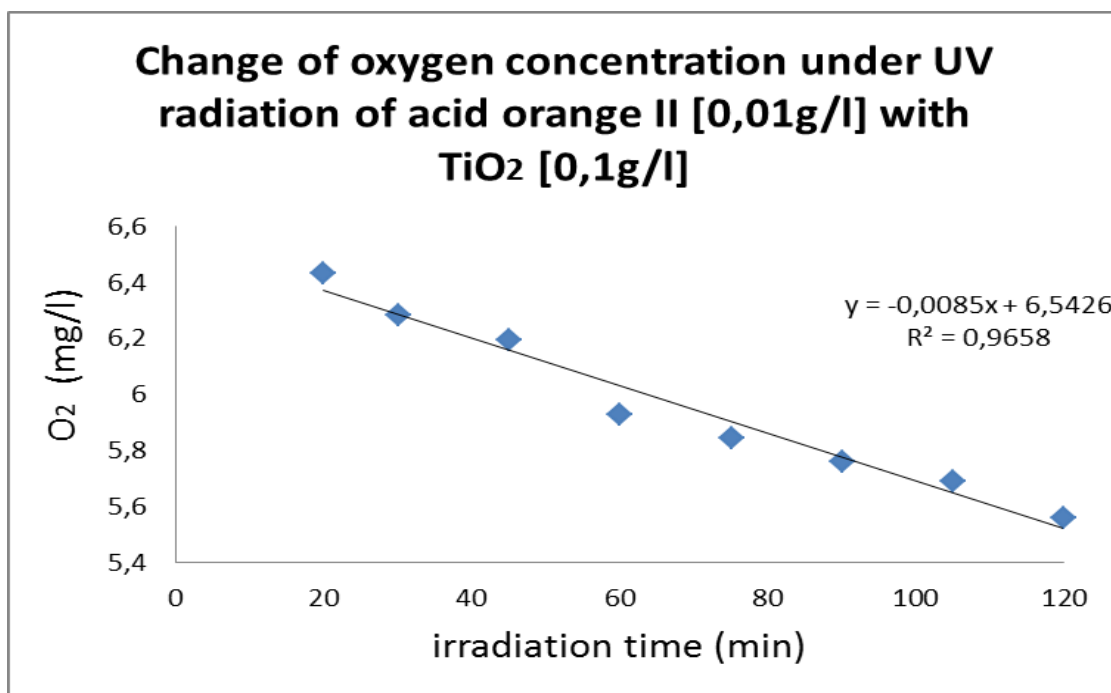
12 Appendices

12.1 Appendix A

Testing of oxymetric method on photocatalytic degradation of acid orange II with TiO_2 for 120 min in open system under UV light

Change of oxygen concentration with time during acid orange degradation

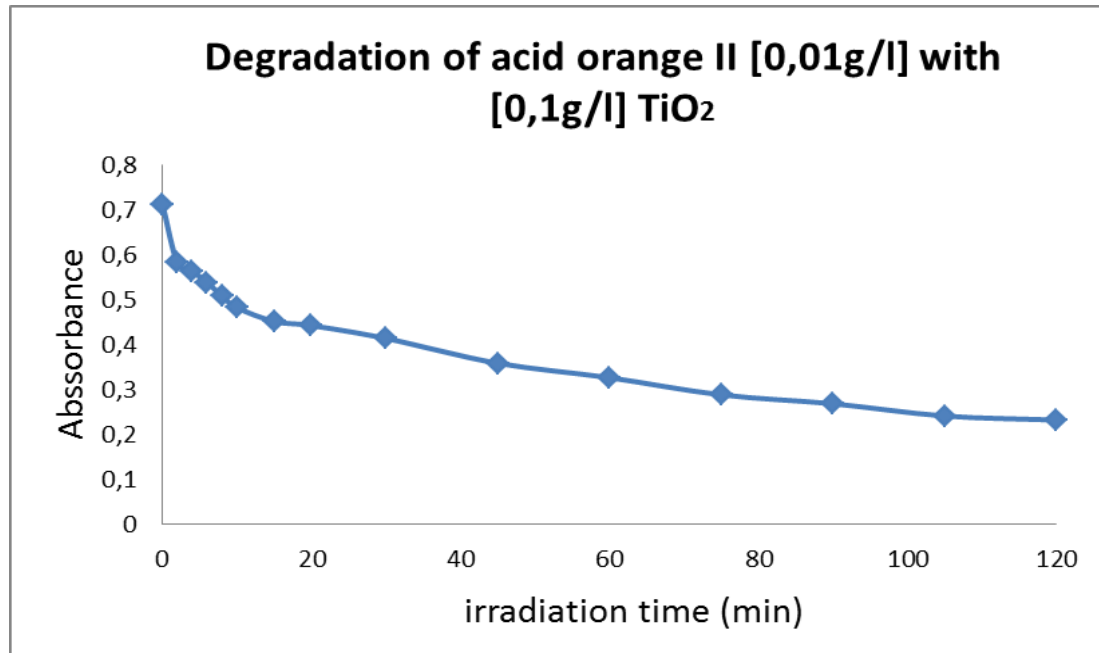
Time (min)	Average temperature °C	O ₂ conc. (mg/l)	O ₂ conc.(mg/l)	O ₂ conc.(mg/l)	O ₂ conc.(mg/l)	Average O ₂ concentration (mg/l)
0	19,2	7,1	7,15	7,825	6,88	7,24
2	18,97	7,1	7	7,78	6,55	7,11
4	19,42	7,1	7,28	7,61	6,6	7,13
6	19,42	7	6,98	7,12	6,52	6,90
8	19,67	6,95	6,91	7,01	6,5	6,84
10	19,45	6,93	6,85	6,82	6,4	6,75
15	19,57	6,8	6,41	6,76	6,37	6,58
20	20,47	6,75	6,6	6,28	6,11	6,44
30	21,02	6,71	6,5	6,21	5,71	6,28
45	22,12	6,6	6,49	6,11	5,59	6,19
60	22,92	6,33	6,19	5,99	5,21	5,93
75	23	6,15	6,14	5,89	5,2	5,84
90	24	6,01	6,09	5,75	5,19	5,76
105	25,12	5,6	5,98	5,99	5,19	5,69
120	24,85	5,5	5,82	5,76	5,17	5,56

Photocatalytic degradation of acid orange II under UV light in the presence of TiO₂

Decrease of dissolved oxygen on acid orange II degradation

Absorbance at 584 nm of the degradation of acid orange II

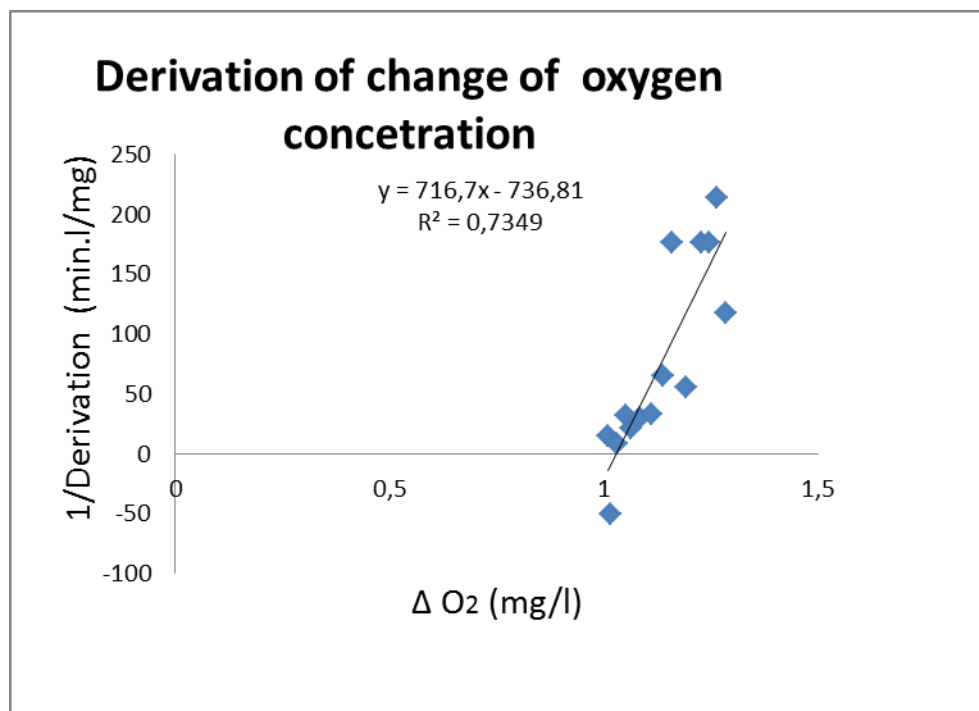
Time(min)	Absorbance A	Absorbance B	Absorbance C	Absorbance D	Average
0	0,588	0,599	0,964	0,698	0,712
2	0,451	0,589	0,6	0,611	0,581
4	0,444	0,576	0,711	0,596	0,563
6	0,439	0,55	0,602	0,56	0,537
8	0,421	0,48	0,573	0,558	0,508
10	0,411	0,452	0,55	0,515	0,482
15	0,4	0,398	0,508	0,499	0,451
20	0,399	0,388	0,573	0,408	0,442
30	0,399	0,362	0,495	0,398	0,413
45	0,385	0,321	0,393	0,334	0,358
60	0,376	0,287	0,384	0,258	0,326
75	0,355	0,263	0,301	0,233	0,288
90	0,32	0,244	0,279	0,23	0,268
105	0,28	0,232	0,277	0,175	0,241
120	0,277	0,21	0,278	0,163	0,232



Photocatalytic degradation of acid orange II under UV light in the presence of TiO₂ at 485 nm

Derivation of oxygen during acid orange degradation

Time (min)	O ₂ (mg/l)	Av. Δ in O ₂ (mg/L)	Derivation (mg/min.L)	1/Derivation (min.L/mg)
0	7,23	1,00	0,065	15,24
2	7,12	1,01	-0,02	-50
4	7,14	1,03	0,121	8,25
6	6,90	1,05	0,031	32
8	6,84	1,06	0,046	21,62
10	6,75	1,08	0,033	30,30
15	6,58	1,11	0,03	33,33
20	6,44	1,14	0,015	65,57
30	6,28	1,16	0,0056	176,47
45	6,19	1,19	0,0178	56,07
60	5,93	1,23	0,0057	176,47
75	5,84	1,25	0,0057	176,47
90	5,76	1,26	0,00467	214,28
105	5,69	1,28	0,0085	117,64
120	5,56	1,30		

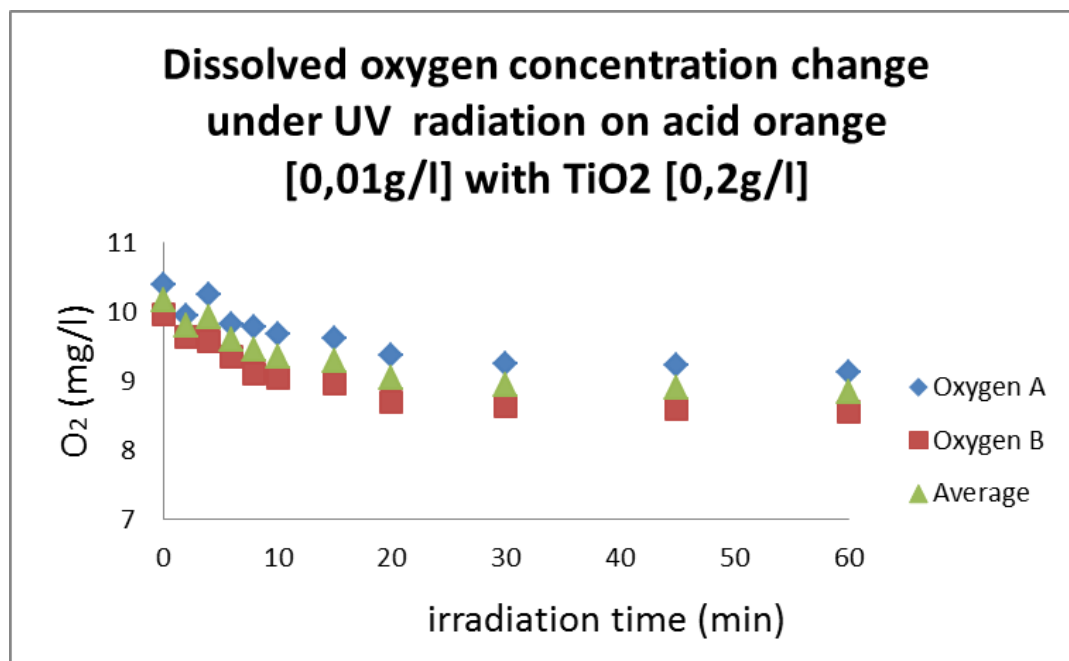


Derivation kinetic model of the change of oxygen concentration during degradation of dye acid orange II

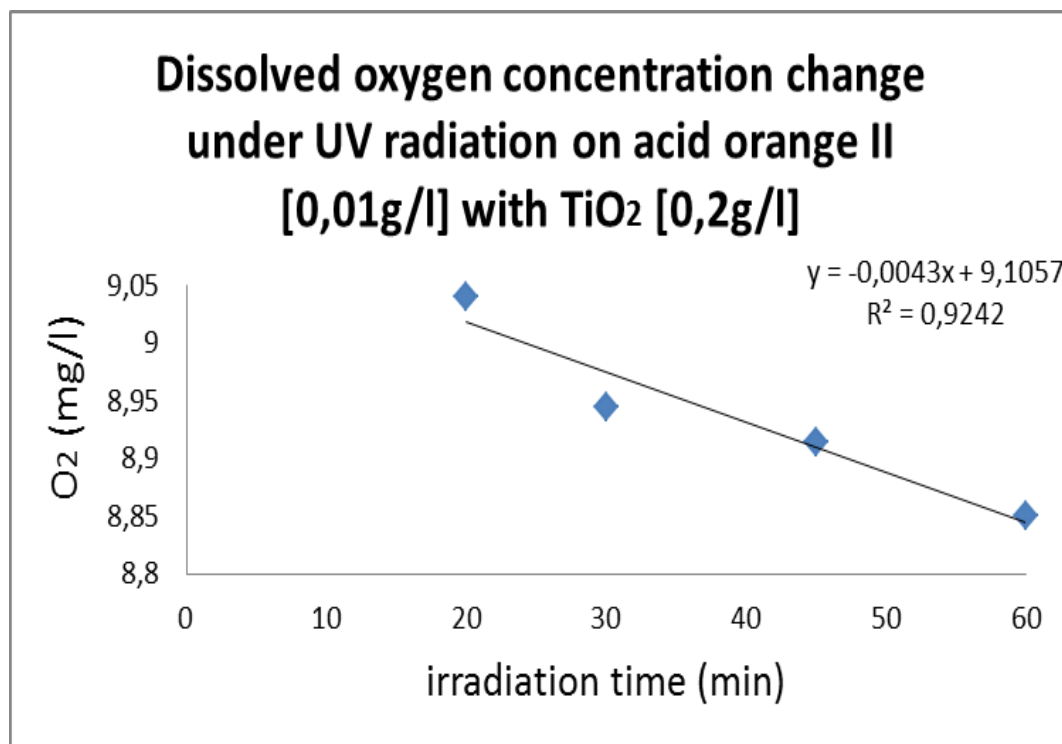
Photocatalytic degradation of acid orange II with TiO_2 for 60 min in an open system under UV light

Oxygen concentration under UV irradiation 0,2 g/l TiO_2 and 0,01 g/l acid orange

Time (min)	Average temperature °C	O ₂ (mg/l) A	O ₂ (mg/l) B	Average
0	12,95	10,39	9,96	10,17
2	12,8	9,94	9,65	9,79
4	12,8	10,26	9,59	9,92
6	12,85	9,83	9,36	9,59
8	12,95	9,78	9,12	9,45
10	12,9	9,68	9,04	9,36
15	12,65	9,63	8,96	9,29
20	12,65	9,38	8,7	9,04
30	12,55	9,25	8,64	8,94
45	12,65	9,23	8,6	8,91
60	12,85	9,14	8,56	8,85



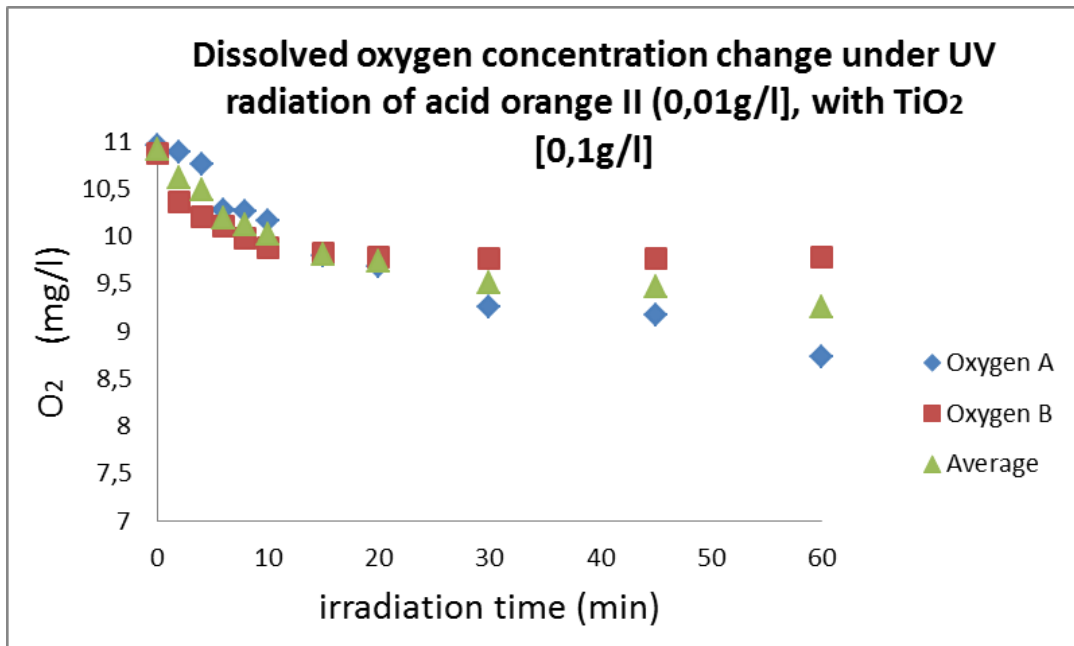
Photocatalytic degradation of acid orange II under UV light in the presence of TiO_2



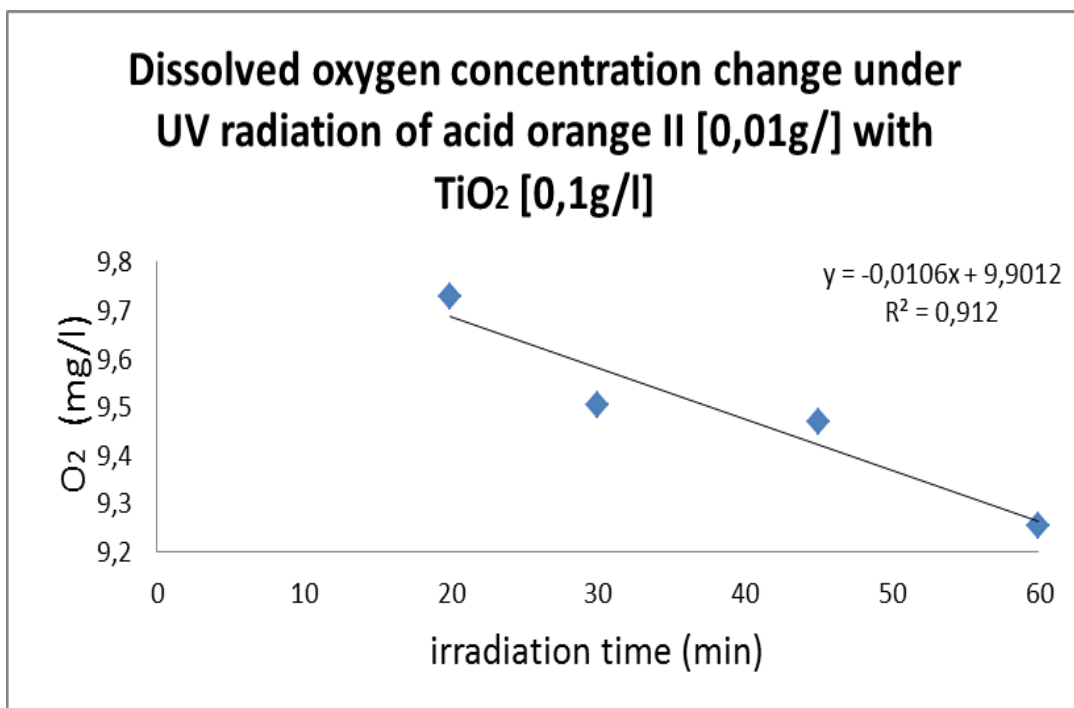
Decrease of oxygen concentration with UV radiation of acid orange

Oxygen concentration change under UV irradiation 0.1 g/l of TiO₂ with 0,01 g/l acid orange

Time (min)	Average temperature °C	O ₂ (mg/l) A	O ₂ (mg/l) B	Average
0	13,65	10,96	10,87	10,91
2	13,5	10,88	10,36	10,62
4	13,45	10,76	10,21	10,48
6	13,4	10,27	10,11	10,19
8	13,45	10,26	9,98	10,12
10	13,45	10,16	9,88	10,02
15	13,5	9,8	9,82	9,81
20	13,55	9,68	9,78	9,73
30	13,85	9,25	9,76	9,51
45	13,75	9,17	9,77	9,47
60	13,55	8,73	9,78	9,25



Photocatalytic degradation of acid orange II under UV light in the presence of TiO₂

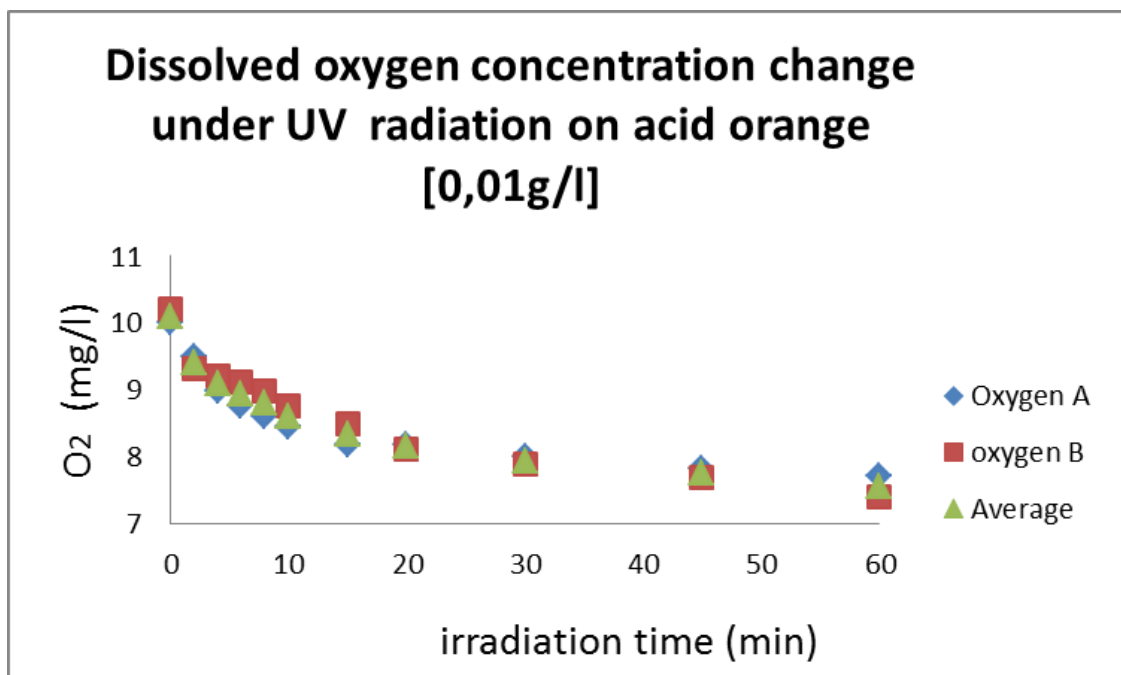


Decrease of oxygen concentration with UV radiation of acid orange II

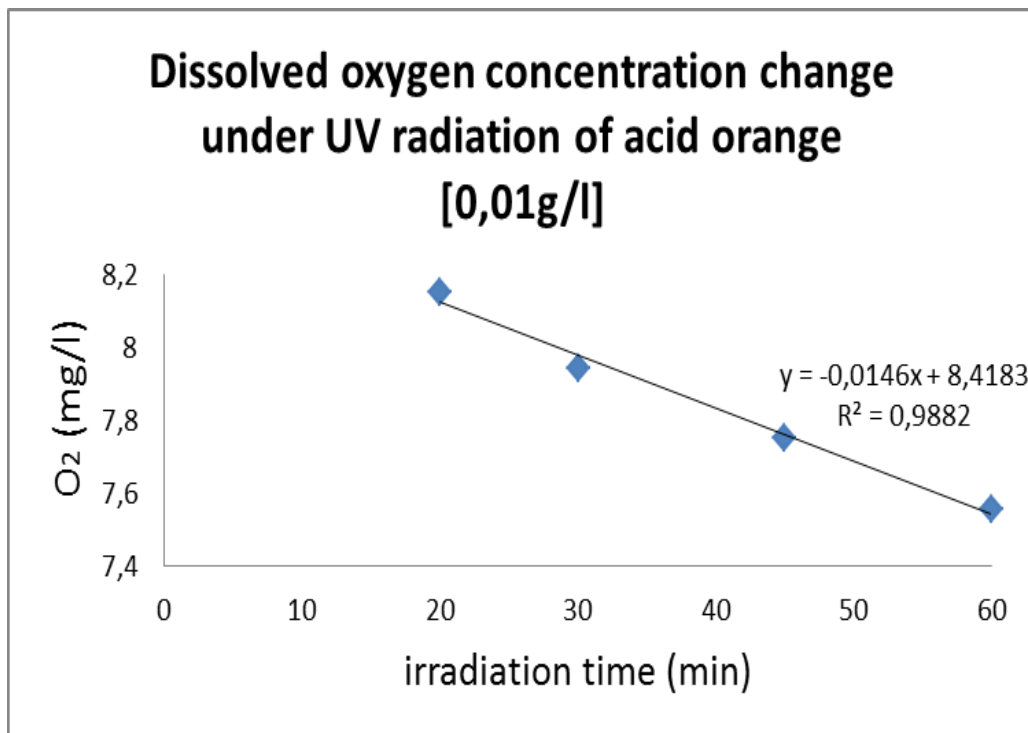
Oxygen concentration change under UV radiation 0 g/l of TiO₂ orange

0,01 g/l acid orange

Time (min)	Average temperature °C	O ₂ (mg/l) A	O ₂ (mg/l) B	Average
0	12,95	9,11	9,4	9,25
2	13,05	9	9,31	9,15
4	13,15	8,99	9,21	9,1
6	13,2	8,76	9,11	8,94
8	13,25	8,61	8,99	8,8
10	13,25	8,45	8,76	8,60
15	13,3	8,31	8,49	8,4
20	73,7	8,19	8,12	8,15
30	13,4	7,99	7,89	7,94
45	13,3	7,82	7,68	7,75
60	13,2	7,71	7,55	7,63



Photocatalytic degradation of acid orange II under UV light in the absence of TiO₂



Decrease of oxygen concentration with UV radiation of acid orange

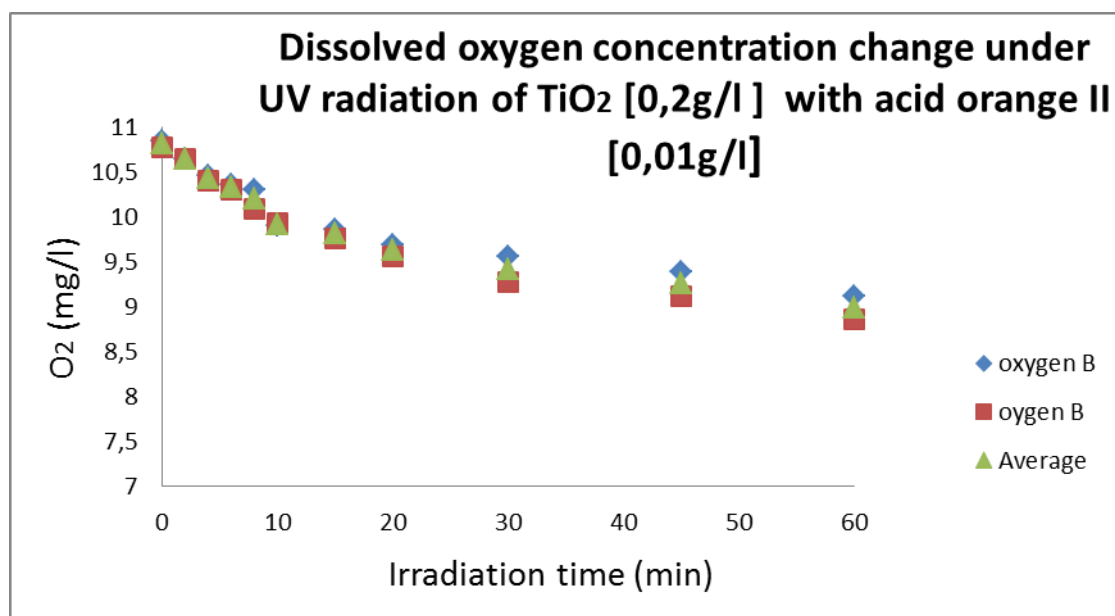
Linear regression result of TiO₂ and acid orange II irradiation under UV light in the an open system

TiO ₂ (mg/l)	Acid orange II (mg/l)	Decrease of oxygen (slope)	Correlation (R ²)
0.2	0.01	0.016	0.912
0.1	0.01	0.0043	0.9242
0	0.01	0.0146	0.9882

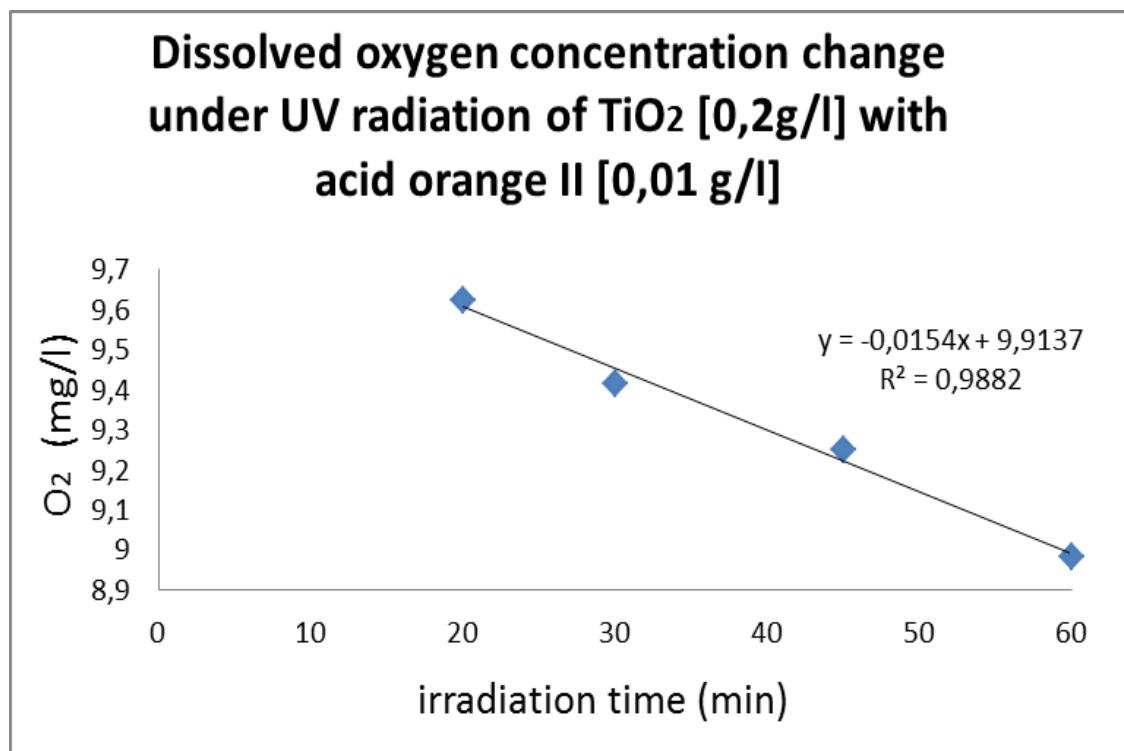
Photocatalytic degradation of acid orange II with TiO_2 for 60 min in a closed system under UV light

Oxygen concentration change under UV radiation 0,2 g/l TiO_2 with 0,01 g/l acid orange

Time (min)	Average temperature °C	O ₂ (mg/l) A	O ₂ (mg/l) B	Average
0	13	10,84	10,77	10,80
2	12,85	10,64	10,64	10,64
4	12,8	10,45	10,39	10,42
6	12,85	10,36	10,29	10,32
8	13	10,3	10,08	10,19
10	13	9,9	9,92	9,91
15	12,8	9,86	9,76	9,81
20	12,6	9,69	9,56	9,63
30	12,35	9,56	9,27	9,42
45	12,2	9,39	9,11	9,25
60	12,2	9,11	8,86	8,98



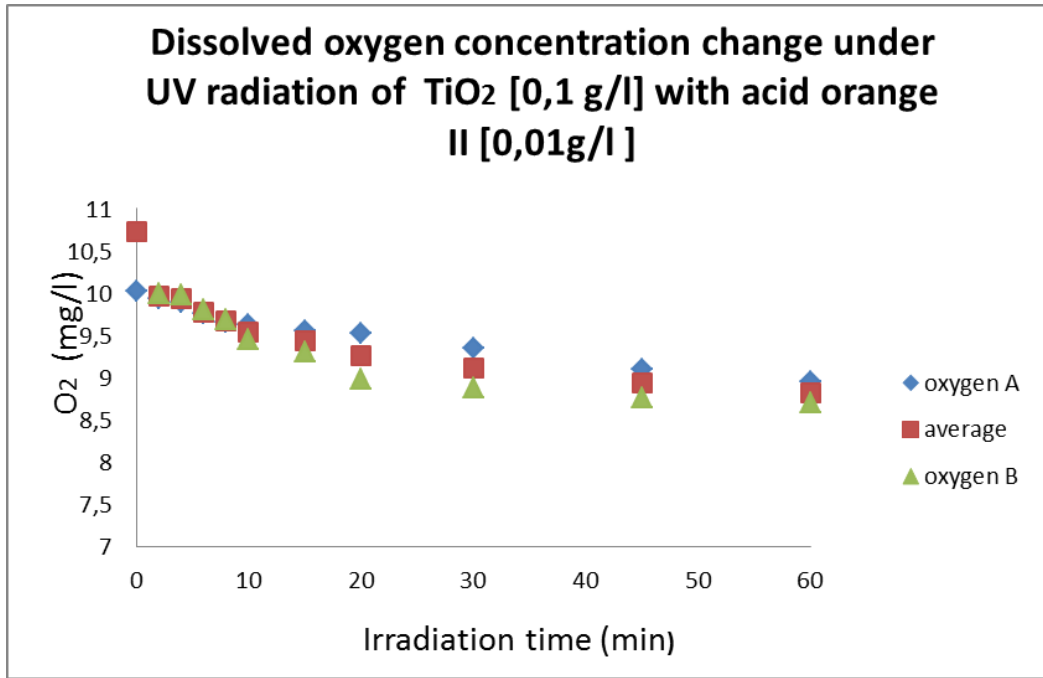
Photocatalytic degradation of acid orange II under UV light in the presence of TiO_2



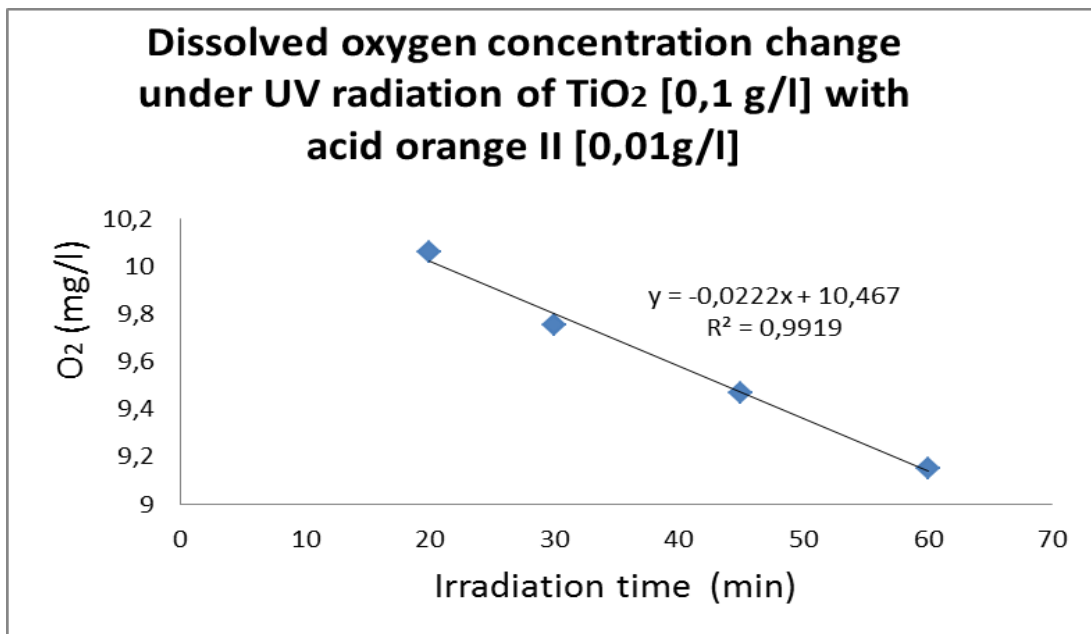
Decrease of oxygen concentration with UV radiation of acid orange II

Oxygen concentration change under UV irradiation 0,1 g/l TiO₂ 0,01 g/l acid orange

Time (min)	Average Temperature °C	O ₂ (mg/l) A	O ₂ (mg/l) B	Average
0	13,05	10,02	10,02	10,02
2	12,65	9,94	9,94	9,94
4	12,5	9,89	9,89	9,89
6	12,3	9,76	9,76	9,76
8	12,25	9,66	9,66	9,66
10	12,3	9,62	9,62	9,62
15	12,25	9,56	9,56	9,56
20	12,3	9,53	9,53	9,53
30	12,35	9,35	9,35	9,35
45	12,3	9,1	9,1	9,1
60	12,3	8,95	8,95	8,95



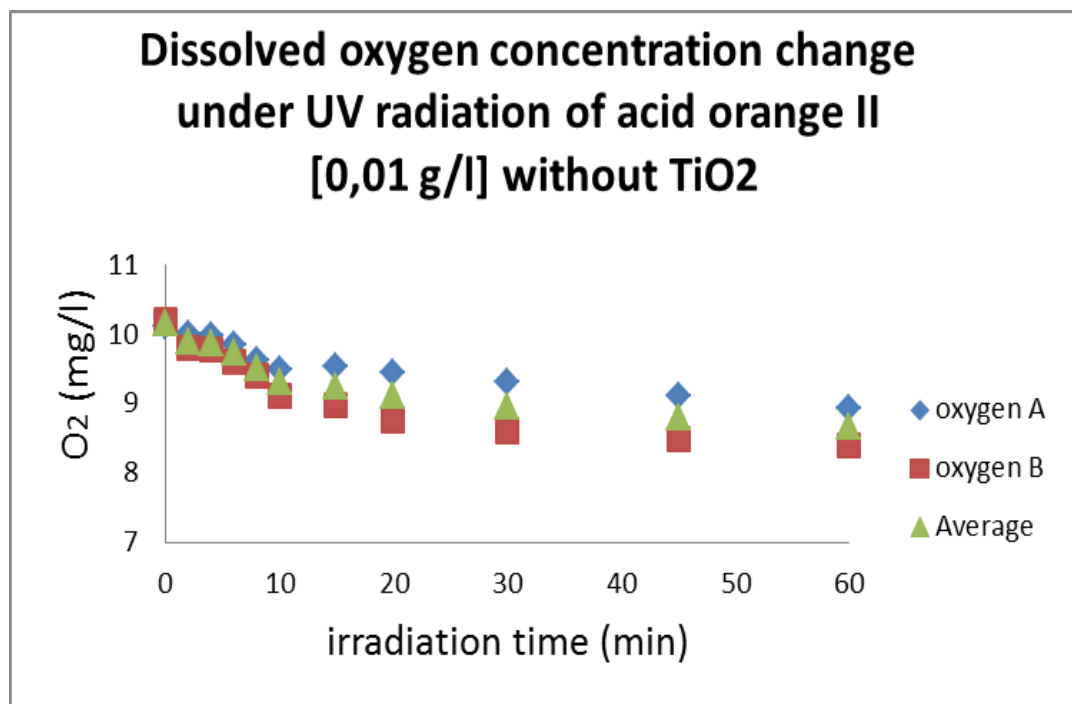
Photocatalytic degradation of acid orange II under UV light in the presence of TiO₂



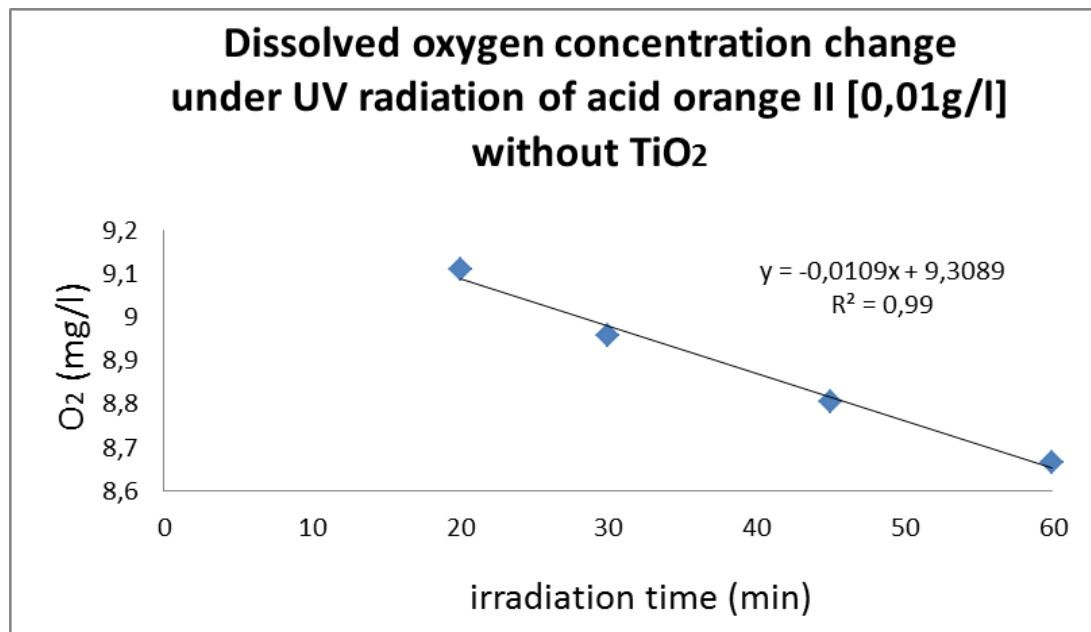
Decrease of oxygen concentration with UV radiation of acid orange II

Oxygen concentration under UV radiation 0 g/l TiO₂ and 0,01 g/l acid orange

Time (min)	Average temperature °C	O ₂ (mg/l) A	O ₂ (mg/l) B	Average
0	13,5	10,12	10,2	10,16
2	13,5	10	9,81	9,90
4	13,5	9,98	9,78	9,88
6	13,5	9,85	9,61	9,73
8	13,5	9,62	9,4	9,51
10	13,5	9,5	9,12	9,31
15	13,5	9,54	8,98	9,26
20	13,5	9,46	8,76	9,11
30	13,5	9,31	8,61	8,96
45	13,5	9,11	8,5	8,80
60	13,5	8,93	8,4	8,66



Change of oxygen concentration in the absence of TiO₂



Decrease of oxygen in the system in the absence of TiO₂

Linear regression result of TiO₂ and acid orange II irradiation under UV light in the closed system

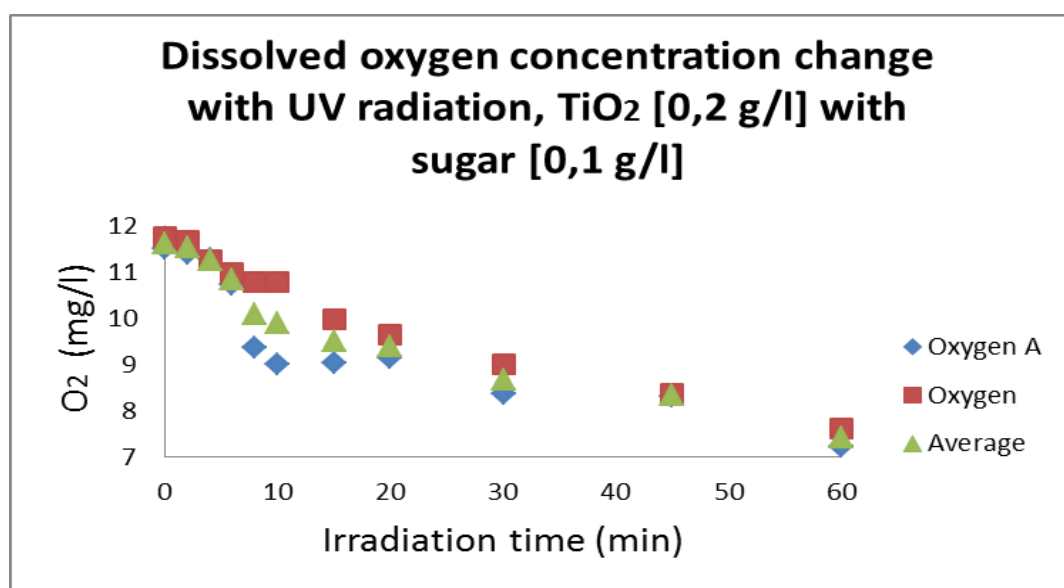
TiO ₂ (mg/l)	Acid orange II (mg/l)	Decrease of oxygen (slope)	Correlation (R ²)
0.2	0.01	0.0154	0.9882
0.1	0.01	0.0108	0.976
0	0.01	0.0109	0.99

12.2 Appendix B

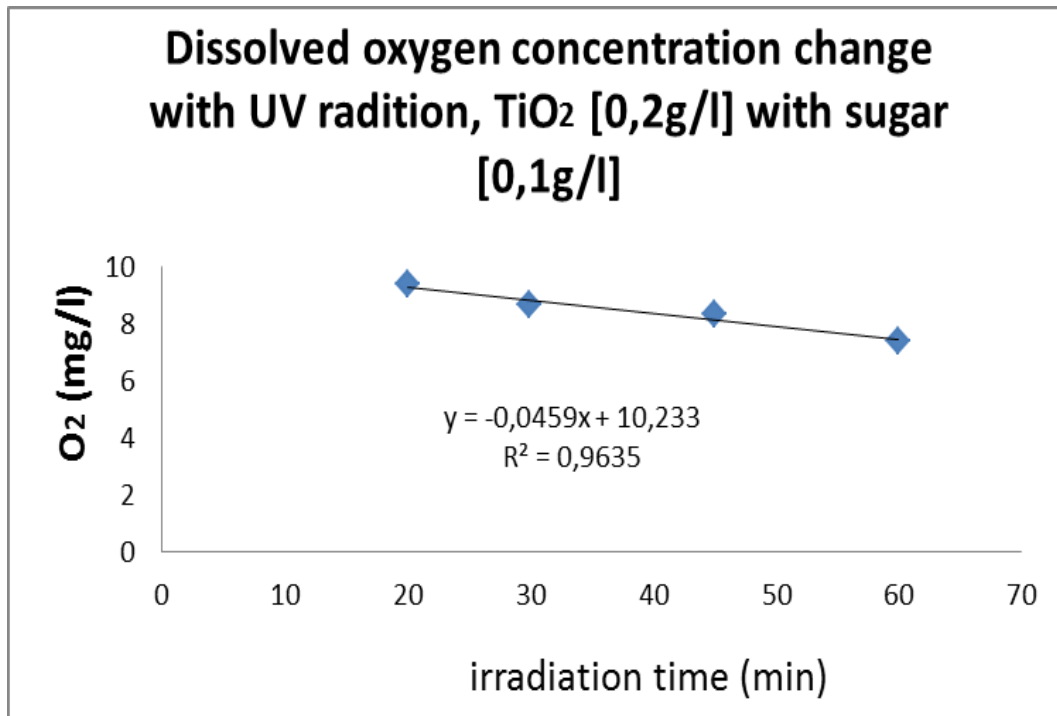
Oxymetric method for testing photocatalysis on a saccharide (sugar) using TiO_2

Oxygen concentration change under UV irradiation 0,2 g/l TiO_2 with 0,1 g/l of sugar

Time(min)	Temperature °C	O ₂ (mg/l) A	O ₂ (mg/l)	Average O ₂
0	13,5	11,5	11,75	11,62
2	13,5	11,4	11,68	11,54
4	13,5	11,28	11,26	11,27
6	13,5	10,73	10,97	10,85
8	13,5	9,38	10,8	10,09
10	13,5	9,01	10,78	9,89
15	13,5	9,04	9,97	9,51
20	13,5	9,13	9,64	9,38
30	13,5	8,35	9	8,67
45	13,5	8,32	8,37	8,34
60	13,5	7,23	7,6	7,41



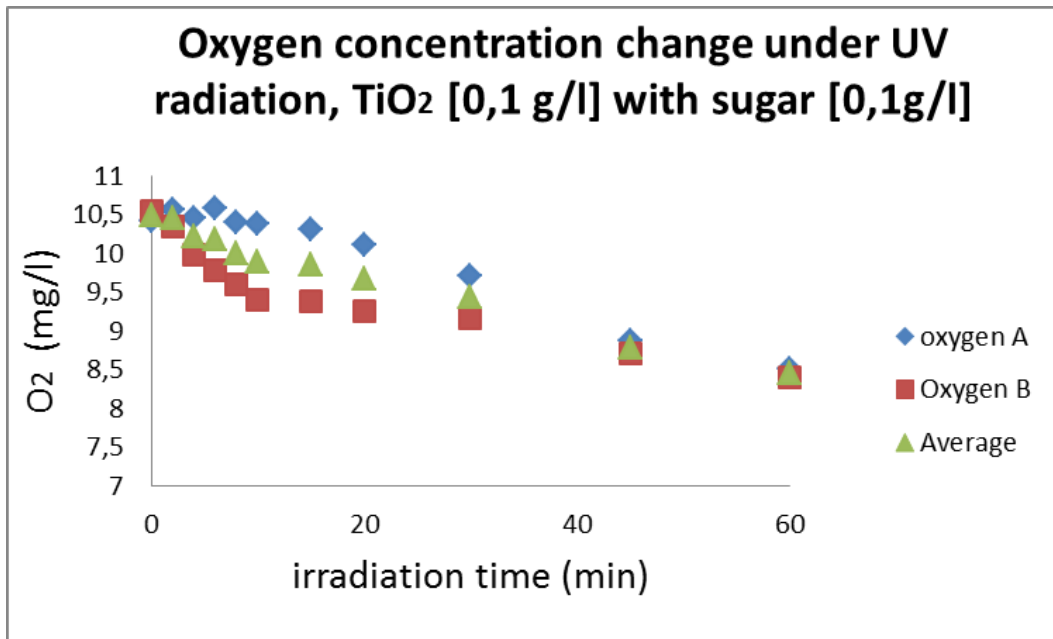
Change in oxygen concentration with radiation time of TiO_2 with sugar



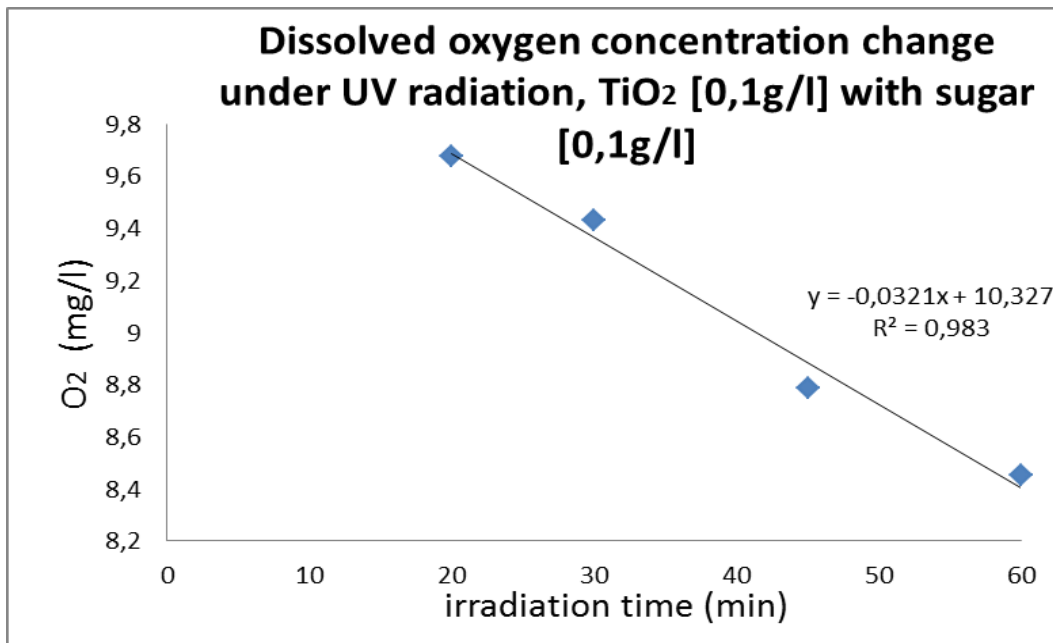
Decrease of oxygen concentration with radiation

Oxygen concentration under UV irradiation 0,1 g/l TiO₂ with 0,1 g/l of sugar

Time(min)	Temperature °C	O ₂ (mg/l) A	O ₂ (mg/l)	Average O ₂
0	13,5	10,42	10,53	10,47
2	13,5	10,55	10,33	10,44
4	13,5	10,44	9,98	10,21
6	13,5	10,57	9,78	10,17
8	13,5	10,4	9,6	10
10	13,5	10,37	9,4	9,88
15	13,5	10,31	9,38	9,84
20	13,5	10,1	9,25	9,6
30	13,5	9,71	9,15	9,43
45	13,5	8,87	8,7	8,78
60	13,5	8,5	8,4	8,45



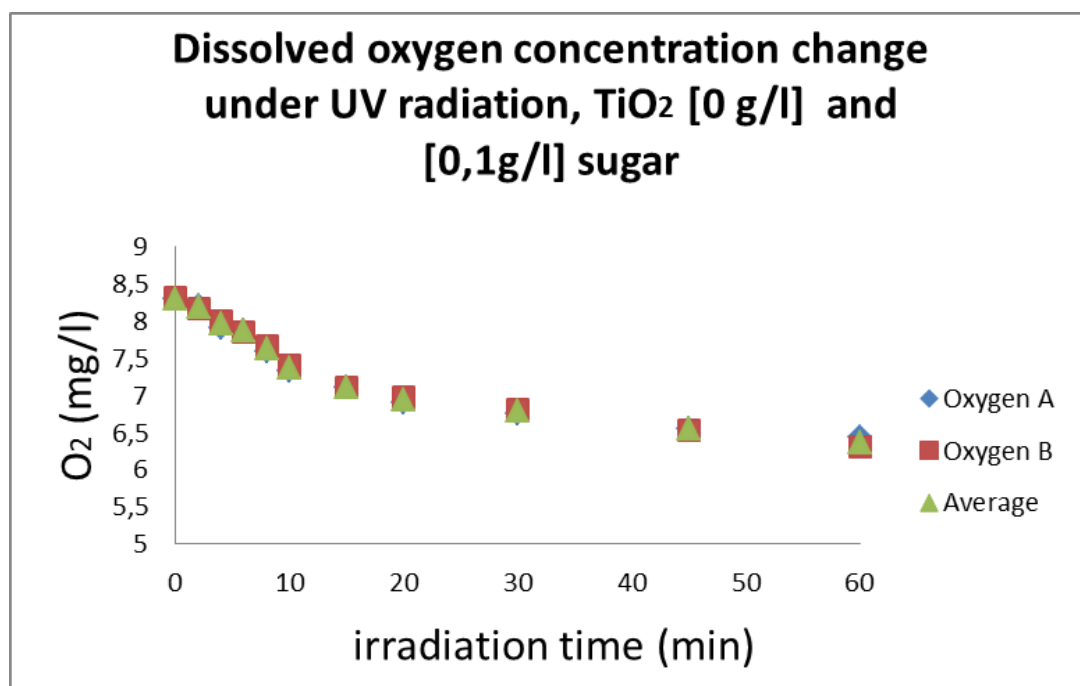
Change in oxygen concentration with radiation time



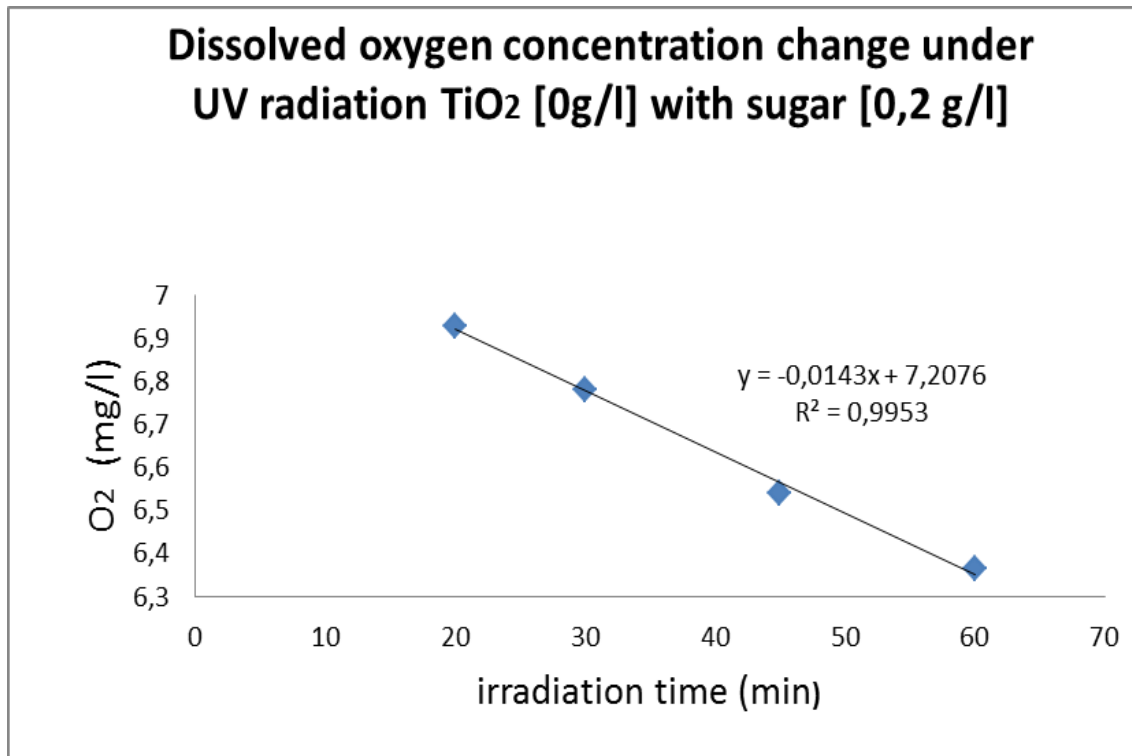
Decrease of oxygen concentration with radiation

Oxygen concentration change under UV radiation 0 g/l TiO₂ with 0,1 g/l of sugar

Time(min)	Temperature °C	O ₂ (mg/l) A	O ₂ (mg/l)	Average O ₂
0	13,5	8,28	8,3	8,29
2	13,5	8,2	8,15	8,18
4	13,5	7,9	8	7,95
6	13,5	7,86	7,85	7,85
8	13,5	7,58	7,65	7,62
10	13,5	7,32	7,4	7,36
15	13,5	7,1	7,11	7,10
20	13,5	6,89	6,97	6,93
30	13,5	6,75	6,81	6,78
45	13,5	6,55	6,53	6,54
60	13,5	6,43	6,3	6,36



Change of oxygen concentration in the absence of TiO₂



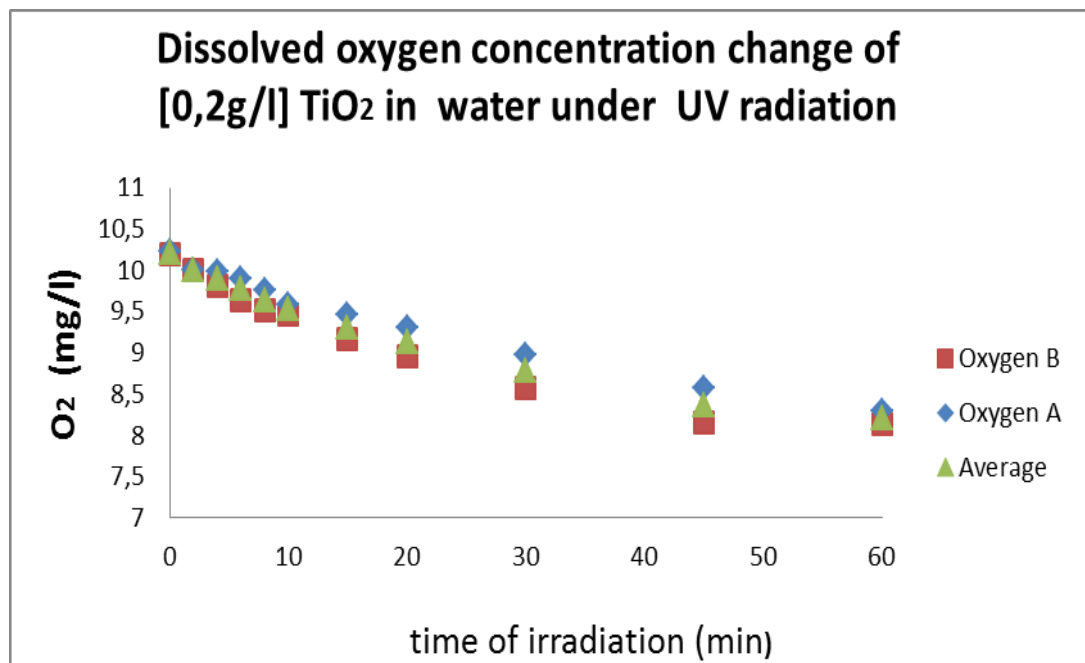
Decrease of oxygen concentration in the absence of TiO₂

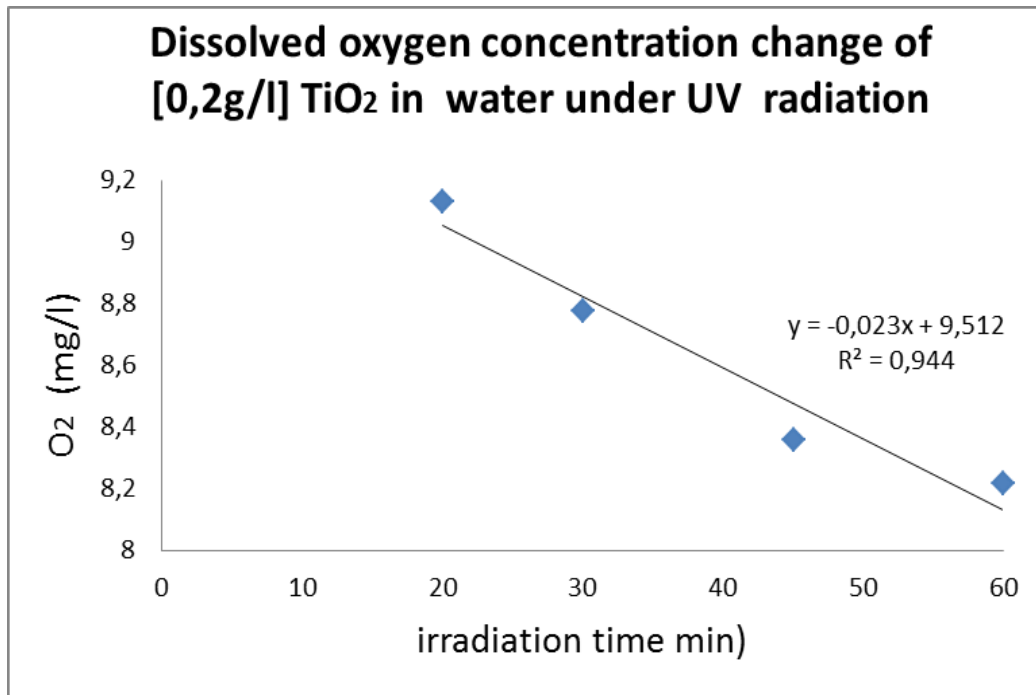
Linear regression results of TiO₂ and sugar irradiation under UV light in the closed system

TiO ₂ (mg/l)	White sugar (mg/l)	Decrease of oxygen (slope)	Correlation (R ²)
0.2	0.1	0.0459	0.9635
0.1	0.1	0.0321	0.983
0	0.1	0.0143	0.9953

Testing of photocatalysis of TiO₂ using Oxymetric methodOxygen concentration under UV irradiation 0,2 g/l TiO₂

Time(min)	Temperature °C	O ₂ (mg/l) A	O ₂ (mg/l)	Average O ₂
0	13,5	10,23	10,2	10,22
2	13,5	10	10	10
4	13,5	9,98	9,81	9,89
6	13,5	9,9	9,64	9,77
8	13,5	9,75	9,51	9,63
10	13,5	9,59	9,46	9,53
15	13,5	9,46	9,16	9,31
20	13,5	9,3	8,96	9,13
30	13,5	8,98	8,57	8,77
45	13,5	8,57	8,15	8,36
60	13,5	8,3	8,13	8,22

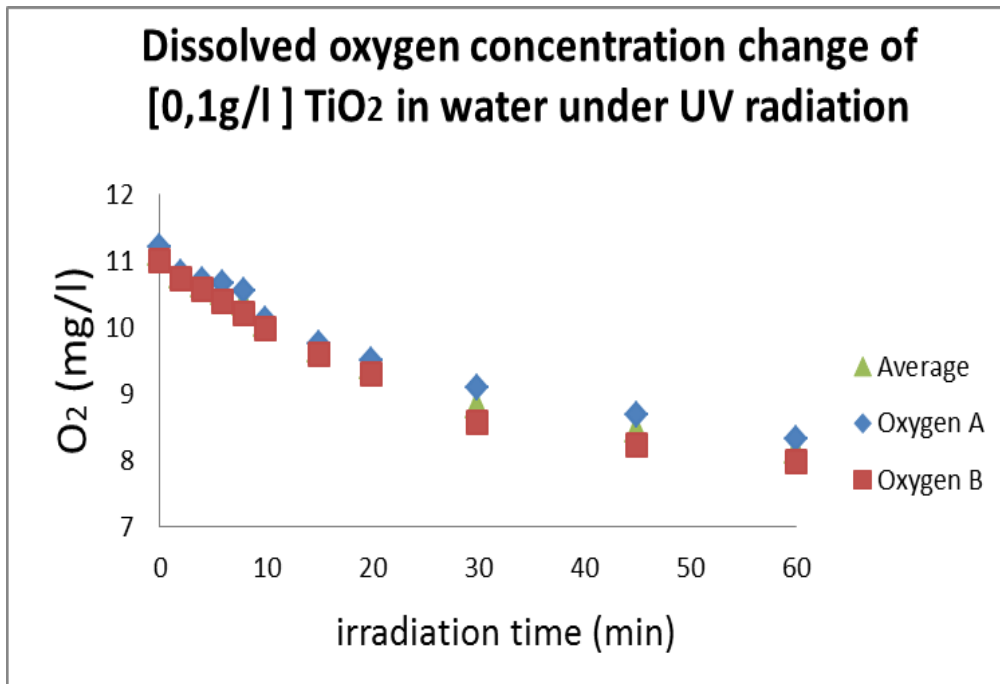
Change in oxygen concentration with radiation time of TiO₂



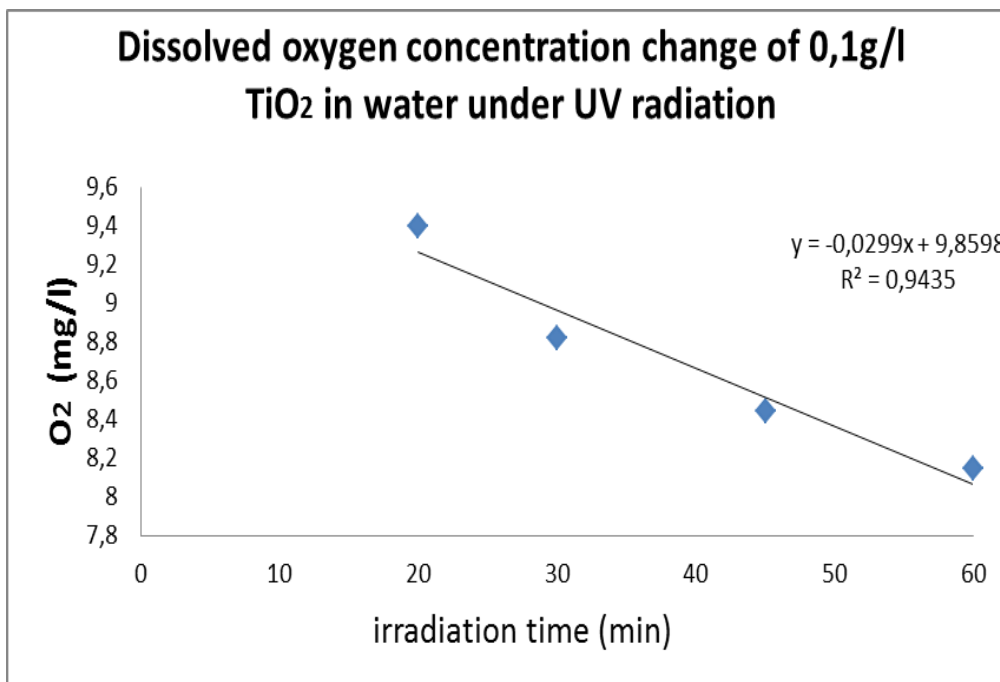
Decrease of oxygen concentration with radiation

Table 12.1: Oxygen concentration under UV irradiation 0.1 g/l TiO₂

Time(min)	Temperature °C	O ₂ (mg/l) A	O ₂ (mg/l)	Average O ₂
0	13,5	11,2	11,2	11,10
2	13,5	10,82	10,82	10,77
4	13,5	10,71	10,71	10,63
6	13,5	10,65	10,65	10,52
8	13,5	10,54	10,54	10,36
10	13,5	10,12	10,12	10,05
15	13,5	9,75	9,75	9,665
20	13,5	9,5	9,5	9,39
30	13,5	9,08	9,08	8,82
45	13,5	8,67	8,67	8,44
60	13,5	8,31	8,31	8,14



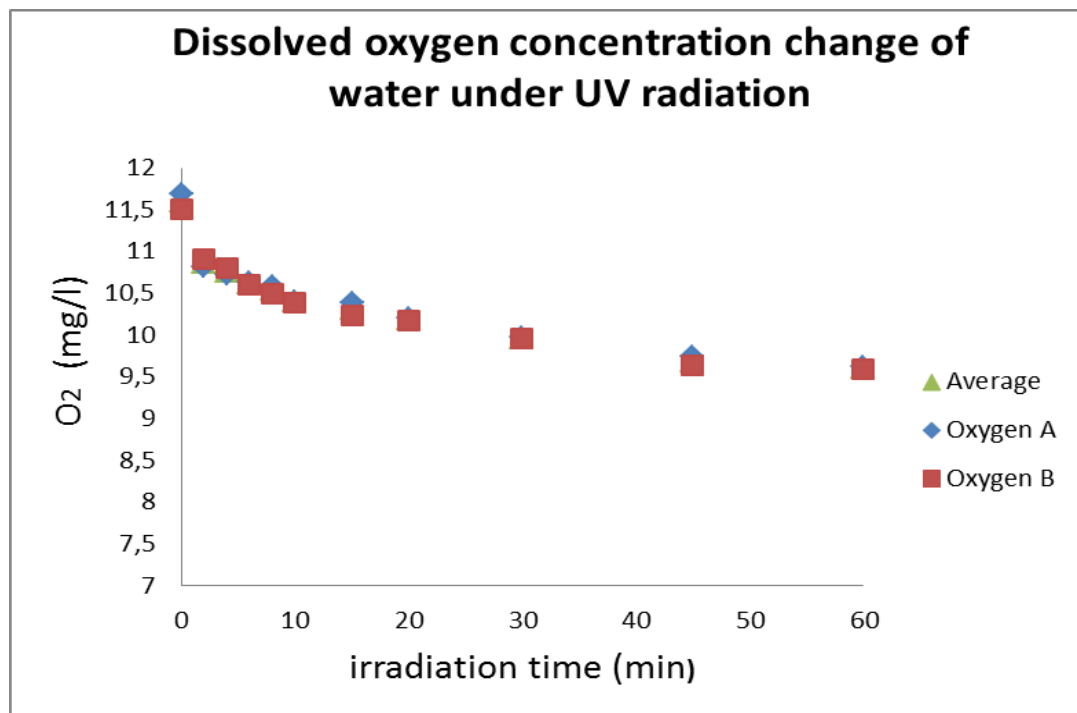
Change in oxygen concentration with radiation time of TiO₂



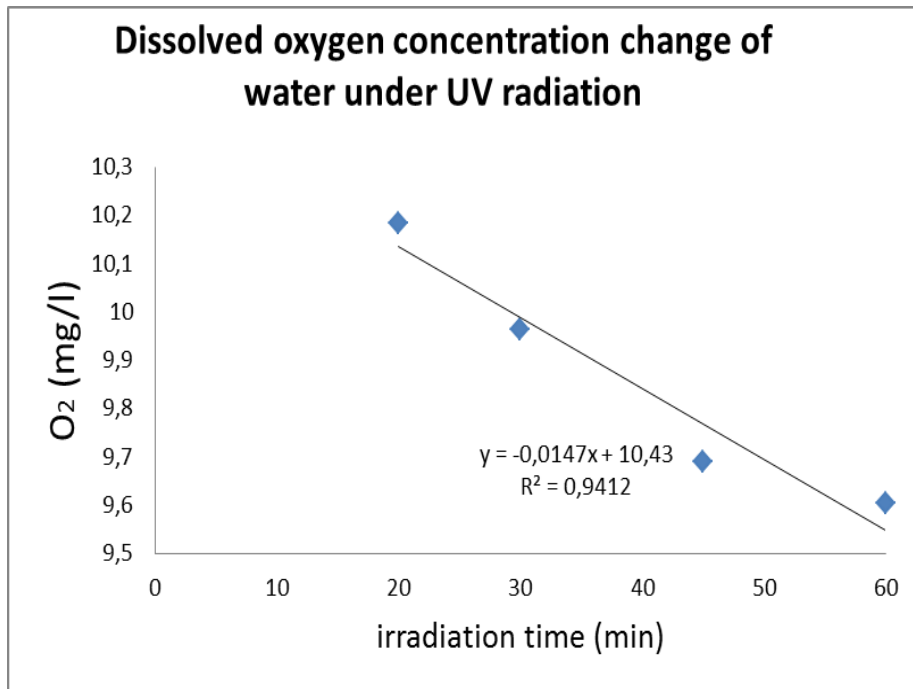
Decrease of oxygen concentration with radiation

Oxygen concentration under UV irradiation 0 g/l TiO₂

Time(min)	Temperature °C	O ₂ (mg/l) A	O ₂ (mg/l)	Average O ₂
0	13,5	11,69	11,5	11,59
2	13,5	10,82	10,91	10,86
4	13,5	10,72	10,8	10,76
6	13,5	10,64	10,6	10,62
8	13,5	10,58	10,5	10,54
10	13,5	10,41	10,39	10,4
15	13,5	10,39	10,23	10,31
20	13,5	10,2	10,17	10,18
30	13,5	9,97	9,96	9,96
45	13,5	9,75	9,63	9,69
60	13,5	9,62	9,59	9,60



Change in oxygen concentration with radiation time of TiO₂



Decrease of oxygen concentration with radiation

Linear regression results of TiO₂ irradiation under UV light in the closed system

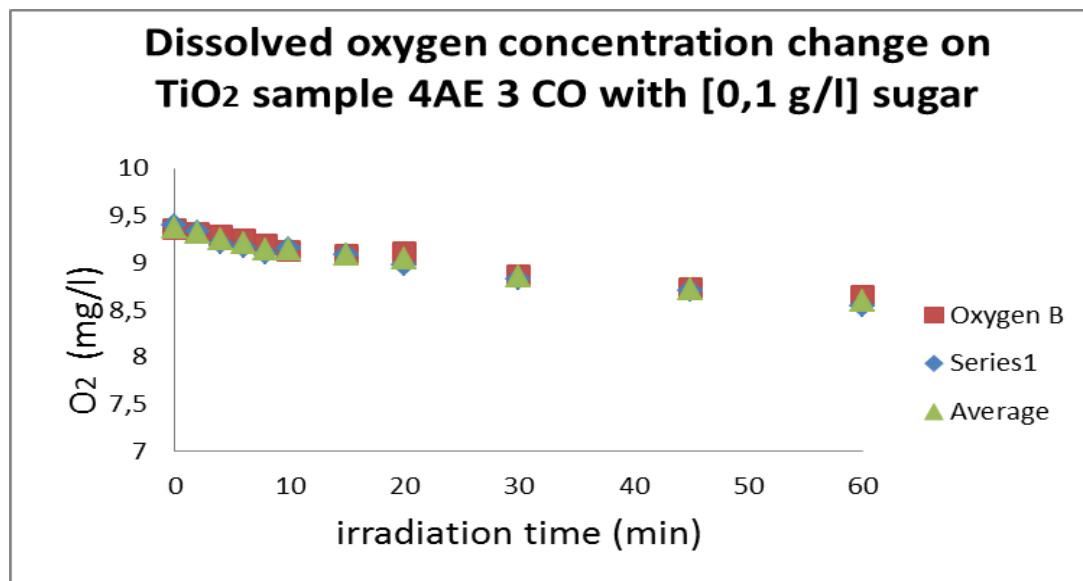
TiO ₂ (mg/l)	Decrease of oxygen (slope)	Correlation (R ²)
0.2	0.023	0.944
0.1	0.0299	0.9435
0	0.0147	0.9412

12.3 Appendix C

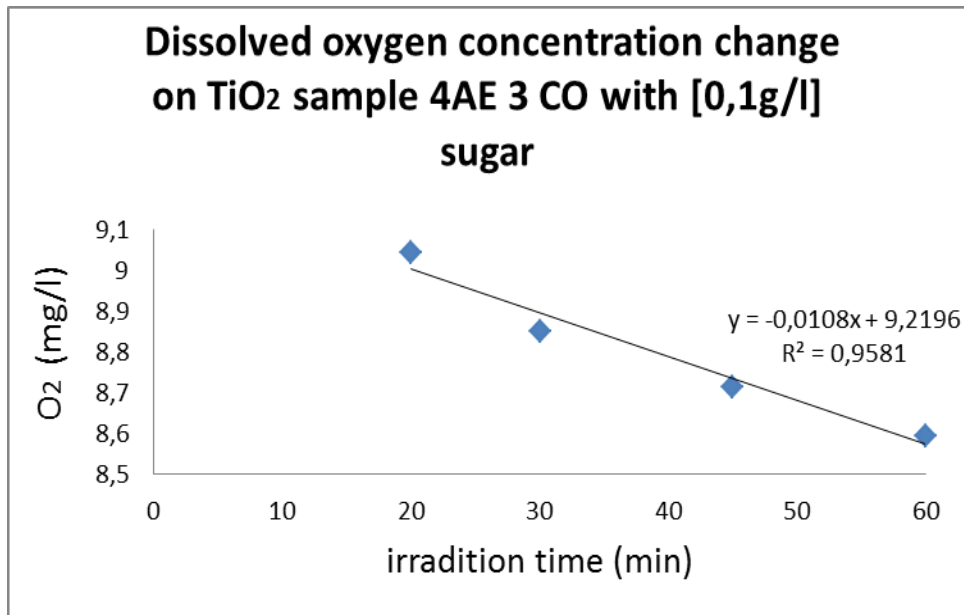
Testing of photocatalysis of TiO₂ using Oxymetric method on cotton samples

Oxygen concentration of cotton sample 4AE3 with 0.1 g/l

Time(min)	Temperature °C	O ₂ (mg/l) A	O ₂ (mg/l)	Average O ₂
0	13,5	9,4	9,35	9,37
2	13,5	9,33	9,31	9,32
4	13,5	9,2	9,29	9,25
6	13,5	9,16	9,25	9,20
8	13,5	9,1	9,19	9,1
10	13,5	9,15	9,13	9,14
15	13,5	9,09	9,08	9,08
20	13,5	8,98	9,11	9,04
30	13,5	8,83	8,87	8,85
45	13,5	8,7	8,73	8,71
60	13,5	8,54	8,65	8,59



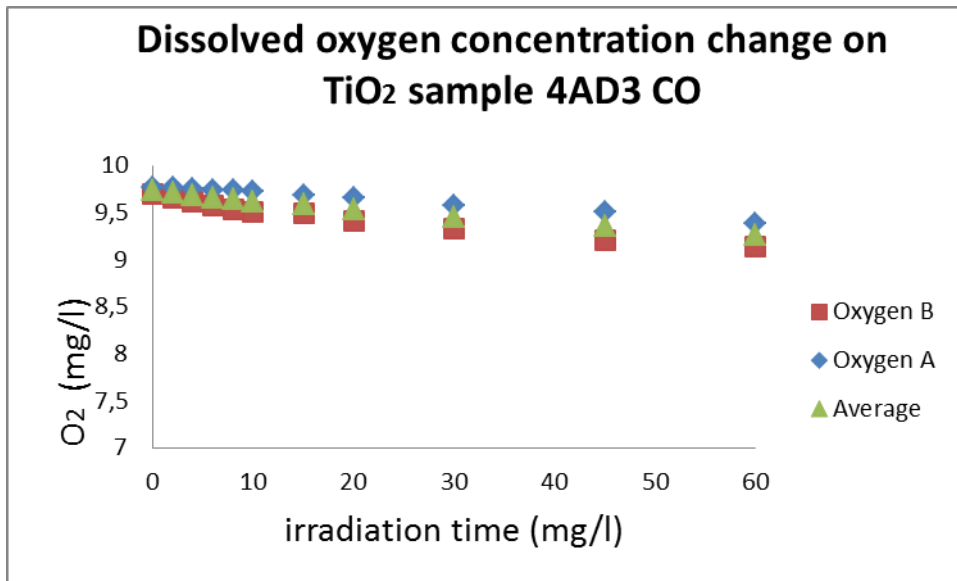
Decrease of dissolved oxygen of TiO₂ coated sample



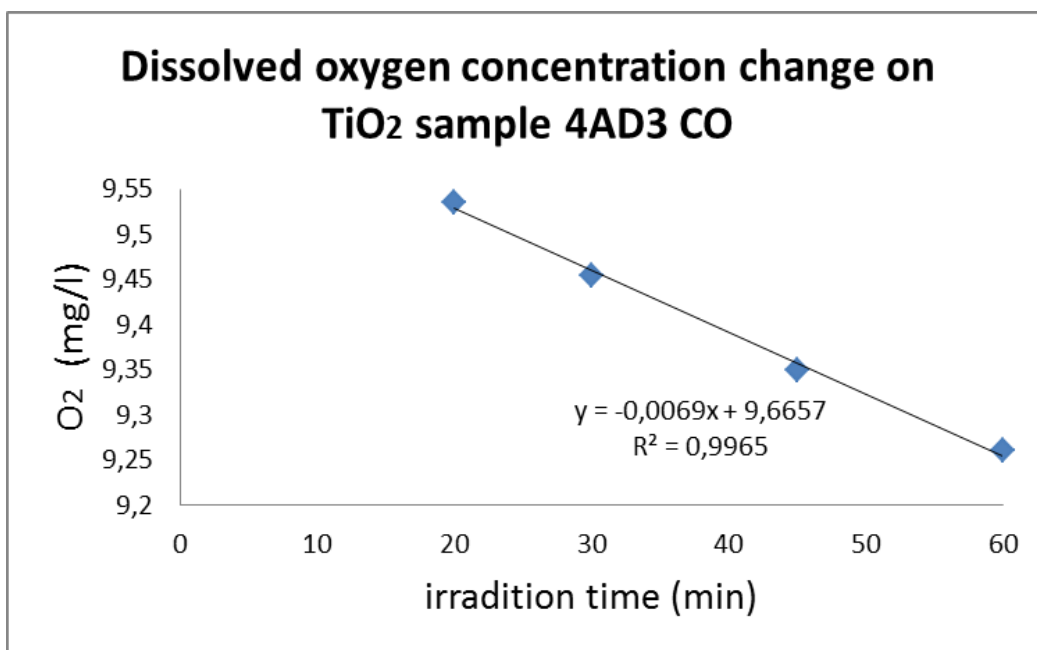
Decrease of dissolved oxygen of TiO₂ coated sample

Oxygen concentration of cotton sample 4AD3 with 0.1 g/l sugar

Time(min)	Temperature °C	O ₂ (mg/l) A	O ₂ (mg/l)	Average O ₂
0	13,5	9,77	9,7	9,73
2	13,5	9,76	9,65	9,70
4	13,5	9,75	9,62	9,68
6	13,5	9,74	9,58	9,66
8	13,5	9,74	9,54	9,64
10	13,5	9,72	9,5	9,61
15	13,5	9,68	9,49	9,58
20	13,5	9,66	9,41	9,53
30	13,5	9,58	9,33	9,45
45	13,5	9,5	9,2	9,35
60	13,5	9,38	9,14	9,26



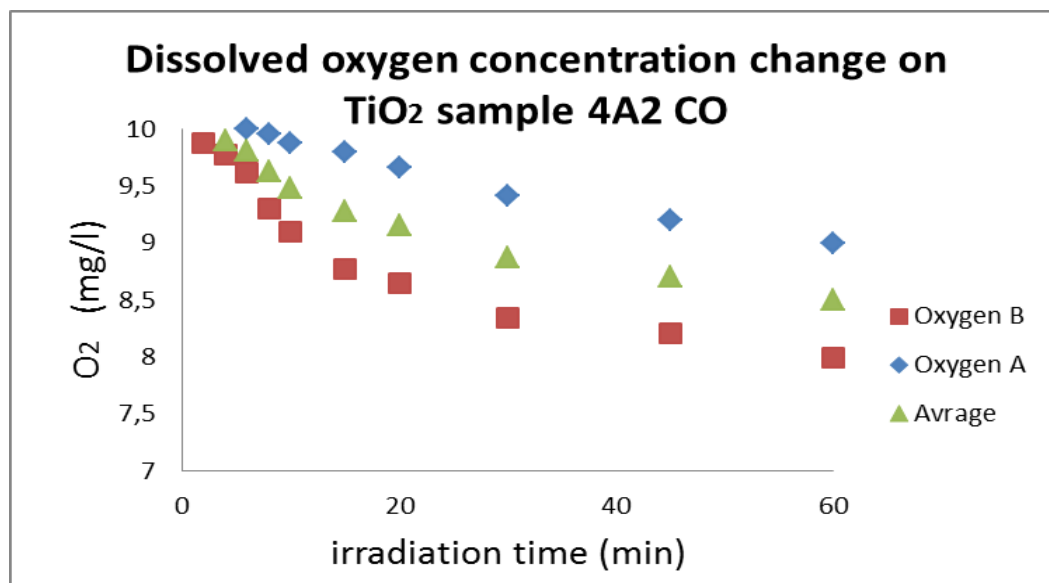
Decrease of dissolved oxygen of TiO₂ coated sample



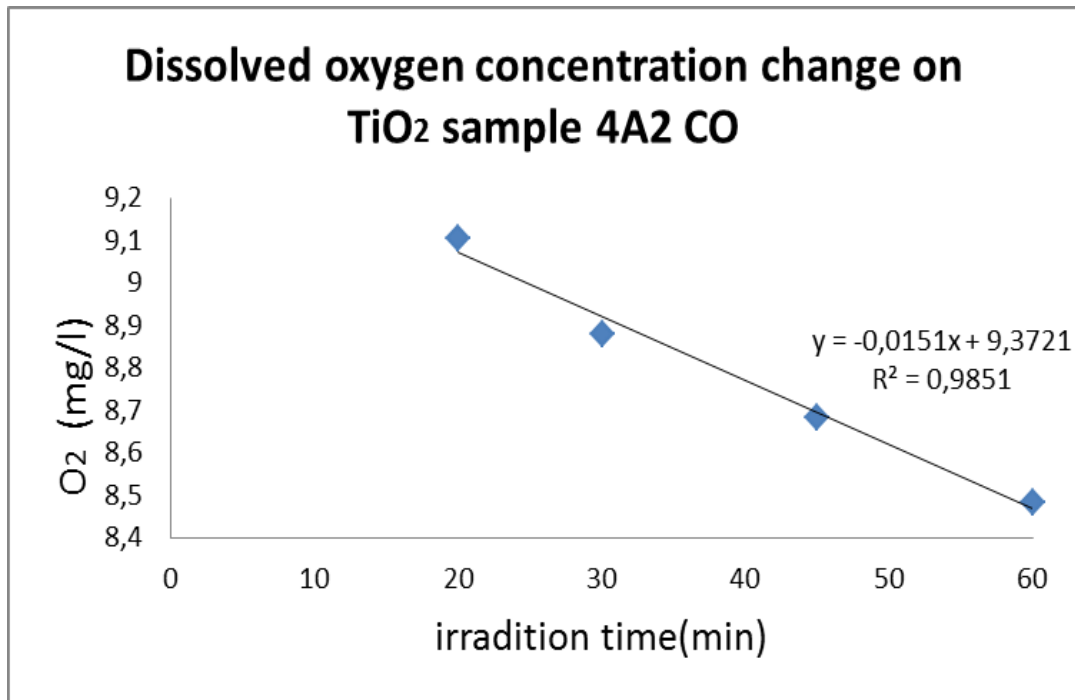
Decrease of dissolved oxygen of TiO₂ coated sample

Oxygen concentration of cotton sample 4A2 with 0.1 g/l sugar

Time(min)	Temperature °C	O ₂ (mg/l) A	O ₂ (mg/l)	Average O ₂
0	13,5	10,34	9,98	10,16
2	13,5	10,14	9,64	9,89
4	13,5	10,03	9,36	9,69
6	13,5	10	9,26	9,63
8	13,5	9,96	8,96	9,46
10	13,5	9,88	8,81	9,34
15	13,5	9,8	8,77	9,28
20	13,5	9,66	8,55	9,10
30	13,5	9,42	8,34	8,88
45	13,5	9,2	8,17	8,68
60	13,5	9	7,97	8,48



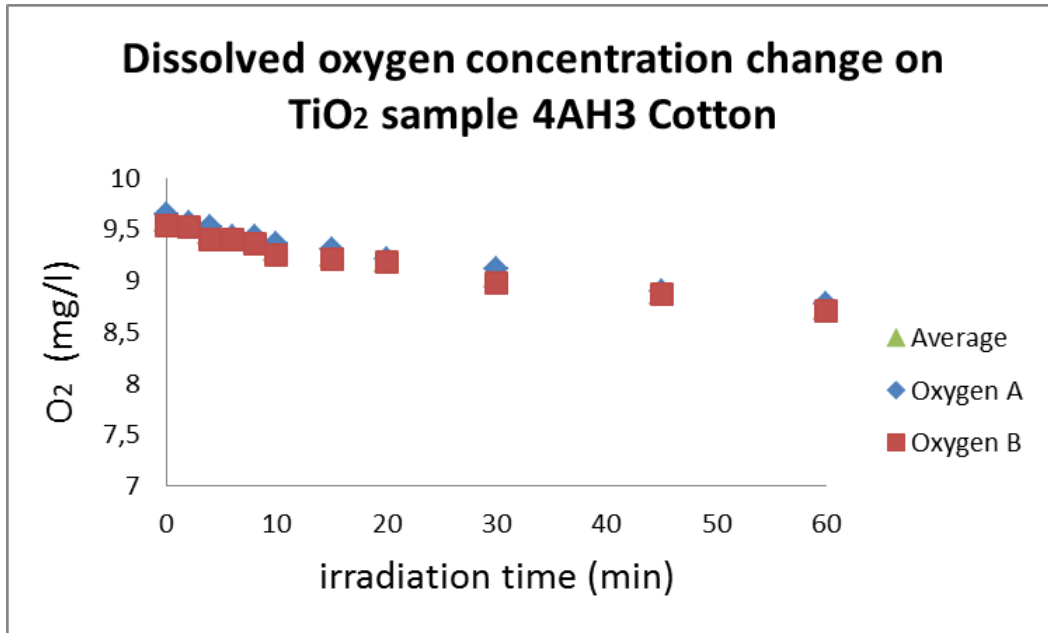
Decrease of dissolved oxygen of TiO₂ coated sample



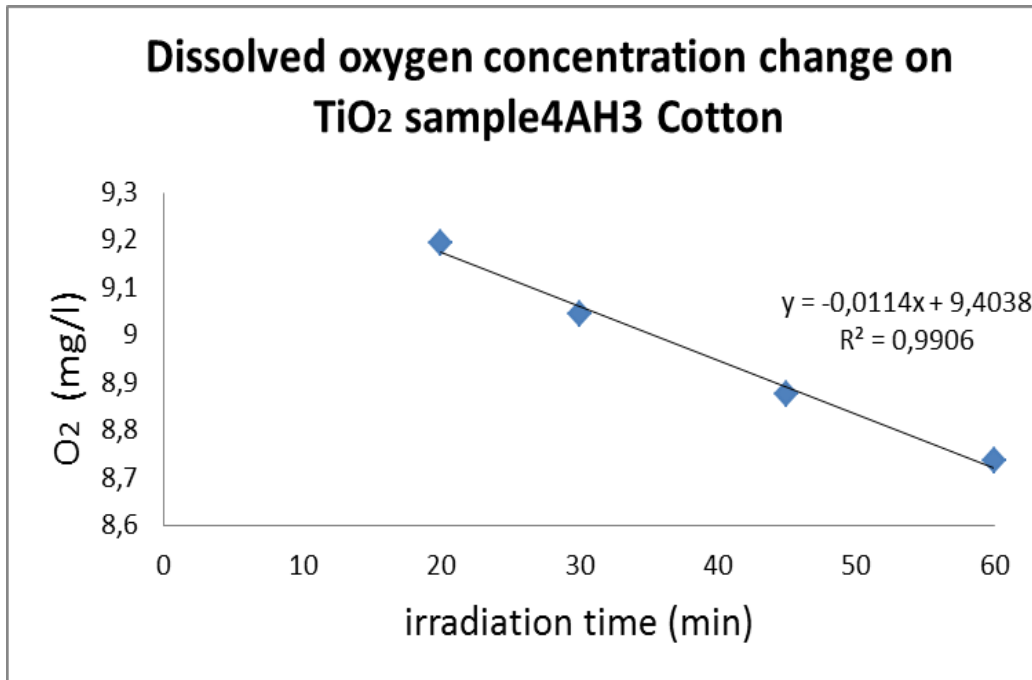
Decrease of dissolved oxygen of TiO₂ coated sample

Oxygen concentration of cotton sample 4AH3 with 0.1 g/l sugar

Time(min)	Temperature °C	O ₂ (mg/l) A	O ₂ (mg/l)	Average O ₂
0	13,5	9,64	9,54	9,59
2	13,5	9,56	9,52	9,54
4	13,5	9,52	9,4	9,46
6	13,5	9,42	9,4	9,41
8	13,5	9,43	9,36	9,39
10	13,5	9,36	9,25	9,30
15	13,5	9,3	9,2	9,25
20	13,5	9,21	9,18	9,19
30	13,5	9,11	8,98	9,04
45	13,5	8,89	8,86	8,87
60	13,5	8,77	8,7	8,74



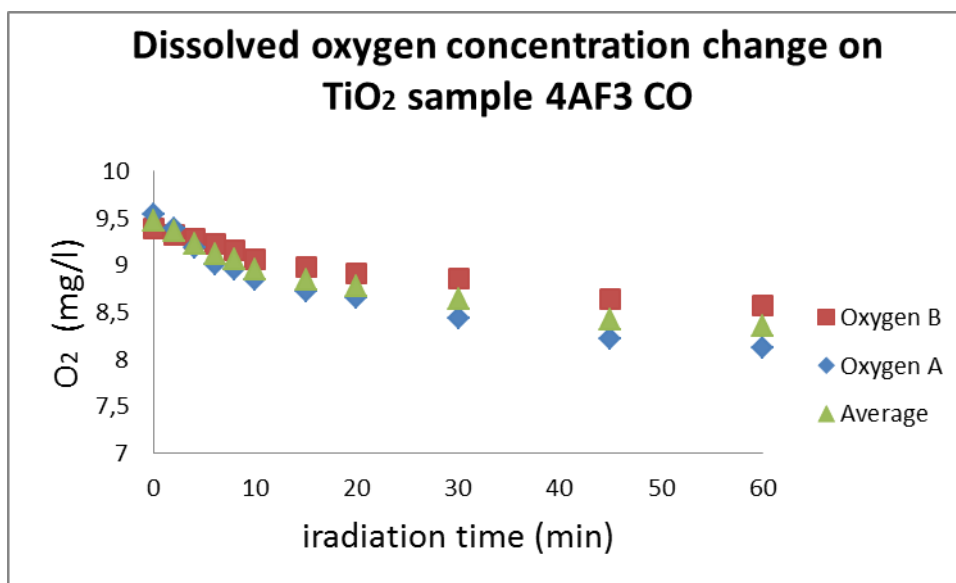
Decrease of dissolved oxygen of TiO₂ coated sample



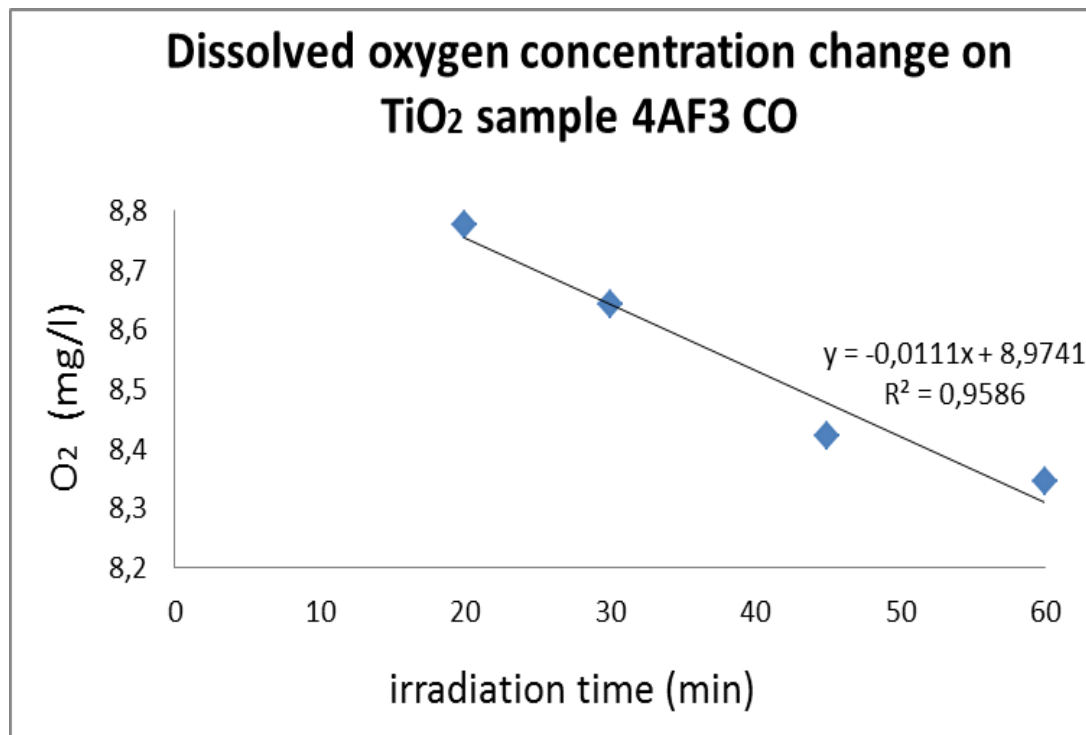
Decrease of dissolved oxygen of TiO₂ coated sample

Oxygen concentration of cotton sample 4AF3 with 0.1 g/l sugar

Time(min)	Temperature °C	O ₂ (mg/l) A	O ₂ (mg/l)	Average O ₂
0	13,5	9,54	9,38	9,46
2	13,5	9,39	9,32	9,35
4	13,5	9,18	9,27	9,22
6	13,5	9	9,22	9,11
8	13,5	8,95	9,15	9,05
10	13,5	8,84	9,05	8,95
15	13,5	8,71	8,98	8,85
20	13,5	8,65	8,9	8,77
30	13,5	8,43	8,85	8,64
45	13,5	8,21	8,63	8,42
60	13,5	8,12	8,57	8,34



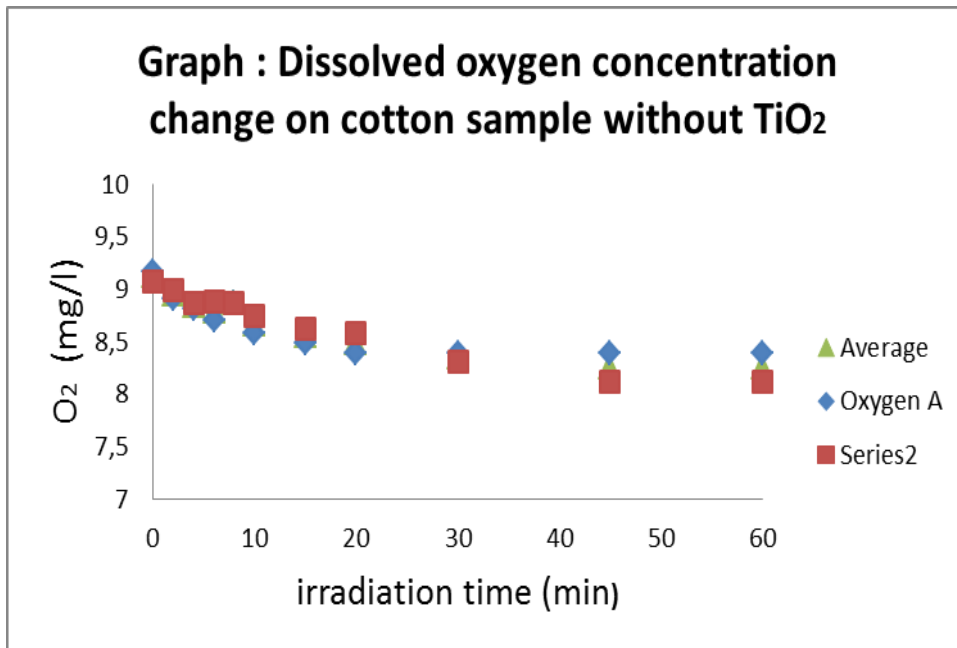
Decrease of dissolved oxygen of TiO₂ coated sample



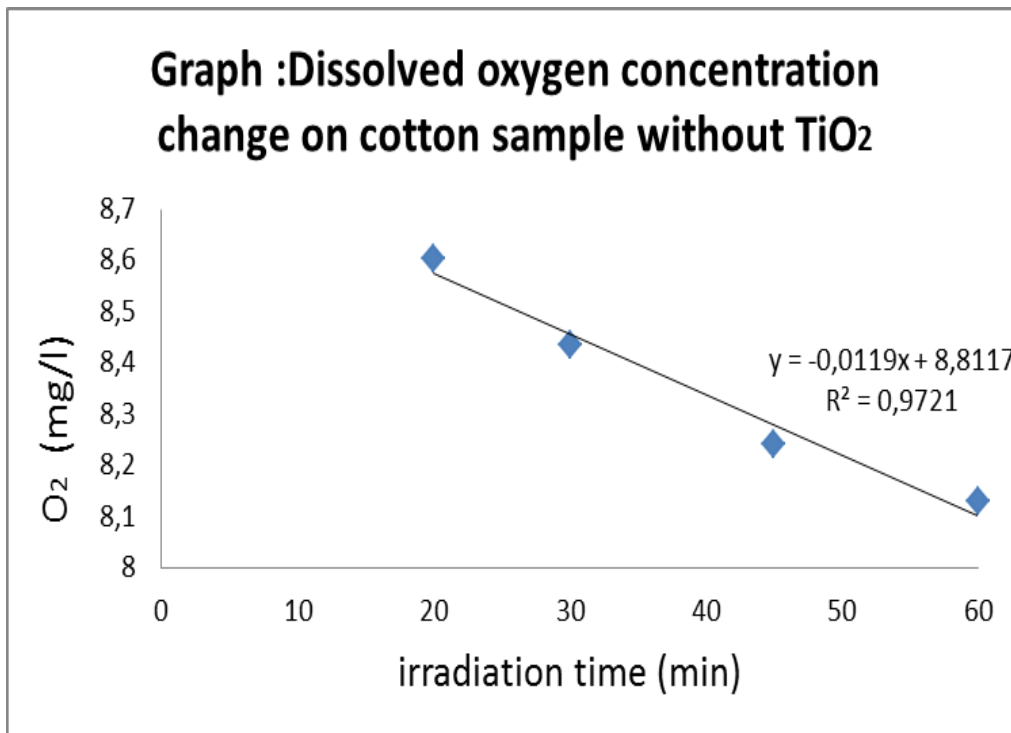
Decrease of dissolved oxygen of TiO₂ coated sample

Oxygen concentration of cotton sample with no TiO₂ and 0.1 g/l sugar

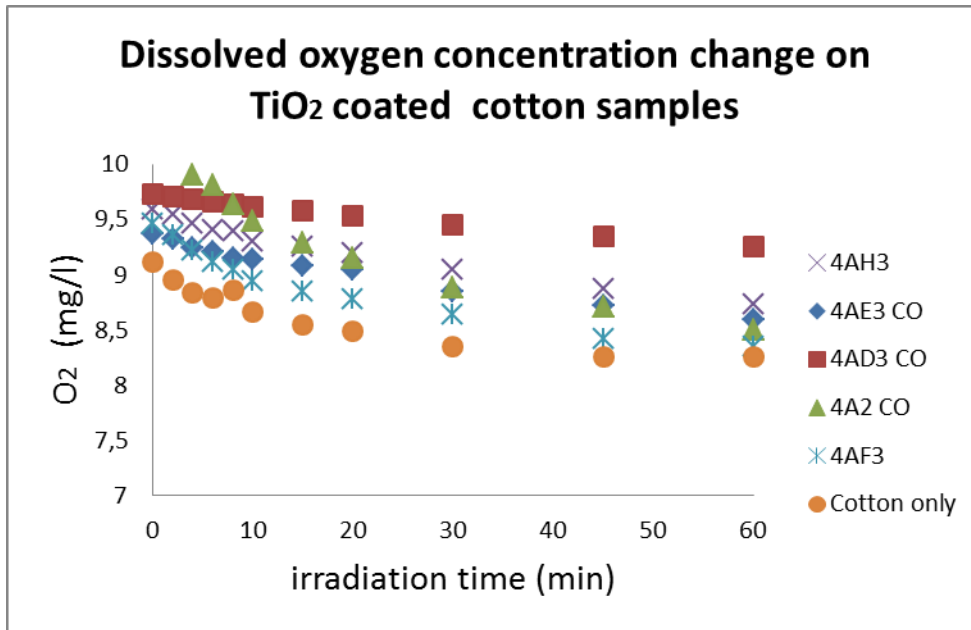
Time(min)	Temperature °C	O ₂ (mg/l) A	O ₂ (mg/l)	Average O ₂
0	13,5	9,26	9,07	9,16
2	13,5	9,16	8,99	9,07
4	13,5	9	8,87	8,94
6	13,5	8,98	8,88	8,93
8	13,5	8,87	8,86	8,86
10	13,5	8,79	8,75	8,77
15	13,5	8,71	8,62	8,66
20	13,5	8,63	8,58	8,60
30	13,5	8,56	8,31	8,44
45	13,5	8,36	8,12	8,24
60	13,5	8,28	7,98	8,13



Decrease of dissolved oxygen of TiO₂ coated sample



Decrease of dissolved oxygen of TiO₂ coated sample

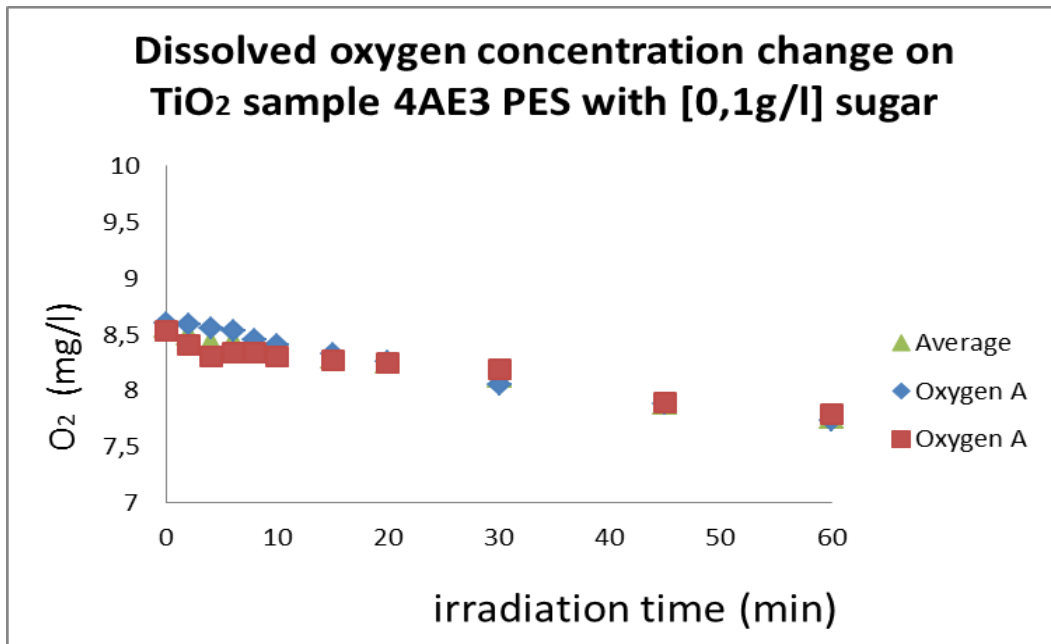


Comparison of the decrease of oxygen concentration of cotton samples

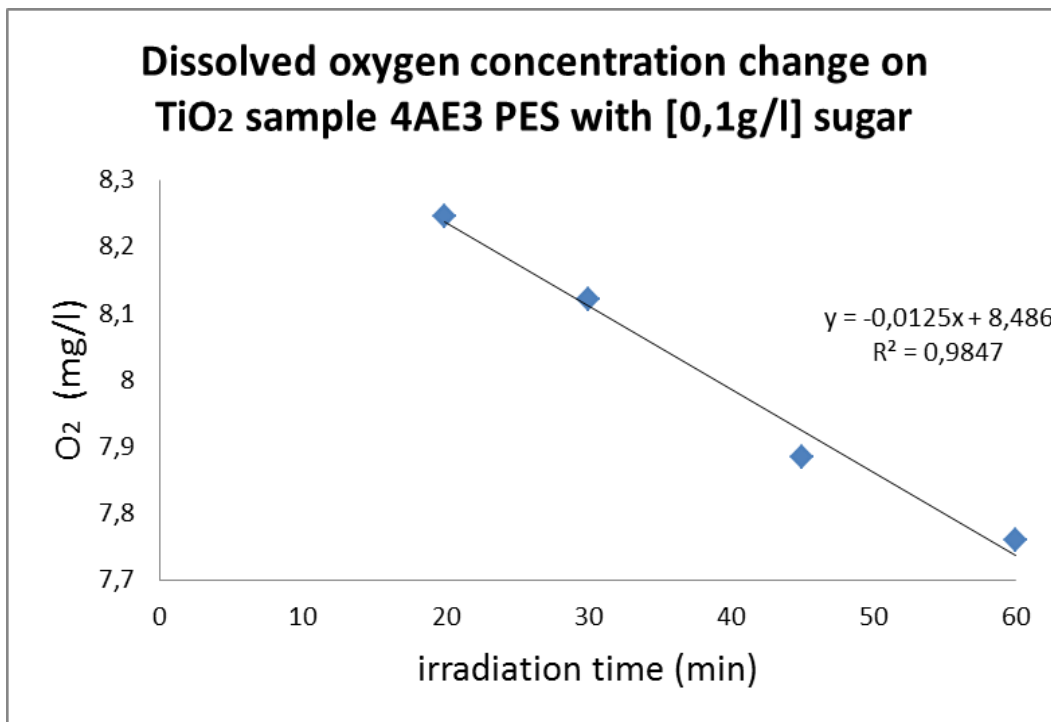
Testing of photocatalysis of TiO₂ using Oxymetric method on polyester samples

Oxygen concentration of polyester sample 4AE3 with 0.1 g/l sugar

Time(min)	Temperature °C	O ₂ (mg/l) A	O ₂ (mg/l)	Average O ₂
0	13,5	8,6	8,53	8,57
2	13,5	8,59	8,4	8,49
4	13,5	8,55	8,3	8,43
6	13,5	8,53	8,34	8,44
8	13,5	8,45	8,33	8,39
10	13,5	8,4	8,3	8,35
15	13,5	8,32	8,27	8,29
20	13,5	8,25	8,24	8,24
30	13,5	8,05	8,19	8,12
45	13,5	7,88	7,89	7,88
60	13,5	7,73	7,79	7,76



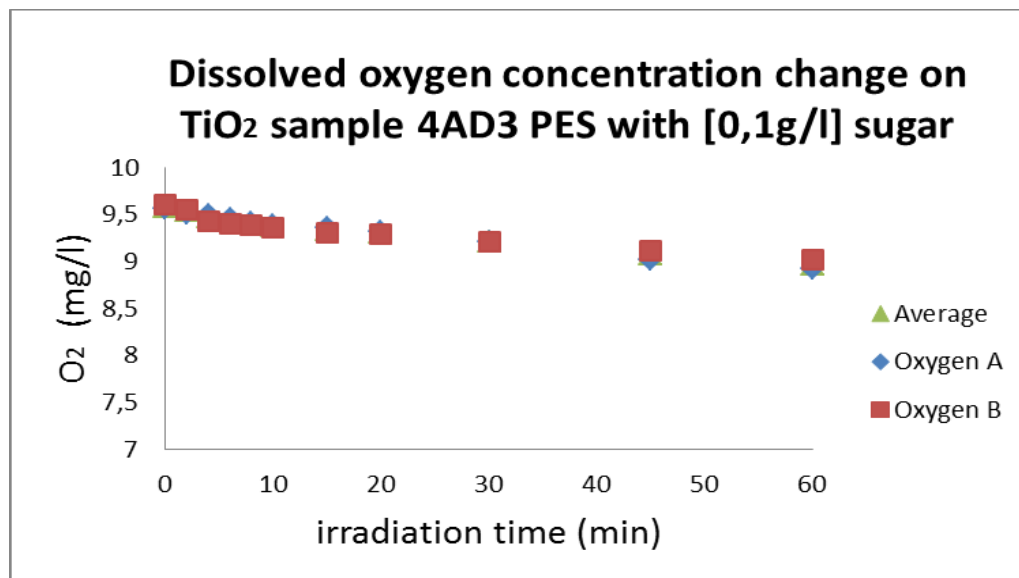
Decrease of dissolved oxygen of TiO₂ coated sample



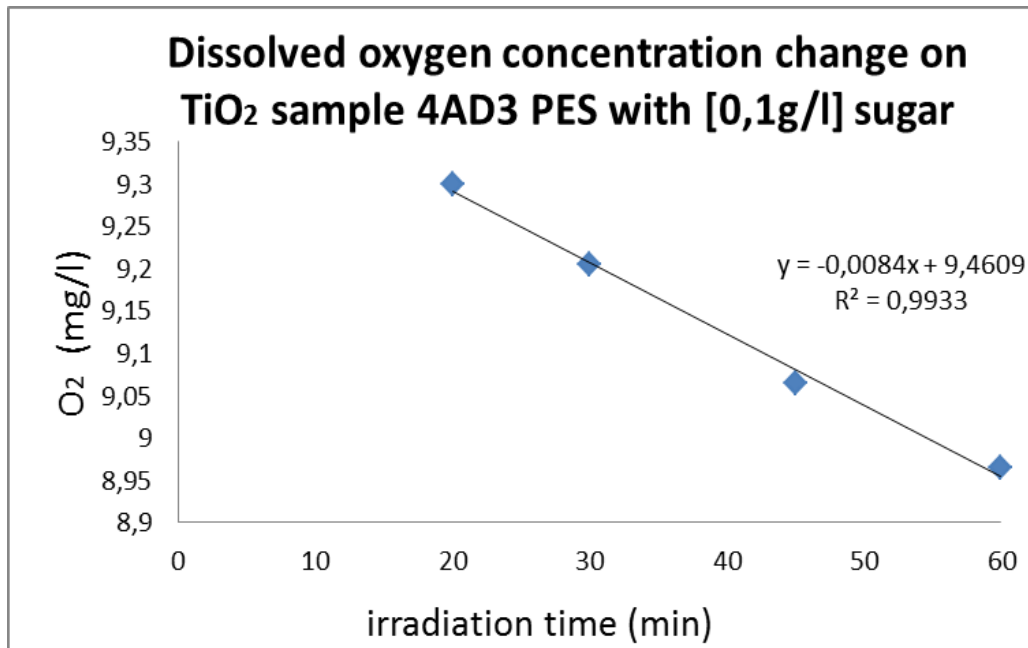
Decrease of dissolved oxygen of TiO₂ coated sample

Oxygen concentration of polyester sample 4AD3 with 0.1 g/l sugar

Time(min)	Temperature °C	O ₂ (mg/l) A	O ₂ (mg/l)	Average O ₂
0	13,5	9,56	9,6	9,58
2	13,5	9,51	9,55	9,53
4	13,5	9,49	9,43	9,46
6	13,5	9,45	9,4	9,42
8	13,5	9,41	9,38	9,39
10	13,5	9,38	9,36	9,37
15	13,5	9,35	9,3	9,32
20	13,5	9,31	9,29	9,3
30	13,5	9,2	9,21	9,20
45	13,5	9,02	9,11	9,06
60	13,5	8,92	9,01	8,96



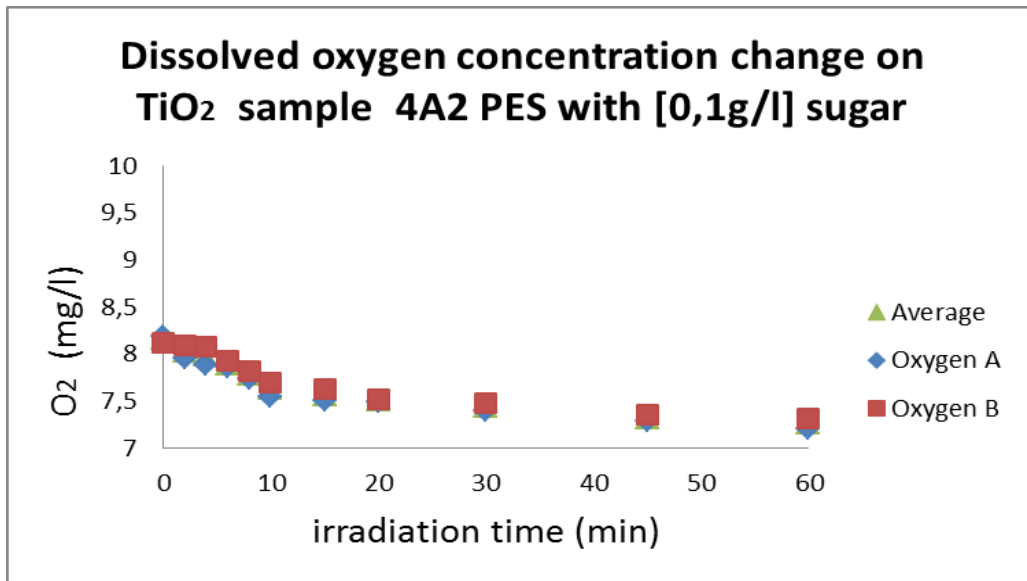
Decrease of dissolved oxygen of TiO₂ coated sample



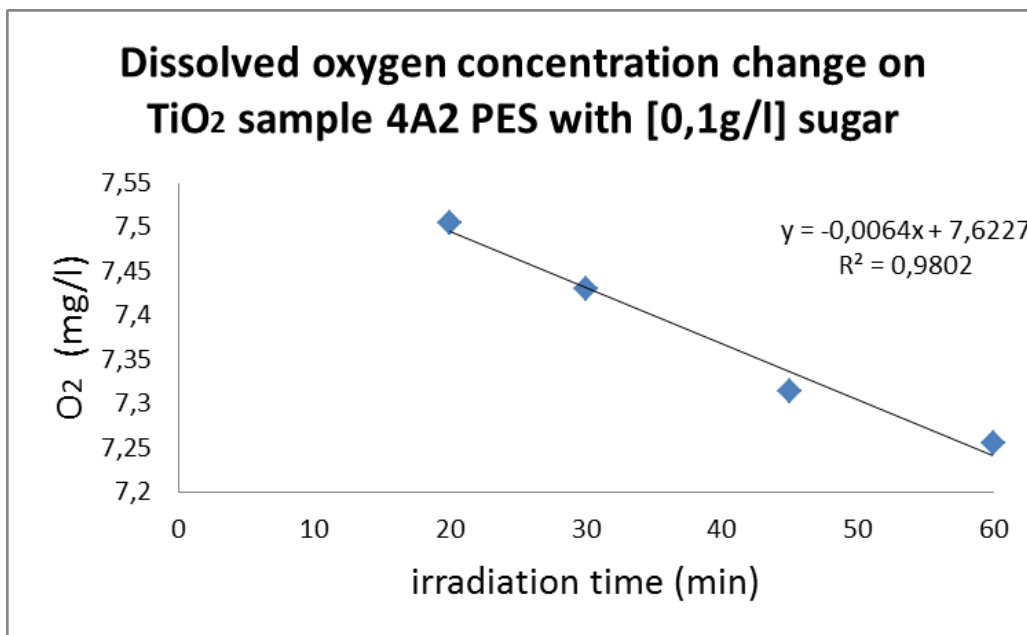
Decrease of dissolved oxygen of TiO₂ coated sample

Oxygen concentration of polyester sample 4A2 with 0.1 g/l sugar

Time(min)	Temperature °C	O ₂ (mg/l) A	O ₂ (mg/l)	Average O ₂
0	13,5	8,19	8,12	8,15
2	13,5	7,95	8,09	8,02
4	13,5	7,89	8,07	7,98
6	13,5	7,86	7,92	7,89
8	13,5	7,73	7,82	7,77
10	13,5	7,54	7,7	7,62
15	13,5	7,5	7,62	7,56
20	13,5	7,49	7,52	7,50
30	13,5	7,39	7,47	7,43
45	13,5	7,28	7,35	7,31
60	13,5	7,2	7,31	7,25



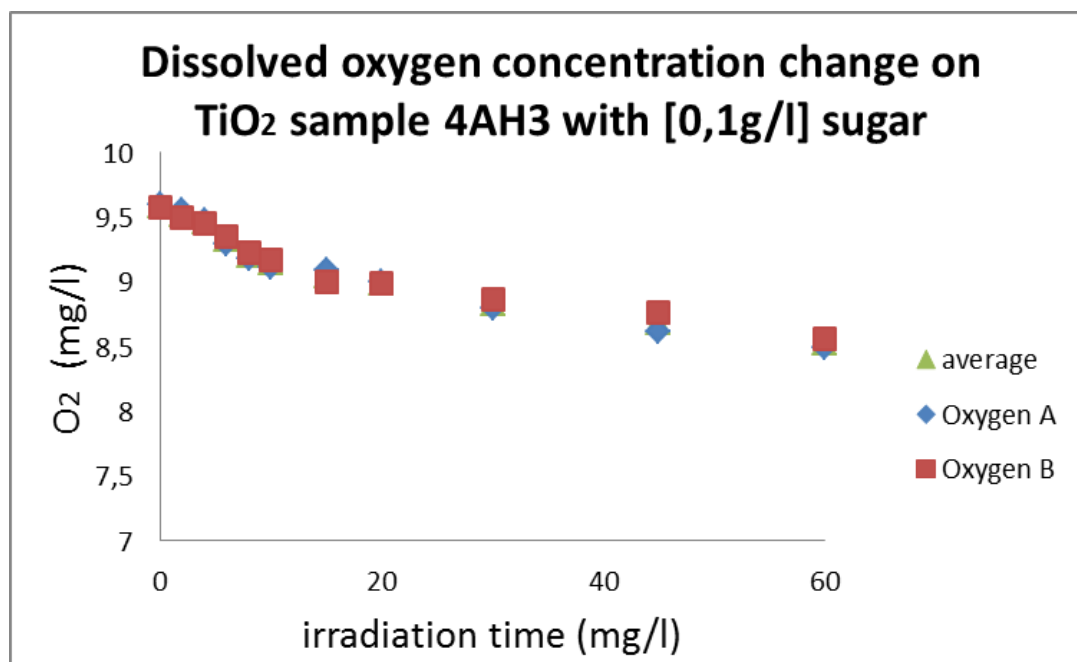
Decrease of dissolved oxygen of TiO₂ coated sample



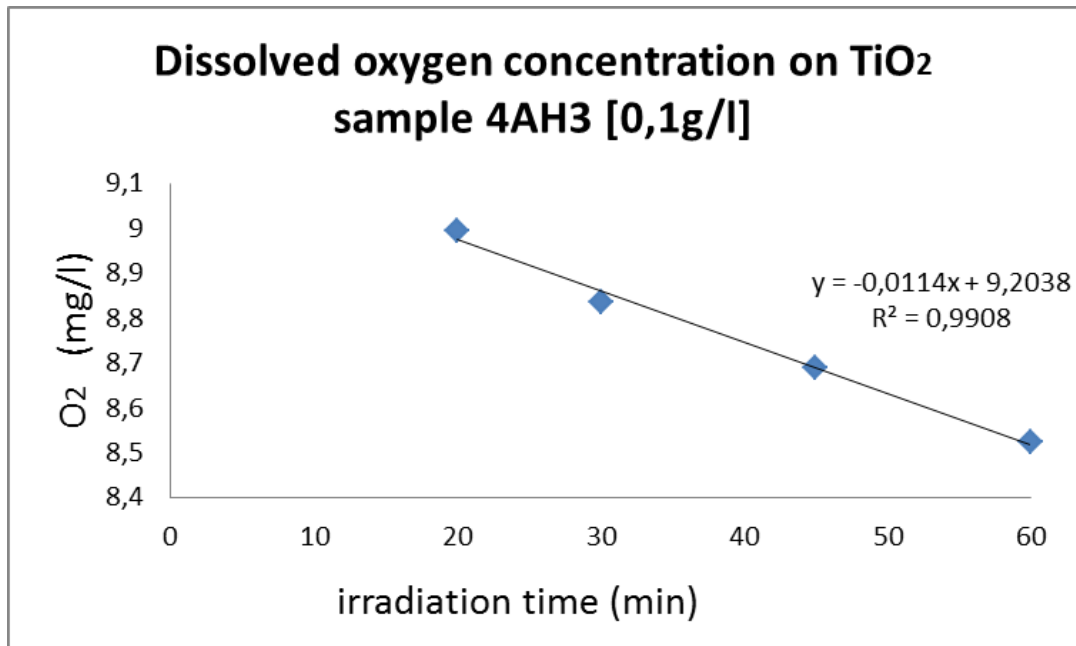
Decrease of dissolved oxygen of TiO₂ coated sample

Oxygen concentration of polyester sample 4AH3 with 0.1 g/l sugar

Time(min)	Temperature °C	O ₂ (mg/l) A	O ₂ (mg/l)	Average O ₂
0	13,5	9,6	9,58	9,59
2	13,5	9,55	9,5	9,52
4	13,5	9,48	9,45	9,46
6	13,5	9,3	9,35	9,32
8	13,5	9,18	9,23	9,20
10	13,5	9,12	9,17	9,14
15	13,5	9,09	9	9,045
20	13,5	9	8,99	8,99
30	13,5	8,8	8,87	8,83
45	13,5	8,62	8,76	8,69
60	13,5	8,49	8,56	8,52



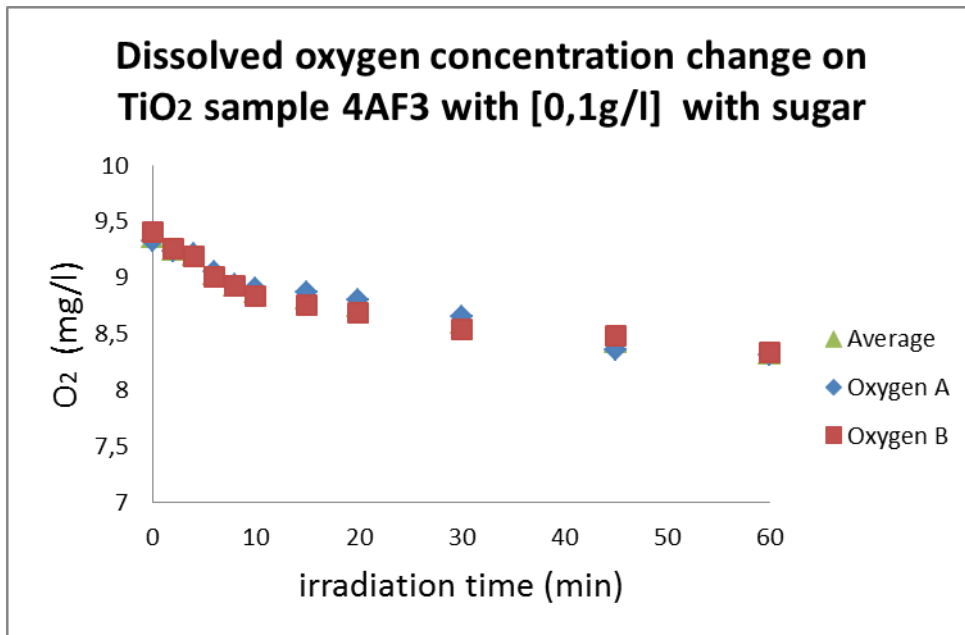
Decrease of dissolved oxygen of TiO₂ coated sample



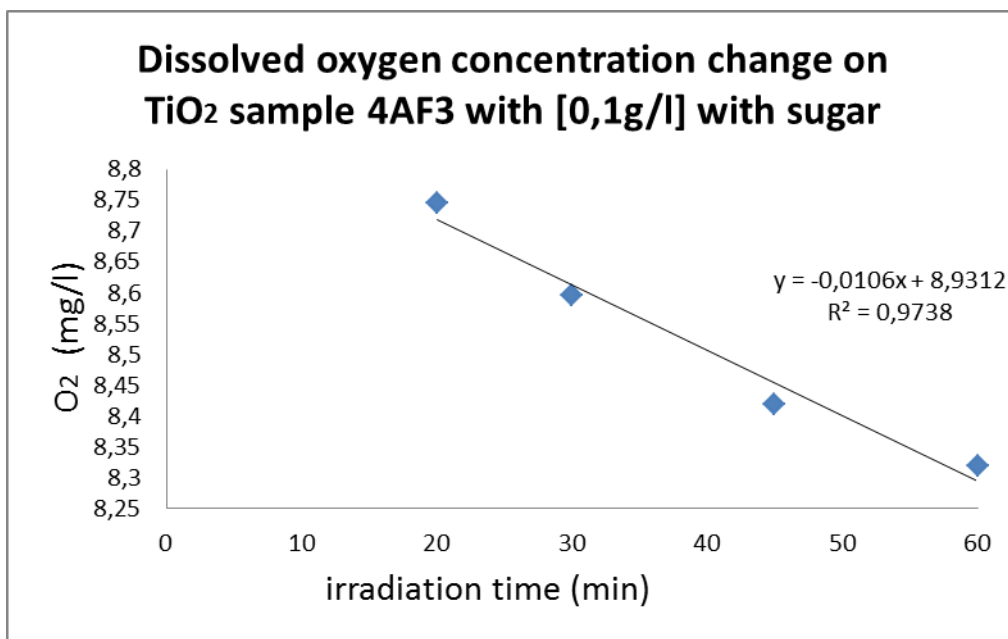
Decrease of dissolved oxygen of TiO₂ coated sample

Oxygen concentration of polyester sample 4AF3 with 0.1 g/l sugar

Time(min)	Temperature °C	O ₂ (mg/l) A	O ₂ (mg/l)	Average O ₂
0	13,5	9,32	9,4	9,36
2	13,5	9,23	9,26	9,245
4	13,5	9,21	9,19	9,2
6	13,5	9,05	9	9,02
8	13,5	8,94	8,92	8,93
10	13,5	8,9	8,84	8,87
15	13,5	8,87	8,76	8,81
20	13,5	8,8	8,69	8,74
30	13,5	8,65	8,54	8,59
45	13,5	8,36	8,48	8,42
60	13,5	8,31	8,33	8,32



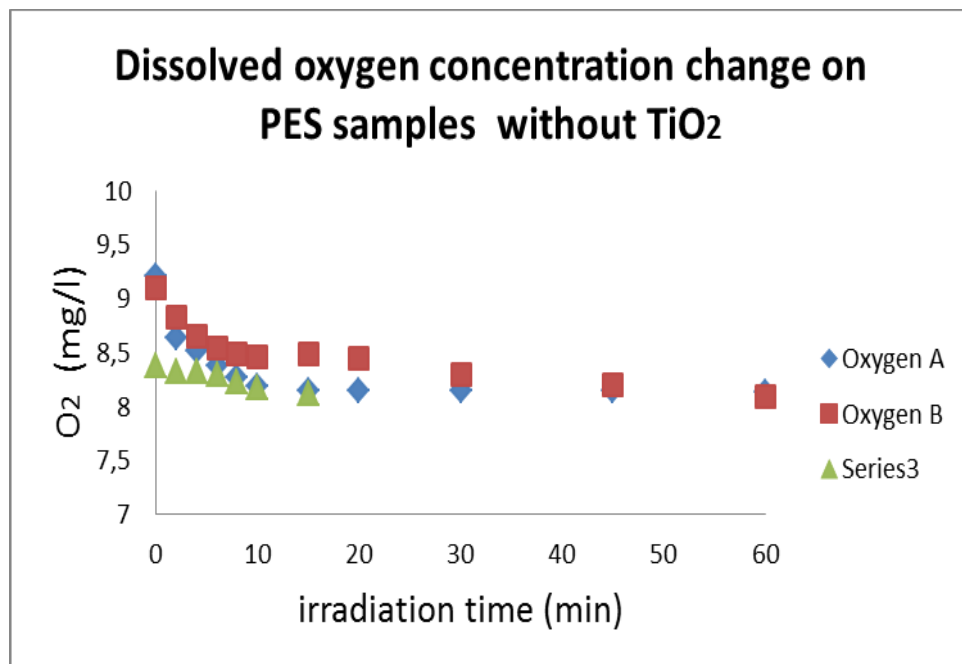
Decrease of dissolved oxygen of TiO₂ coated sample



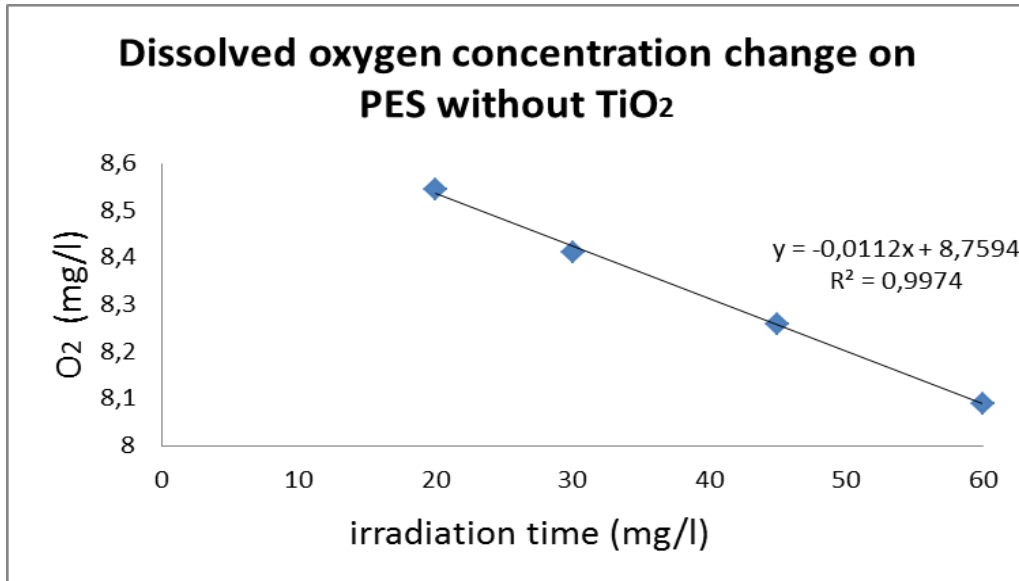
Decrease of dissolved oxygen of TiO₂ coated sample

Oxygen concentration of polyester sample without TiO₂ with 0.1 g/l sugar

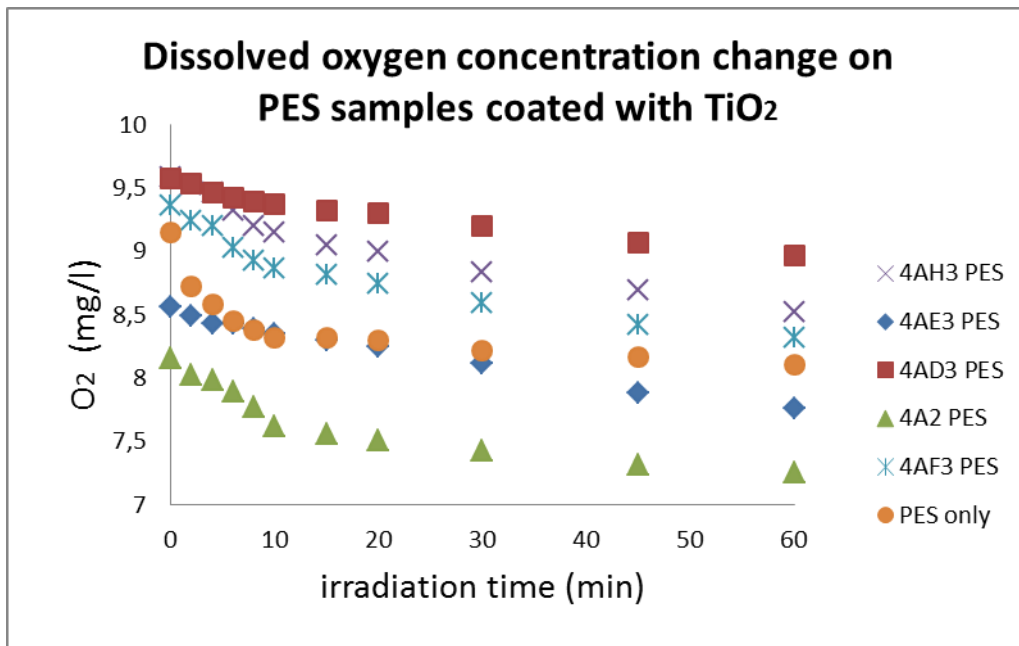
Time(min)	Temperature °C	O ₂ (mg/l) A	O ₂ (mg/l)	Average O ₂
0	13,5	9,84	9,91	9,87
2	13,5	9,48	8,82	9,15
4	13,5	8,97	8,65	8,81
6	13,5	8,93	8,54	8,73
8	13,5	8,91	8,48	8,69
10	13,5	8,85	8,46	8,65
15	13,5	8,68	8,49	8,55
20	13,5	8,64	8,45	8,55
30	13,5	8,52	8,3	8,41
45	13,5	8,32	8,2	8,26
60	13,5	8,09	8,09	8,09



Decrease of dissolved oxygen of TiO₂ coated sample



Decrease of dissolved oxygen of TiO₂ coated sample



Comparison of the decrease of oxygen concentration on polyester samples